The stage joins the show: Aspects of perturbed spacetimes

by

© **Uzair Hussain**

A thesis submitted to the School of Graduate Studies in partial fulfillment of the requirements for the degree of Doctor of Philosophy.

Theoretical Physics Program

Memorial University

September 2017

St. John's, Newfoundland and Labrador, Canada

Abstract

In this thesis we present projects that cover various topics in black hole physics. The central theme of the thesis is perturbation theory of black holes. The techniques developed to study the perturbations of spacetime allows us to explore and elucidate many other topics in gravitational physics.

The recent discovery of gravitational waves provides strong evidence for the existence of black hole mergers. Using perturbation theory we study the problem of black hole mergers with an extreme mass ratio in an asymptotically flat spacetime, and proceed to demonstrate how the event horizon and the apparent horizon of the larger black hole deform. In this thesis we also study problems concerning perturbation of black holes that are more theoretical in nature. In the context of the fluid/gravity duality, we precisely establish the relationship between standard perturbation theory of spherically symmetric black holes i.e., the master equation, with near equilibrium dual fluid perturbations on the boundary of asymptotically Anti de Sitter (AdS) black holes. By the use of this relationship and a numerical evolution of the master equation we argue for the existence of non-Newtonian fluids in the fluid/gravity duality. The last project concerns itself with a generalization of the first law of black hole mechanics to include five dimensional solutions of spacetime called solitons. We verify this law for spacetimes containing solitons.

To the current residents of Zarigul

Acknowledgements

I am eternally grateful to my supervisors, Dr. Ivan Booth and Dr. Hari Kunduri. Both of them have a wealth of knowledge of the field which they enthusiastically shared. Their doors were always open for all my inquiries, even the annoying ones. Their pedagogical skills, expertise, intellect, patience and understanding made the arduous process of learning theoretical physics much easier. Dr. Booth's composure is remarkable, I would go in his office anxious and come out tranquil. This together with Dr. Kunduri's quick-witted humour and boldness helped relieve stress. Aside from academic matters, Dr. Booth and Dr. Kunduri have also given me invaluable advice on general matters of life which I certainly cherish.

I would also like to thank my committee members Dr. Jahrul Alam, and Dr. Stephanie H. Curnoe for their advice and wisdom.

I am grateful of the advice and input I got from Dr. Viqar Husain, Dr. Eduardo Martinez Pedroza, Dr. Chris Radford and Dr. Sanjeev Seahra. I am thankful of the long and stimulating talks I had with Dr. Andrey Shoom and Dr. Jonathan Ziprick, they were always open to hear and critique my nebulous views.

Through the course of my Ph.D. I fostered many friendships, I am thankful of all my friends, especially the "field hallers". The late nights spent at Field Hall will truly be unforgettable.

My time spent in St. John's was truly transforming because it was here that I met my fiancé, Shirin Modarresi. My Ph.D. would have been tremendously more difficult if it was not for her unwavering support and unconditional love.

Last but not least I would like to thank my family especially my dear parents, without their infinite support and encouragement I would not have been capable of this achievement.

Statement of contributions

I am the sole author of Chapter 1, Chapter 4 and Chapter 7. The co-authorship statement of the manuscripts is given in Chapter 2.

Table of contents

List of tables

List of figures

List of symbols

We follow the sign conventions of Misner, Thorne, and Wheeler [46]

GR	General Relativity
EFE	Einstein's Field Equations
AdS	Anti-de Sitter
CFT	Conformal field theory
EMR	Extreme mass ratio
EH	Event horizon
AH	Apparent horizon
$I^+(S)$	Chronological future of set S
$I^-(S)$	Chronological past of set S
$J^+(S)$	Causal future of set S
$J^-(S)$	Causal past of set S
$D^+(S)$	Future domain of dependence of S
$D^-(S)$	Past domain of dependence of S
i^+	Future timelike infinity
i^0	Spatial infinity
i^-	Past timelike infinity
$\mathscr{I}^+$	Future null infinity
$\mathscr{I}^-$	Past null infinity
$\mathcal{L}$	Lie derivative
Λ	Cosmological constant
L	AdS length
$\eta_{\mu\nu}$	Minkowski metric
Ω_{AB}	Metric on unit sphere
Y^{lm}	Spherical harmonics
Y^{lm}_A	Even vector harmonics
Y^{lm}_{AB}	Even tensor harmonics
X^{lm}_A	Odd vector harmonics
X^{lm}_{AB}	Odd tensor harmonics
$M_\odot$	Unit solar mass

Chapter 1

Introduction

In November 1915, Einstein presented his theory of General Relativity (GR) before the Prussian Academy of Sciences in Berlin [56]. Sitting on the throne of the theory were a set of notoriously difficult coupled non-linear partial differential equations, now famous as Einstein's Field Equations (EFEs). In tensor notation they have a deceptively simple form[1]:

$$R_{\mu\nu} - \frac{1}{2}Rg_{\mu\nu} = C_E T_{\mu\nu}, \tag{1.1}$$

where C_E is a constant, $R_{\mu\nu}$ is the Ricci tensor, R is the Ricci scalar, $g_{\mu\nu}$ is the metric tensor, and $T_{\mu\nu}$ is the stress energy tensor. Meanwhile in Russia, Karl Schwarzschild, an established German astronomer was voluntarily serving in the military [13]. It took Schwarzchild a mere two months to write down the first ever exact solution of EFEs [55] by assuming $T_{\mu\nu} = 0$:

$$ds^2 = -f(r)dt^2 + \frac{1}{f(r)}dr^2 + r^2 d\Omega_2^2 \tag{1.2}$$

[1] Omitting the cosmological constant for now.

where $f(r) = 1 - \frac{2M}{r}$ and $d\Omega_2^2$ is the line element of a 2-sphere. This solution describes a black hole of mass M, one of the most astonishing predictions of GR. It is a region of spacetime which is surrounded by a closed surface called an event horizon. Once the event horizon is crossed it is impossible to fight the pull of gravity and escape. The gravitational pull is so strong that even light cannot escape.

Compelling observational evidence that strongly suggests that there are objects in the universe which are most effectively described by a black hole solution continues to accumulate. At the center of our own galaxy, the Milky Way, there is a bright radio source over a very compact region of space. This radio source is named Sagittarius A* (Sgr A*). It is believed that Sgr A* is a black hole, this is concluded by observing the orbits of stars near it. The shape of the orbits are consistent with an object which is $4.3 \times 10^6 M_\odot$ and confined to a region which has a diameter of about 0.004 light years [24]. This is still not conclusive of a black hole, but a black hole is top on the list of possible theoretical models explaining this observation. As matter is accreted by the black hole it forms a disk, called an accretion disk. At very small radial distances from the black hole the matter has a very large amount of angular momentum. This creates friction and heats up the disc which causes it to emit tremendous amounts of radiation in the X-ray band [44]. There are direct observations of this X-ray signal, with the first one coming from the Hubble telescope in 2011 [47]. In 2014 NASA's NuSTAR captured a remarkable event, the inner part of the accretion disk that emits X-rays was observed to move inwards towards the black hole [49]. More direct evidence as to existence of black holes is expected to come from the now active Event Horizon telescope, which aims to observe Sgr A* at an angular resolution which will allow effects close to the event horizon to be better observed [59].

Until the end of this year, when the Event Horizon telescope should deliver reliable results, the current gold medallist in the Olympics of black hole observations is the

recent detection of gravitational waves by LIGO from the merger of a binary black hole system [1]. The reason this discovery is so significant is because in addition to providing evidence for the existence of black holes it also confirms the existence of the long sought after gravitational waves. Just as electromagnetic waves are caused by small perturbations of the electromagnetic field, gravitational waves are small perturbations of spacetime itself. These perturbations cause test particles in spacetime to move in a specific pattern. If mirrors are attached to these test masses then an interferometer can detect these movements.

Gravitational waves were predicted as early as 1893 by Oliver Heaviside [31] and in 1905 by Henri Poincare [52]. In the context of EFEs, Einstein predicted gravitational waves in 1916 [15]. A particularly important scenario concerning gravitational waves comes from studying perturbations of the Schwarzschild geometry (1.2). This was first done by Regge and Wheeler in 1957 to test the stability of the solution [54]. The perturbations are considered to be small and this allows the EFEs to be linearized. Although this offers some simplification the equations are still quite complex. Regge and Wheeler exploited the spherical symmetry of the Schwarzschild black hole by expanding the perturbation to the metric in scalar, vector and tensor spherical harmonics. By doing this they were able to encode all the dynamics into a simple 1+1 dimensional wave equation, called the master equation. This equation will play a central role in this thesis and will be applied to the study of black hole mergers as well as in the fluid/gravity correspondence which we now introduce.

The two major advancements of 20^{th} century theoretical physics were General Relativity and Quantum Mechanics. In the later half of the 20^{th} century physicists had developed the Standard Model, which is the theory of the interactions of elementary particles. The Standard Model arose from applying the principles of Einstein's Special Theory of Relativity (SR) to quantum mechanics. The quest of physicists in the late

20^{th} century and the early 21^{st} century has been to find a quantum theory for gravity. The two main schools of thought for quantum gravity are string theory and loop quantum gravity. So far neither has entirely succeeded in its goal but both theories have tremendous mathematical richness.

In the past two decades string theory has been in the spotlight due to its celebrated AdS/CFT correspondence. Here AdS means anti-de Sitter and an AdS spacetime is a solution to EFEs but with a negative cosmological constant included. CFT means a conformal field theory, i.e., a field theory that is invariant under conformal transformations of the metric. The correspondence was developed by Juan Maldacena's seminal work in 1998 [41]. The attractive feature of AdS/CFT is that it connects a gravitational theory in the D-dimensional AdS spacetime, usually called the bulk, with a $D-1$ dimensional CFT without gravity. The CFT lives on the boundary of the D-dimensional AdS space. These correspondences are frequently called holographic since they bear similarity to a 2-dimensional hologram which encodes 3-dimensional data. An offshoot of AdS/CFT is the fluid/gravity correspondence, which is the long wavelength limit. Here rather than having a CFT on the boundary, the bulk is dual to the conservation equations for a fluid. The bulk is taken to be a black hole or a black brane whose perturbations correspond to perturbations of the fluid. We will discuss the fluid/gravity correspondence, and how it relates to gravitational perturbations, in detail below.

More generally, string theory utilizes radical ideas to explain Nature. One of these is the use of higher dimensional spacetimes than the usual four that we can perceive. This has been a fruitful endeavour in many ways. Statistical calculations of black hole entropy using string theory were first done using five dimensional black holes [57]. The AdS/CFT duality motivates research into higher dimensional bulk solutions to explain four dimensional non-gravitational dual systems. There is also a possibility that small

higher dimensional black holes may be produced in particle colliders [35]. Higher dimensional gravity is also studied just for its mathematical richness. Understanding higher dimensional solutions can provide insight into features that are peculiar to just four dimensions [19].

The research papers presented in this thesis will delve into all the topics touched upon above, such as black hole mergers, perturbations of black holes, fluid/gravity correspondence and higher dimensional solutions of EFEs. In Section 1.1 of this introduction we provide the relevant background for the papers, and then in Section 1.2 we present a brief overview of the research papers.

1.1 Background

1.1.1 Event and apparent horizons

A great deal of information about the structure of spacetime can be acquired by simply analysing the different types of curves living in the spacetime. In the following subsections we will demonstrate how studying curves in spacetime facilitates the identification of different regions in spacetime. This will allow us to construct precise definitions of the event and apparent horizon. This section closely follows [64].

Future and past directed curves

A curve $\gamma(t)$ is called a future directed timelike curve if at each $p \in \gamma$ the tangent vector t^μ is a future directed timelike vector. Further, γ is called a future directed causal curve if at each $p \in \gamma$, t^μ is either a future directed timelike or null vector. We can also construct identical definitions for past directed curves.

Chronological future and past

The chronological future, $I^+(p)$, of a point p in some Lorentzian manifold M, is defined to be the set of points that can be reached by a future directed timelike curve starting from p. Note that since we can perform small deformations around an endpoint q of a timelike curve while still preserving its timelike nature, the set $I^+(p)$ is an open set. Then it follows that for any subset $S \subset M$, we can define $I^+(S) = \cup_{p\in S} I^+(p)$. Again, identical definitions can be constructed for the past.

Causal future and past

The causal future of $p \in M$, denoted $J^+(p)$ is defined analogously to $I^+(p)$ except now we have future directed causal curves instead of future directed timelike curves, and similarly for a subset $S \subset M$ we have $J^+(S) = \cup_{p\in S} J^+(p)$. Analogous definitions hold for the causal pasts, $J^-(p)$ and $J^+(S)$.

Future and past domain of dependence

A subset $S \subset M$ is said to achronal if there exist no pairs of points $p, q \in S$ such that $q \in I^+(p)$. If S is a closed achronal set we can define the future domain of dependence of S, denoted $D^+(S)$, as the all points $p \in M$ such that every past inextendible causal curve through p intersects S. This means that all possible signals that can arrive at $p \in D^+(S)$, must have passed through S. Analogously we can define the past domain of dependence of S, $D^-(S)$ in the same way as $D^+(S)$ but with future replaced by past in the definition. Further the domain of dependence, $D(S)$, is naturally defined as, $D(S) = D(S)^- \cup D^+(S)$.

Cauchy surface

A closed achronal set Σ for which $D(\Sigma) = M$ is called a Cauchy surface, and a spacetime M that possesses a Cauchy surface Σ is said to globally hyperbolic. It is assumed that all physical realizable spacetimes are globally hyperbolic. It can be shown that for a globally hyperbolic spacetime $J^+(S)$ is a closed set.

Conformal transformations

We demonstrate how we can use a conformal transformation on a spacetime to 'bring infinity in'. Consider Minkowski space in spherical coordinates,

$$ds^2 = dt^2 + dr^2 + r^2(d\theta^2 + \sin^2\theta d\phi^2). \tag{1.3}$$

We may define double null coordinates, $v = t + r$ and $u = t - r$, followed by a further transformation $V = 1/v$, so the the region $v \to \infty$ is now at $V = 0$. The metric is then

$$ds^2 = \frac{1}{V^2} du dV + \frac{1}{4}\left(\frac{1}{V} - u\right)^2 (d\theta^2 + \sin^2\theta d\phi^2). \tag{1.4}$$

But now this metric is singular at $V = 0$. If we do a conformal transformation by multiplying the metric by V^2, we arrive at the unphysical but non-singular spacetime,

$$ds^2 = du dV + \frac{1}{4}(1 - uV)^2 (d\theta^2 + \sin^2\theta d\phi^2). \tag{1.5}$$

However we can do better. By choosing the conformal factor appropriately we can make finite all infinite asymptotic regions instead of just $v \to \infty$ finite in the sense of the above procedure. Defining the conformal transformation as $\tilde{g}_{\mu\nu} = \Omega^2 \eta_{\mu\nu}$ and choosing

$$\Omega^2 = 4(1 + v^2)^{-1}(1 + u^2)^{-1} \tag{1.6}$$

and introducing the following coordinate transform,

$$T = \tan^{-1} v + \tan^{-1} u \quad \text{and} \quad R = \tan^{-1} v - \tan^{-1} u \tag{1.7}$$

with $-\pi < T + R < \pi$, $-\pi < T - R < \pi$ and $0 \leq R$, metric becomes,

$$ds^2 = -dT^2 + dR^2 + \sin^2 R(d\theta^2 + \sin^2 \theta d\phi^2). \tag{1.8}$$

Interestingly, this is the same metric as the Einstein static universe, but with coordinates restricted by (1.7).

Past time like infinity	i^-	$R = 0$, $T = -\pi$
Past null infinity	$\mathscr{I}^-$	$T = -\pi + R$ for $0 < R < \pi$
Spatial infinity	i^0	$R = \pi$, $T = 0$
Future null infinity	$\mathscr{I}^+$	$T = \pi - R$ for $0 < R < \pi$
Future timelike infinity	i^+	$R = 0$, $T = \pi$

Table 1.1: Various regions of the asymptotic boundary.

On asymptotically flat spacetimes[2] a similar conformal transformation can be performed to a new 'unphysical' spacetime with properties similar to those of Minkowski. However we make two modifications. First since we do not want the spacetime to be flat at some fixed point in the interior at very late and early times, we do not impose flatness at i^+ and i^-. Secondly, we will relax[3] the conditions of smoothness and differentiability of the conformally transformed metric, $\tilde{g}_{\mu\nu}$ at spatial infinity i^0.

Event and apparent horizons

Now that we have reviewed the appropriate definitions we can give a precise definition of event and apparent horizons. Intuitively we may define the black hole as a region

[2]See [30] for a precise definition of asymptotically flat spacetimes.
[3]Please see [64] for more details.

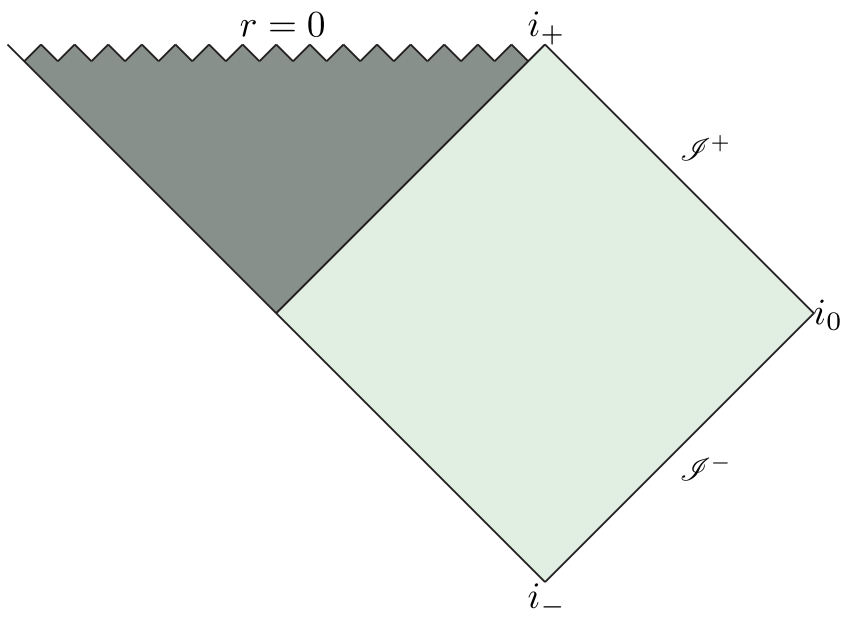

Figure 1.1: The conformal spacetime diagram for the Schwarzschild black hole.

B such that timelike and null geodesics originating from B cannot escape to i^+ and $\mathscr{I}^+$ respectively. More concretely we may define it in the following manner. Let $(M, g_{\mu\nu})$ be an asymptotically flat spacetime which we associate with an unphysical spacetime, $(\tilde{M}, \tilde{g}_{\mu\nu})$ with a conformal transformation, Ω. Then if in the unphysical spacetime there is an open region $\tilde{V} \subset \tilde{M}$ with $\overline{M \cap J^-(\mathscr{I}^+)} \subset \tilde{V}$ such that $(\tilde{V}, \tilde{g}_{\mu\nu})$ is globally hyperbolic then $(M, g_{\mu\nu})$ is called strongly asymptotically predictable. Such a spacetime is said to contain a black hole if M is not contained in $J^-(\mathscr{I}^+)$. The black hole region, B is then defined to be $B = [M - J^-(\mathscr{I}^+)]$ and the boundary of B, denoted H, is such that $H = \partial J^-(\mathscr{I}^+) \cap M$. H is called the event horizon.

Next we define the apparent horizon. Let Σ be an asymptotically flat Cauchy surface for $\tilde{V}$, so it passes through i^0 and is spacelike. Then let $C \subset \Sigma \cap M$ be a closed subset of Σ which is a 3-dimensional manifold with a boundary and further assume that the two-dimensional boundary $S = \partial C$ is such that the expansion, θ, of the outgoing family of null geodesics orthogonal to S satisfies $\theta \leq 0$. Such a surface S is called an outer marginally trapped surface, and C is called a trapped region.

Consider then $\mathscr{T}$, defined to be the closure of the union of all trapped regions, C, on Σ. The boundary $\mathscr{A} = \partial\mathscr{T}$ is called the apparent horizon. This makes $\mathscr{A}$ an outer marginally trapped surface with orthogonal outgoing null geodesics having expansion, $\theta = 0$. Further, if the weak or strong energy condition holds, then $R_{\mu\nu}k^\mu k^\nu \geq 0$ where k^μ is any null vector, and it can be shown that the apparent horizon always lies inside or coincides with the event horizon [51].

When the spacetime is stationary the apparent horizon coincides with the event horizon. This is not true for dynamical spacetimes for which the apparent horizon is found to be inside the event horizon [7]. This can be demonstrated by finding the spherically symmetric apparent horizon in a simple yet dynamical spacetime such as Vaidya [62]:

$$ds^2 = -f dv^2 + 2dvdr + r^2 d\Omega_2^2 \quad \text{with} \quad f = 1 - \frac{2M(v)}{r}. \tag{1.9}$$

This metric satisfies EFEs with stress tensor,

$$T_{\mu\nu} = \frac{dM/dv}{4\pi r^2} l_\mu l_\nu \tag{1.10}$$

where $l_\mu = \partial_\mu v$ is tangent to ingoing null geodesics. We may then consider the scenario where $M(v)$ models a black hole of mass M_1 irradiated with null dust for a finite time such that the mass is increased to M_2 [53],

$$M(v) = \begin{cases} M_1 & v \leq v_1 \\ M_{12}(v) & v_1 < v < v_2 \\ M_2 & v \geq v_2 \end{cases} \tag{1.11}$$

In Figure 1.2 we can see an illustration of what the apparent horizon and event

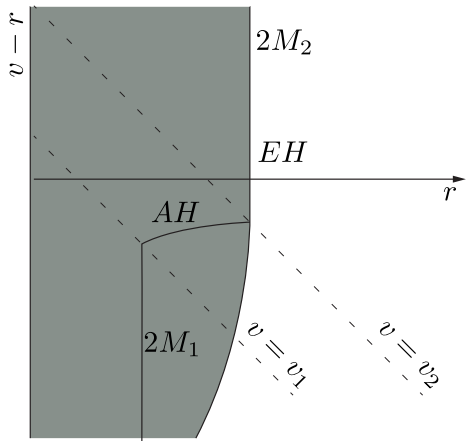

Figure 1.2: Difference in apparent horizon (AH) and event horizon (EH) for Vaidya spacetime.

horizon of the Vaidya spacetime look like. As the figure suggests, and can be verified [53], the apparent horizon is a spacelike surface in the interval $v_1 \leq v \leq v_2$ and null otherwise, unlike the event horizon which is null throughout. But more intriguing than that is the teleological nature of the event horizon. This is demonstrated by how the event starts to grow at $v \ll v_2$. This is in contrast to the apparent horizon which is more local in nature and changes only in the interval where it encounters the null dust. Finally notice that after v_2 the apparent horizon and event horizon coincide.

1.1.2 Static and stationary axially symmetric spacetimes

This section starts with a brief review of Weyl static axially symmetric spacetimes in four dimensions and then generalizes to stationary axially symmetric spacetimes in D dimensions.

Static axially symmetric spacetimes

In this section we review Weyl solutions of the EFEs, these are solutions that have commuting Killing vector fields ∂_t and ∂_ϕ. A canonical form of the metric of such a spacetime is [26],

$$ds^2 = -\mathrm{e}^{2U}dt^2 + \mathrm{e}^{-2U}\left[\mathrm{e}^{2\gamma}(d\eta^2 + d\xi^2) + \rho^2 d\phi^2\right] \tag{1.12}$$

where U, γ and ρ depend only on the coordinates η and ξ, and $\rho \in [0, \infty)$, $z \in (-\infty, \infty)$ and $\phi \in [0, 2\pi)$. When this metric is inserted into the EFEs equations with a vanishing cosmological constant, one of the equations implies that ρ is a harmonic function,

$$\left(\partial_\eta^2 + \partial_\xi^2\right)\rho = 0. \tag{1.13}$$

Due to this feature it is more convenient to use coordinates $\rho(\eta, \xi)$ and $z(\eta, \xi)$, such that $\rho + iz$ is analytic. Then the metric is

$$ds^2 = -\mathrm{e}^{2U}dt^2 + \mathrm{e}^{-2U}\left[\mathrm{e}^{2\gamma}(d\rho^2 + dz^2) + \rho^2 d\phi^2\right] \tag{1.14}$$

and now U and γ are functions of ρ and z. For U the EFEs give,

$$\partial_\rho^2 U + \frac{1}{\rho}\partial_\rho U + \partial_z^2 U = 0. \tag{1.15}$$

Notice that this is the Laplacian for the unphysical metric $ds^2 = d\rho^2 + \rho^2 d\theta^2 + dz^2$, with U not having a dependence on θ. For γ we get the following equations,

$$\partial_\rho \gamma = \rho\left[(\partial_\rho U)^2 + (\partial_z U)^2\right] \quad \text{and} \quad \partial_z \gamma = 2\rho\partial_\rho U \partial_z U. \tag{1.16}$$

If we take $U = 0$ and $\gamma = 0$ we recover the Minkowski spacetime. But consider the solution $U = \log \rho$ and $\gamma = \log \rho$. This leads to the metric

$$ds^2 = -\rho^2 dt^2 + d\rho^2 + dz^2 + \rho^2 d\phi^2. \tag{1.17}$$

Notice that this is Minkowski in Rindler coordinates with acceleration in the ρ direction. Further we see that the function U can be interpreted as the Newtonian potential of an infinitely long rod along the z-axis with mass density $1/2$. There is just one other solution for Minkowski space [26],

$$U = \frac{1}{2}\log\left(\sqrt{\rho^2 + z^2} + z\right) \qquad \gamma = \frac{1}{2}\log\left(\frac{\sqrt{\rho^2 + z^2} + z}{2\sqrt{\rho^2 + z^2}}\right). \tag{1.18}$$

Now the function U has the Newtonian interpretation as the potential of a semi-infinite rod located on the negative z-axis with mass density $1/2$. Doing a transformation $\rho = \tilde{z}\tilde{\rho}$, $z = \frac{1}{2}(\tilde{z}^2 - \tilde{\rho}^2)$ then leads to the following metric,

$$ds^2 = -\tilde{z}^2 dt^2 + d\tilde{z}^2 + d\tilde{\rho}^2 + \tilde{\rho}^2 d\phi^2. \tag{1.19}$$

This is also a Rindler spacetime but now the acceleration direction is $\tilde{z}$. Let us now consider the Schwarzschild solution. If we apply the transformation $r = m(x+1)$ and $\cos(\theta) = y$, the metric becomes [26],

$$ds^2 = -\frac{x-1}{x+1}dt^2 + m^2\frac{x+1}{x-1}dx^2 + m^2\frac{(x+1)^2}{1-y^2}dy^2 + m^2(x+1)^2(1-y^2)d\phi^2 \tag{1.20}$$

where $|y| < 1$ and m is the mass. The region $r > 2m$ now corresponds to $x > 1$, in this region it is possible to make the further transformation $\rho = m\sqrt{(x^2-1)(1-y^2)}$ and $z = mxy$. This allows us to write the Schwarzschild metric in the form of (1.14)

Figure 1.3: Finite rod for Schwarzschild spacetime.

with,

$$e^{2U} = \frac{R_+ + R_- - 2m}{R_+ + R_- + 2m} \qquad e^{2\gamma} = \frac{(R_+ + R_-)^2 - 4m^2}{4R_+R_-} \tag{1.21}$$

where $R_\pm^2 = \rho^2 + (z \pm m)^2$. This naturally leads to,

$$U = \frac{1}{2}\log\left(\frac{R_- + z - m}{R_+ + z + m}\right). \tag{1.22}$$

This is the Newtonian potential for a finite rod located along $|z| < m$, again with a mass density of $1/2$.

Stationary axially symmetric spacetimes

So far we have discussed the approach for obtaining axisymmetric solutions for static spacetimes in four dimensions, now we shall discuss how this is generalized to D dimensional stationary solutions. We follow the treatment of [28]. Consider a D dimensional spacetime with $D-2$ linearly independent Killing vector fields $V_{(i)}$, $i = 1, \ldots, D-2$. Further, assume these vector fields commute,

$$\left[V_{(i)}, V_{(j)}\right] = 0 \tag{1.23}$$

Since the vector fields commute we set up a coordinate system adapted to the fields, i.e., we can find coordinates x^i and y^a such that,

$$V_{(i)} = \frac{\partial}{\partial x^i}. \tag{1.24}$$

This implies that the metric will only depend on the coordinates y^1 and y^2. It is shown in [28] that for any point there exists a two-dimensional surface which includes the point and further that all tangent vectors on this hypersurface are orthogonal to the $V_{(i)}$. Hence we can write the metric as,

$$ds^2 = G_{ij}dx^i dx^j + \hat{g}_{ab}dy^a dy^b \tag{1.25}$$

where G_{ij} and $\hat{g}_{ab}$ are functions of y^1 and y^2 only. Now we define a new coordinate,

$$r = \sqrt{\det(G_{ij})} \tag{1.26}$$

where r is not a constant, then we can find a coordinate z, and two functions $\nu(y^1, y^2)$ and $\Lambda(y^1, y^2)$, so that the metric now takes the form,

$$ds^2 = G_{ij}dx^i dx^j + \mathrm{e}^{2\nu}(dr^2 + \Lambda dz^2) \tag{1.27}$$

where now G, ν and Λ are functions of r and z. For a given solution of the EFEs we can divide the z-axis into rods based on how G behaves as $r \to \infty$ (we will drop the ij when there is no confusion). If we take G to be a matrix then since $|\det G| = r^2$ we see that the product of eigenvalues of G goes to zero as $r \to 0$ and clearly $\dim(\ker(G(0, z))) \geq 1$. We will restrict ourselves to cases where $\dim(\ker(G(0, z))) = 1$, except at isolated values of z. This is because if we have more than one eigenvalue going to zero it implies that we have a curvature singularity at that point [28]. If we denote the isolated values of z as $a_1, a_2, \ldots, a_N$ with $a_1 < a_2 < \ldots < a_N$ then the z-axis can be divided into $N + 1$ intervals, $[-\infty, a_1], [a_1, a_2], \ldots, [a_{N-1}, a_N]$ and $[a_N, \infty]$. These $N + 1$ intervals are called the rods of the solution. We may also associate a vector to each rod. Consider then the $N + 1$ vectors $v_{(k)}$ in $\mathbb{R}^{D-2}$ for $k = 1, \ldots, N + 1$, which

are defined by,

$$G(0,z)v_{(k)} = 0 \quad \text{for} \quad z \in [a_{k-1}, a_k] \tag{1.28}$$

with $v_{(k)} \neq 0$. Notice that this simply means that $v_{(k)} \in \ker(G(0,z))$. These vectors are called the direction of the corresponding rod and the specification of all the rods and their directions is called the rod structure [28]. Notice that the vectors $v_{(k)}$ are only defined up to a scalar multiplication, hence they could be made arbitrarily long. This implies they are members of the projective space, $v_{(k)} \in \mathbb{R}P^{D-3}$. Now let v be a rod in specific interval $[a_m, a_{m+1}]$, then we can write v as,

$$v = v^i \frac{\partial}{\partial x^i} \tag{1.29}$$

and from (1.28) we know that $G_{ij}(0,z)v^j = 0$. Further if $G_{ij}v^iv^j/r^2 < 0$ the rod is timelike, and if $G_{ij}v^iv^j/r^2 > 0$ the rod is spacelike. Consider then the case where v is a spacelike rod, and let us introduce a new set of coordinates η^i such that,

$$\frac{\partial}{\partial \eta^1} = v = v^i \frac{\partial}{\partial x^i}. \tag{1.30}$$

Then to avoid a conical singularity η^1 must be a compact direction with period,

$$\Delta\eta^1 = 2\pi \lim_{r\to\infty} \sqrt{\frac{r^2 \mathrm{e}^{2\nu}}{G_{ij}v^iv^j}}. \tag{1.31}$$

If η_1 is a timelike direction we can perform a Wick rotation, $\tilde{\eta}_1 \to i\eta_1$, and find an associated temperature. A finite timelike rod corresponds to a horizon and a semi-infinite timelike rod corresponds to an acceleration horizon, as in (1.18). Semi-infinite spacelike rods correspond to an axis of symmetry and finite spacelike rods correspond to "bolts" or "bubbles". We will see in a later chapter spacetimes which consist of

such bolts with topology S^2.

We now consider the rod structure of the Kerr solution [28]. In Boyer-Lindquist coordinates the metric is given by,

$$ds^2 = -\frac{\Delta - a^2\sin^2\theta}{\Sigma}dt^2 - 2a\sin^2\theta\frac{\rho^2+a^2-\Delta}{\Sigma}dtd\phi \tag{1.32}$$

$$+\frac{(\rho^2+a^2)^2 - \Delta a^2\sin^2\theta}{\Sigma}\sin^2\theta d\phi^2 + \frac{\Sigma}{\Delta}d\rho^2 + \Sigma d\theta^2 \tag{1.33}$$

with

$$\Delta = \rho^2 - 2M\rho - a^2 \quad \text{and} \quad \Sigma = \rho^2 + a^2\cos^2\theta. \tag{1.34}$$

It is clear that the two Killing fields are $\partial_t = (1,0)$ and $\partial_\phi = (0,1)$, and it can be shown that $\det G = -\Delta\sin^2\theta$, which implies that $r = \sqrt{\Delta}\sin\theta$. Then, if we take $z = (\rho - M)\cos\theta$, we can bring the metric into the canonical form (1.27). But it will be more convenient to introduce prolate spherical coordinates (x, y), similar to the Schwarzschild case (1.20), with the role of ρ (defined below (1.20)) now played by the canonical coordinate r,

$$r = \alpha\sqrt{(x^2-1)(1-y^2)} \quad \text{and} \quad z = \alpha xy \tag{1.35}$$

where $\alpha = \sqrt{M^2 - a^2}$, $x \geq 1$ and $-1 \leq y \leq 1$. Then in terms of the Boyer-Lindquist coordinates,

$$x = \frac{\rho - M}{\sqrt{M^2 - a^2}} \quad y = \cos\theta. \tag{1.36}$$

Then in these coordinates it can be shown that [28],

$$G_{11} = -\frac{x^2\cos^2\lambda + y^2\sin^2\lambda - 1}{(1 + x\cos\lambda)^2 + y^2\sin^2\lambda} \quad G_{12} = -2a\frac{(1-y^2)(1+x\cos\lambda)}{(1+x\cos\lambda)^2 + y^2\sin^2\lambda} \tag{1.37}$$

$$e^{2\nu} = \frac{(1+x\cos\lambda)^2 + y^2\sin^2\lambda}{(x^2-y^2)\cos^2\lambda} \quad \text{with} \quad \sin\lambda = \frac{a}{M}\ . \tag{1.38}$$

The G_{22} component can be found from the det $G = r$ condition.

$$G_{22} = \frac{G_{12}^2 - \alpha^2(x^2-1)(1-y^2)}{G_{11}} \ . \tag{1.39}$$

To arrive at the rod structure we need to set $r = 0$. From (1.35) we see that we can set $y = \pm 1$, then for $y = -1$, $x = -z/\alpha$ and since $x \geq 1$ we get the rod $[-\infty, -\alpha]$. Similarly for $y = 1$, $x = z/\alpha$, we the the rod $[\alpha, \infty]$. We can see from (1.37) and (1.39) that $G_{12} = G_{22} = 0$ for $y = \pm 1$. This means that both the rods are spacelike and point in the direction of $\partial_\phi = (0, 1)$. We may also get $r = 0$ by setting $z = 1$ which implies that $y = z/\alpha$, then since $-1 \leq y \leq 1$ we get the rod $[-\alpha, \alpha]$. It can be shown that the direction v of this rod is given by [28],

$$v = (1, \Omega) \quad \Omega = \frac{\sin\lambda}{2M(1+\cos\lambda)}. \tag{1.40}$$

Figure 1.4: Rod diagram for the Kerr spacetime, the finite rod in the center corresponds to the event horizon and the two semi-infinite rods correspond to the axis of symmetry.

Further we find that $G_{ij}v^iv^j/r^2 < 0$ for $r \to 0$, which means that the rod is timelike and corresponds to an event horizon. Notice that Ω is the angular velocity of the black hole. Also note that we get the rod for the Schwarzschild solution if we set $a = 0$, then $\alpha = M$.

1.1.3 Energy in General Relativty

Defining the energy of a closed volume of space is not a straightforward matter in general relativity, see [58] for a review. Here we briefly describe how one kind of

energy, the Brown-York energy, is derived from the action of EFEs using Hamilton-Jacobi methods. This will find applications in the fluid/gravity duality in Section 1.1.8.

Classical mechanics

Consider the action of a free non-relativistic particle, $S[\dot{q}(t)] = \int_{t_1}^{t_2} \frac{1}{2} m\dot{q}^2 dt$. The Euler-Lagrange equation has the solution, $q(t) = q_1 + \frac{q_2 - q_1}{t_2 - t_1}(t - t_1)$. Inserting this solution into the action we have,

$$S(q_2, t_2, q_1, t_1) = \frac{1}{2} m \frac{(q_2 - q_1)^2}{t_2 - t_1}. \tag{1.41}$$

Then notice that we have,

$$\frac{\partial S}{\partial q_2} = p \quad \text{and} \quad \frac{\partial S}{\partial t_2} = -E. \tag{1.42}$$

These relationships are a manifestation of the Hamilton-Jacobi equation. Usually when one varies a Lagrangian, the variations of position at t_1 and t_2 are taken to be zero, and there is no variation of time. But if one does not impose this condition then the variation yields [58],

$$\delta S_1[q(t)] = \int_{t_1}^{t_2} \left(\frac{\partial L}{\partial q} - \frac{d}{dt}\frac{\partial L}{\partial \dot{q}} \right) (\delta q - \dot{q}\delta t)\, dt + \frac{\partial L}{\partial \dot{q}} \delta q \Big|_{t_1}^{t_2} - \left(\frac{\partial L}{\partial \dot{q}} \dot{q} - L \right) \delta t \Big|_{t_1}^{t_2}. \tag{1.43}$$

The terms under the integral vanish because $q(t)$ solves the Euler-Lagrange equations, and if we take the variations to vanish at t_1 we recover (1.42). Notice though that we can always take a new action $S[q(t)] = S_1[q(t)] - S_0[q(t)]$ where,

$$S_0[q(t)] = \int_{t_1}^{t_2} (dh/dt) dt \tag{1.44}$$

where $h = h(q(t), t)$ and it will not effect the equations of motion (since it only contributes at the boundaries), but it does change the momentum, $p \to p - \partial h/\partial q$, and the energy, $E \to E + \partial h/\partial t$.

Einstein-Hilbert action

Let's do a lightning review of the action for EFEs. We start with the Einstein-Hilbert action [53],

$$S_H[g] = \frac{1}{16\pi} \int_V R\sqrt{-g} d^4x. \tag{1.45}$$

Variation of this action with respect to the metric with vanishing boundary conditions results in [53],

$$(16\pi)\delta S_H = \int_V G_{\mu\nu}\delta g^{\mu\nu}\sqrt{-g}d^4x - \int_{\partial V} \epsilon h^{\mu\nu} n^\sigma \partial_\sigma \delta g_{\mu\nu} \sqrt{|h|} d^3y \tag{1.46}$$

where $G_{\mu\nu} = R_{\mu\nu} - \frac{1}{2}Rg_{\mu\nu}$, $h_{\mu\nu}$ is the induced metric on the (nowhere null) boundary ∂V, n^σ is the normal to ∂V, and $\epsilon = +1$ when ∂V is timelike and $\epsilon = -1$ when ∂V is spacelike. If we impose the condition that the derivative of the variation of the metric must also vanish on ∂V then we simply get $G_{\mu\nu} = 0$, which are the vacuum EFEs. If we don't impose this condition we can take another route. Consider the trace of the extrinsic curvature $K = \nabla_\mu n^\mu$ of ∂V. Its variation leads to [53],

$$\delta K = \frac{1}{2} h^{\mu\nu} n^\sigma \partial_\sigma \delta g_{\mu\nu} \tag{1.47}$$

which is half of the integrand of the second term appearing in (1.46). So, if we define our initial action to be,

$$S[g] = \frac{1}{16\pi} \int_V R\sqrt{-g}d^4x + \frac{1}{8\pi} \int_{\partial V} \epsilon K \sqrt{|h|} d^3y, \tag{1.48}$$

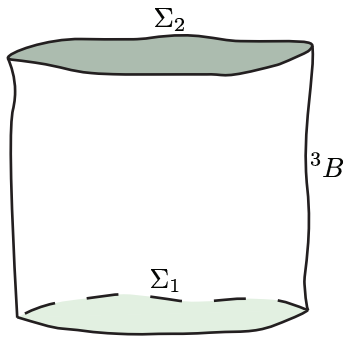

Figure 1.5: An illustration of the boundary, ∂V, split into two spacelike surfaces Σ_1 and Σ_2, and a timelike surface ^3B.

and vary it, we get rid of the boundary term appearing in (1.46). This is usually called the "trace K action" in the literature.

Brown-York energy

We want to apply the Hamilton Jacobi method outlined above for classical mechanics to the action for EFEs and define a quasi-local energy in a similar way. This was first done by Brown and York [8]. They split the boundary, ∂V, into two spacelike surfaces Σ_1 and Σ_2, which belong to a family of spacelike surfaces Σ_t which foliate the space time, and a time like surface ^3B as shown in Figure 1.5. Then the action can be written as,

$$S[g] = \frac{1}{16\pi}\int_V R\sqrt{-g}d^4x + \frac{1}{8\pi}\int_{t_1}^{t_2}\chi\sqrt{|h|}d^3y - \frac{1}{8\pi}\int_{^3B}\Theta\sqrt{-\gamma}d^3z \tag{1.49}$$

where χ is the extrinsic curvature of the surfaces Σ_t with metric $h_{\mu\nu}$ and Θ is the extrinsic curvature on ^3B with metric $\gamma_{\mu\nu}$. If one varies this action without vanishing

boundary conditions one arrives at,

$$\begin{aligned}\delta S =&(\text{terms giving EFEs})\\ &+\frac{1}{16\pi}\int_{\Sigma_2}\left(\chi^{\mu\nu}-\chi h^{\mu\nu}\right)\delta h_{\mu\nu}\sqrt{|h|}d^3y\\ &-\frac{1}{16\pi}\int_{\Sigma_1}\left(\chi^{\mu\nu}-\chi h^{\mu\nu}\right)\delta h_{\mu\nu}\sqrt{|h|}d^3y\\ &-\frac{1}{16\pi}\int_{{}^3B}\left(\Theta^{\mu\nu}-\Theta\gamma^{\mu\nu}\right)\delta\gamma_{\mu\nu}\sqrt{-\gamma}d^3z. \end{aligned}\tag{1.50}$$

Here, the second and third line are analogous to the conjugate momentum terms, $\partial L/\partial\dot{q}\delta q|_{t_1}^{t_2}$ in (1.43). Also, this is precisely the conjugate momentum of the ADM formalism [3]. The last term then, is the analogue of the energy in (1.43). Notice though that it is not a scalar energy as in the classical mechanics case. The 3-metric, $\gamma_{\mu\nu}$ on ${}^3B$, contains information about the proper time elapsed (the lapse function) between the slices, which is roughly related to the energy, but, $\gamma_{\mu\nu}$ also contains spatial distance information on ${}^3B$ [8]. Hence, rather than a scalar quantity we get a surface energy-momentum tensor $\Theta^{\mu\nu}-\Theta\gamma^{\mu\nu}$. Again, as in the classical mechanics case, this surface energy-momentum tensor is not unique, since we can always take a new action $S^1=S-S^0$, where S^0 is assumed to an arbitrary function of the three-metric on the boundary $\partial V=\Sigma_2\ \cup\ {}^3B\ \cup\ \Sigma_1$. Then the surface stress tensor is given by [58],

$$T^{\mu\nu}=\frac{1}{8\pi}\left(\Theta^{\mu\nu}-\Theta\gamma^{\mu\nu}\right)+\frac{2}{\sqrt{|\gamma|}}\frac{\delta S^0}{\delta\gamma_{\mu\nu}}.\tag{1.51}$$

1.1.4 Black hole mechanics

Above we demonstrated how one can define the Brown-York energy by considering the Einstein-Hilbert action. In the following sections we show how for asymptotically flat spacetimes we have a canonical method to derive the energy and momentum of the

spacetime. We then use these definitions to show the first law of black hole mechanics.

The non-dynamical boundary term

In (1.49) we had introduced the "trace-K action" for EFEs,

$$S[g] = \frac{1}{16\pi}\int_V R\sqrt{-g}d^4x + \frac{1}{8\pi}\int_{\partial V}\epsilon K\sqrt{|h|}d^3y \tag{1.52}$$

There is an inherent pathology in this action which can be made prominent when one considers a flat spacetime, $R = 0$. Then the action is simply,

$$S[g] = \frac{1}{8\pi}\int_{\partial V}\epsilon K\sqrt{|h|}d^3y \tag{1.53}$$

Now lets take the boundary ∂V such that it consists of two hypersurfaces $t = t_1$ and t_2, and a three-cylinder. Clearly $K = 0$ on the t_1 and t_2 hypersufaces. On the 3-cylinder the metric is given by, $ds^2 = -dt^2 + \rho^2 d\Omega^2$ which immediately implies that $|h|^{1/2} = \rho^2 \sin\theta$. The unit normal is $n_\mu = \partial_\mu r$ then, $\epsilon = 1$ and $K = \nabla_\mu n^\mu = 2/\rho$. This gives [53],

$$\int_{\partial V}\epsilon K|h|^{1/2}d^3y = 8\pi\rho(t_2 - t_1) \tag{1.54}$$

which diverges as $\rho \to \infty$. This problem does not go away when one considers curved spacetimes and thus implies that the action is not well defined for asymptotically flat spacetimes. To remedy this, we subtract from the action the following term,

$$S_0 = \frac{1}{8\pi}\int_{\partial V}\epsilon K_0|h|^{1/2}d^3y, \tag{1.55}$$

where K_0 is the extrinsic curvature of ∂V when it is isometrically embedded in flat spacetime [53].

Hamiltonian formulation of general relativity

Now we briefly describe how one may arrive at the Hamiltonian formulation of EFEs. The starting point is to foliate the spacetime with the constant-t surfaces, Σ_t, of a scalar time function $t(x^\nu)$. Let the vector t^μ be such that $t^\mu \partial_\mu t = 1$. Further if n^μ is the normal to Σ_t then the vector t^μ can be written as,

$$t^\mu = N n^\mu + N^\mu \tag{1.56}$$

where N is a scalar function called the lapse and the N^μ is a vector tangent to the slice Σ_t and is called the shift vector. These are thus named because the lapse function measures how much proper time has elapsed from one slice to next and the shift vector measures how the coordinate grid translates spatially from one slice to next.

In this foliation the action becomes [53],

$$\begin{aligned} S[g] =& \frac{1}{16\pi} \int_{t_1}^{t_2} dt \Bigg[\int_{\Sigma_t} \left({}^3R + K^{\mu\nu} K_{\mu\nu} - K^2 \right) N \sqrt{h} d^3y \\ &+ 2 \int_{S_t} (k - k_0)\, N \sqrt{\sigma} d^2\theta \Bigg] \end{aligned} \tag{1.57}$$

where, ${}^3R$ is the Ricci scalar for the slice Σ_t, k is the extrinsic curvature of the two dimensional surface S_t, and k_0 is the extrinsic curvature of S_t isometrically embedded in flat space. The metric on the hypersurface Σ_t is denoted by $h_{\mu\nu}$ and let $\dot{h}_{\mu\nu} = \mathcal{L}_t h_{\mu\nu}$, be its Lie derivative with respect to the vector t^μ. Then one can show that [53],

$$K_{\mu\nu} = \frac{1}{2N} \left(\dot{h}_{\mu\nu} - D_\mu N_\nu - D_\nu N_\mu \right) \tag{1.58}$$

where D_μ is the covariant derivative compatible with the metric $h_{\mu\nu}$. Then the momentum conjugate to $h_{\mu\nu}$ is given by,

$$p^{\mu\nu} = \frac{\partial}{\partial \dot{h}_{\mu\nu}} \left(\sqrt{-g}L\right) \tag{1.59}$$

where L is the 'volume part' of the action since the boundary term does not depend on $\dot{h}_{\mu\nu}$. Further in light of (1.58), we may write,

$$p^{\mu\nu} = \frac{\partial K_{\sigma\gamma}}{\partial \dot{h}_{\mu\nu}} \frac{\partial}{\partial K_{\sigma\gamma}} \left(\sqrt{-g}L\right) \tag{1.60}$$

which gives us [53],

$$(16\pi)p^{\mu\nu} = \sqrt{h}\left(K^{\mu\nu} - Kh^{\mu\nu}\right). \tag{1.61}$$

Then we can compute the Hamiltonian density from, $H = p^{\mu\nu}\dot{h}_{\mu\nu} - \sqrt{-g}L$, after integrating over Σ_t and adding the boundary terms we arrive at,

$$(16\pi)H_G = \int_{\Sigma_t} \left[N(K^{\mu\nu}K_{\mu\nu} - K^2 - {}^3R) - 2N_\mu D_\nu (K^{\mu\nu} - Kh^{\mu\nu})\right] \sqrt{h} d^3y \tag{1.62}$$

$$- 2\int_{S_t} \left[N(k - k_0) - N_\mu (K^{\mu\nu} - Kh^{\mu\nu}) r_\nu\right] \sqrt{\sigma} d^2\theta \tag{1.63}$$

where r_ν is the spacelike normal to S_t. Variation of this Hamiltonian with respect to $h_{\mu\nu}$ and $p_{\mu\nu}$ give us Hamilton's equations which are equivalent to Einstein's evolution equations, and variation with respect to the lapse N and the shift N^μ give us the Hamiltonian and momentum constraints [53].

ADM mass and angular momentum

Let us examine the 'on-shell' Hamiltonian, i.e, evaluated on a solution to the EFEs, we have,

$$H_G^{\text{solution}} = -\frac{1}{8\pi}\int_{S_t}\left[N(k-k_0) - N_\mu r_\nu(K^{\mu\nu} - Kh^{\mu\nu})\right]\sqrt{\sigma}d^2\theta \tag{1.64}$$

where the part under the integral over Σ_t vanishes on a solution. This equation is remarkably illuminating. We know from classical physics that the Hamiltonian of a theory is related to the energy content. Yet thus far we have not made this connection. If the spacetime is asymptotically flat then we can relate H_G^{solution} to the energy and momentum of the spacetime. To do so let us demand that at spatial infinity the hypersurface Σ_t must coincide with a surface of constant time in the asymptotic Minkowski space. Let $(\bar{t}, \bar{x}, \bar{y}, \bar{z})$ be coordinates of the asymptotically Minkowski spacetime, y^a be the coordinates on Σ_t and x^μ the coordinates of the whole spacetime. Now as we approach asymptotic infinity we have the relations $y^a \to y^a(\bar{x}, \bar{y}, \bar{z})$ and $x^\mu \to x^\mu(\bar{t}, \bar{x}, \bar{y}, \bar{z})$. We know that $\bar{t}$ is the proper time of an observer at rest in the Minkowski region, thus the four velocity of the observer is given by, $u^\mu = \partial x^\mu/\partial\bar{t}$. This vector is normalized and orthogonal to the $\bar{t}$ = constant surfaces, it coincides with the normal n^μ for Σ_t in the asymptotic region, thus we have that $n^\mu \to \partial x^\mu/\partial\bar{t}$. Then from (1.56) we have [53],

$$t^\mu \to N\left(\frac{\partial x^\mu}{\partial\bar{t}}\right) + N^\mu\left(\frac{\partial x^\mu}{\partial y^a}\right). \tag{1.65}$$

We then define the mass of an asymptomatically flat spacetime as the limit of H_G^{solution} as the two dimensional surface S_t extends out to spatial infinity, with lapse chosen as

$N = 1$ and the shift as $N^\mu = 0$,

$$M = -\frac{1}{8\pi} \lim_{S_t \to \infty} \int_{S_t} (k - k_0) \sqrt{\sigma} d^2\theta. \tag{1.66}$$

For a Schwarzschild spacetime this formula produces the correct mass, M, which appears in the metric. What we have done is connect the 'time flow' vector t^μ with $\partial x^\mu / \partial \bar{t}$ which generates time translations in the Minkowski region. Hence we have made the familiar connection of time translations with energy. We can use an analogous line of reasoning to define the angular momentum of the spacetime. The generator of rotations in the asymptotic region is given by, $\partial x^\mu / \partial \phi$, hence we need $t^\mu \to \phi^\mu = \partial x^\mu / \partial \phi$, this can be accomplished by the choice $N = 0$ and $N^\mu = \phi^\mu$. Hence, the angular momentum of an asymptotically flat spacetime is given by,

$$J = -\frac{1}{8\pi} \lim_{S_t \to \infty} \int_{S_t} (K_{\mu\nu} - K h_{\mu\nu}) \phi^\mu r^\nu \sqrt{\sigma} d^2\theta. \tag{1.67}$$

Notice the extra minus is inserted to account for the right-hand rule for angular momentum. These expressions are called the ADM mass and angular momentum [3]. An attractive feature of these expressions is that they do not rely on a coordinate system.

Komar formulae

There are other equivalent expressions that can define the mass and angular momentum of a spacetime in a similar coordinate independent way. An example are the Komar formulae for mass and angular momentum [36]. They rely on the Killing fields of the spacetime and are given by [53],

$$M = -\frac{1}{8\pi} \lim_{S_t \to \infty} \int_{S_t} \nabla^\mu \xi^\nu_{(t)} dS_{\mu\nu} \tag{1.68}$$

$$J = \frac{1}{16\pi} \lim_{S_t \to \infty} \int_{S_t} \nabla^\mu \xi^\nu_{(\phi)} dS_{\mu\nu} \tag{1.69}$$

where $\xi^\nu_{(t)}$ is the timelike Killing field responsible for time translations and $\xi^\nu_{(\phi)}$ is the spacelike Killing field responsible for rotations. Further the two-dimensional volume form is given by,

$$dS_{\mu\nu} = -2n_{[\mu} r_{\nu]} \sqrt{\sigma} d^2\theta \tag{1.70}$$

where n_μ and r_ν are the timelike and spacelike normals to S_t respectively. It can be shown that Killing fields satisfy $\Box \xi^\mu = -R^\mu{}_\nu \xi^\nu$, then by invoking Stokes' theorem we have,

$$\int_S \nabla^\mu \xi^\nu dS_{\mu\nu} = 2 \int_\Sigma R^\mu{}_\nu \xi^\nu d\Sigma_\mu \tag{1.71}$$

where S is the boundary of the spacelike slice Σ and $d\Sigma_\mu = -n_\mu \sqrt{h} d^3y$, where n_μ is the normal to Σ. Then if we have an asymptotically flat spacetime which contains a spinning black hole and matter with stress energy tensor $T_{\mu\nu}$, and Σ is a hypersurface which extends from the horizon, $\mathcal{H}$, to spatial infinity, then Σ has two boundaries, one at the horizon and one at infinity. Making use of EFEs and (1.71), the mass and angular momentum of the spacetime is given by,

$$M = M_H + 2 \int_\Sigma \left(T_{\mu\nu} - \frac{1}{2} T g_{\mu\nu} \right) n^\mu t^\nu \sqrt{h} d^3y \tag{1.72}$$

where t^μ is a timelike Killing field. The angular momentum of the spacetime is given by,

$$J = J_H - \int_\Sigma \left(T_{\mu\nu} - \frac{1}{2} T g_{\mu\nu} \right) n^\mu \phi^\nu \sqrt{h} d^3y \tag{1.73}$$

where t^μ is the timelike Killing field for time translations, ϕ^μ is the spacelike Killing field for rotations, and,

$$M_H = -\frac{1}{8\pi}\int_{\mathcal{H}} \nabla^\mu t^\nu dS_{\mu\nu} \quad \text{and} \quad J_H = \frac{1}{16\pi}\int_{\mathcal{H}} \nabla^\mu \phi^\nu dS_{\mu\nu}. \tag{1.74}$$

The stress tensor encodes information for energy momentum fluxes, we can use this information to compute how much energy (or mass) and momentum gets transferred across a surface. To do so consider the vector fields,

$$\varepsilon^\mu = -T^\mu{}_\nu t^\nu \quad \text{and} \quad l^\mu = T^\mu{}_\nu \phi^\nu. \tag{1.75}$$

Then ε^ν is an energy flux vector and l^μ is an angular momentum flux vector. Both these vectors are divergenceless as a consequence of the conservation equations, $\nabla^\mu T_{\mu\nu} = 0$, and the antisymmetry of $\nabla_\mu \xi_\nu$. By Stokes' theorem we have that,

$$\int_{\partial V} \varepsilon^\nu d\Sigma_\nu = 0 \quad \text{and} \quad \int_{\partial V} l^\nu d\Sigma_\nu = 0 \tag{1.76}$$

where ∂V is the boundary of a four dimensional region of space V. The above integrals imply that the total transfer of energy or momentum across the boundary is zero, i.e, said quantity is conserved. But we may speak of the transfer across one piece of ∂V. Say one of the pieces of ∂V is the hypersurface Σ then mass transferred across Σ is given by,

$$\delta M = \int_\Sigma \varepsilon^\mu d\Sigma_\mu \tag{1.77}$$

and the angular momentum transferred across Σ is,

$$\delta J = \int_\Sigma l^\mu d\Sigma_\mu. \tag{1.78}$$

First law of black hole mechanics

Now we have all the tools necessary to calculate the effect of mass and angular momentum flux through the horizon of a black hole. Consider then, a stationary axisymmetric blackhole of mass M and angular momentum J. Then we assume that there is some low energy matter in the spacetime described by the stress energy tensor $T^{\mu\nu}$. Then from (1.76), the mass transferred into the blackhole is given by,

$$\delta M = -\int_{\mathcal{H}} T^{\mu}{}_{\nu} t^{\nu} d\Sigma_{\nu} \tag{1.79}$$

and the angular momentum is given by,

$$\delta J = \int_{\mathcal{H}} T^{\mu}{}_{\nu} \phi^{\nu} d\Sigma_{\nu} \tag{1.80}$$

where $\mathcal{H}$ is the horizon and $d\Sigma_{\nu} = -\xi_{\nu} dv dS = -(t_{\nu} + \Omega\phi_{\nu}) dv dS$, where Ω is the angular velocity of the black hole, and dS is the area element of the two dimensional slice on the event horizon and dv is the null direction along the event horizon. Then we have,

$$\delta M - \Omega \delta J = \int_{\mathcal{H}} T_{\mu\nu}(t^{\mu} + \Omega\phi^{\mu}) \xi^{\nu} dv dS \tag{1.81}$$

$$= \int dv \int_{\mathcal{H}|_v} T_{\mu\nu} \xi^{\mu} \xi^{\nu} dS. \tag{1.82}$$

Using the Raychaudri equation up to linear order we have that $d\theta/dv = \kappa\theta - 8\pi T_{\mu\nu}\xi^{\mu}\xi^{\nu}$, where θ is the expansion and κ is the surface gravity. Inserting this into (1.81) and assuming that the black hole is stationary both before and after the perturbation, and using the definition of expansion as the fractional rate of change of

area dS, we can show that,

$$\delta M - \Omega \delta J = \frac{\kappa}{8\pi} \delta A \tag{1.83}$$

where δA is the change in the black holes surface area. This relationship between mass, spin and area is called the first law of black hole thermodynamics due to its resemblance to the first law of thermodynamics. If the black hole also contains charge which then is also perturbed, the above relationship gets modified to

$$\delta M = \frac{\kappa}{8\pi} \delta A + \Omega \delta J + \Phi_H \delta Q \tag{1.84}$$

where Φ_H is the electrostatic potential at the horizon and δQ is the change in the charge of the black hole.

1.1.5 First law of soliton mechanics

This section closely follows [37]. In Section 1.1.4 we saw that we can take a charged, spinning black hole and add linear perturbations to the charge δQ, angular momentum δJ, and mass δM. We showed that these perturbations satisfy the first law of black hole thermodynamics,

$$\delta M = \frac{\kappa}{8\pi} \delta A + \Omega \delta J + \Phi_H \delta Q. \tag{1.85}$$

where κ is the surface gravity, A is the area of the event horizon and Φ_H is the electrostatic potential at the horizon.

This was derived for black holes in dimensions of spacetime $D = 4$. As mentioned above, there has been active interest in the solutions for EFE's in dimensions $D > 4$, especially motivated by string theory and the AdS/CFT correspondence. The natural step is to consider asymptotically flat solutions for $D = 5$. A generalization of the Kerr solution in $D = 5$, for example, has a horizon topology of S^3 [48]. A more exotic

solution which does not have a counterpart in $D = 4$ is the black ring solution whose horizon has a topology $S^1 \times S^2$ [18].

There is an interesting class of solutions in $D = 5$ dimensions of the Einstein-Maxwell called gravitational solitons. These solutions are stationary and asymptotically flat and do not contain horizons. This makes solitons different from black hole solutions. In $D = 5$ solitons are characterized by having a non-trivial homology[4], specifically we have that $H_2(\Sigma) \neq 0$, where Σ is a spacelike surface. This allows for non-trivial 2-cycles or "bubbles". A 2-cycle is a two dimensional closed manifold (compact and no boundary) that is itself not a boundary. It has been shown that in $D = 4$ solitons cannot exist [23], this is due to the requirement that in $D = 4$, the domain of outer communication has to be simply connected [21]. These 2-cycles or bubbles can carry charge and magnetic flux as a result of the Maxwell fields. They also contribute to the mass, angular momentum and electric charge of the solution.

It is natural to expect that the counterpart of the first law of black hole thermodynamics, (1.85), will be different in $D = 5$ and for spacetimes containing solitons. In [38] the first law of thermodynamics was derived for spacetimes containing black holes and solitons. More precisely, consider black hole and soliton solutions $(\mathcal{M}, g)$ for $D = 5$ coupled to an arbitrary number of Maxwell fields $F^I, I = 1 \dots N$ and neutral scalar fields $\chi^A, A = 1 \dots n$. These spacetimes are stationary and bisymmetric, i.e, they have isometries $\mathbb{R}_t \times U(1)^2$. This is chosen because for stationary black holes, the rigidity result of Hollands, Ishibashi and Wald [33] shows that the spacetime must admit at least one $U(1)$ isometry. We will assume an additional $U(1)$, i.e. $U(1)^2$ isometry, as this case most closely resembles the four-dimensional case, in the sense

[4]Homology is a precise way of counting the number of holes in a manifold. For example for a solid torus $S^1 \times D^2$, is $H_1(S^1 \times D^2) = \mathbb{Z}$, this means that we have 1-cycle (a closed loop) that will not contract, i.e, it goes through the hole in the centre of the solid torus. For a hollow torus, we have $H_1(S^1 \times S^1) = \mathbb{Z}^2$, which means now there are two loops which will not close, one of them is the same as $S^1 \times D^2$ the other is around the inside waist of the torus. Further, $H_2(S^1 \times S^1) = \mathbb{Z}$, this is the hollow region inside of the torus. Similarly $H_1(S^2) = 0$ and $H_2(S^2) = \mathbb{Z}$.

that the 'orbit space' formed by quotienting the spacetime by the symmetry group is two-dimensional. Further it is assumed that the matter fields in the spacetime also follow these symmetries, i.e,

$$\mathcal{L}_{\xi_\alpha} g = \mathcal{L}_{\xi_\alpha} F^I = \mathcal{L}_{\xi_\alpha} \chi^A = 0 \tag{1.86}$$

where $\xi_\alpha = (\xi, m_i)$, ξ is the generator of time translations, m_i are the generators of the rotational symmetries and $\mathcal{L}$ is the Lie derivative. This implies that all spacetime fields depend only on the two-dimensional orbit space $\mathcal{B} = \mathcal{M}/\mathbb{R}_t \times U(1)^2$. $\mathcal{B}$ is simply connected with boundary $\partial\mathcal{B}$. On $\partial\mathcal{B}$ the matrix of scalar products $g(m_i, m_j)$ has rank 1 and is divided into intervals I, or "rods" analogous to the ones introduced in Section 1.1.2. For the spacetimes including a black hole the corresponding rod is $I_H = H/U(1)^2$. The remaining part of $\partial\mathcal{B}$ we have spheres where a linear combination $v^i m_i$, $v^i \in \mathbb{Z}$ vanish. For the sphere we have corresponding finite rods where the end points of the rod correspond to the poles of the sphere. Axes of rotation correspond to semi-infinite rods, similar to the Kerr case above.

The action for the spacetimes for which the first law can be found is given by,

$$S = \tfrac{1}{16\pi} \int \star R - f_{AB}(\chi) \mathrm{d}\chi^A \wedge \star \mathrm{d}\chi^B - g_{IJ}(\chi) F^I \wedge \star F^J - \frac{1}{6} C_{IJK} F^I \wedge F^J \wedge A^K \tag{1.87}$$

where $F^I = dA^I$ for a locally defined gauge potential A^I. Then we can define the mass spin and charge, by using Komar expressions analogous to (1.68) and (1.69),

$$M = -\frac{3}{32\pi} \int_{S_\infty} \star \mathrm{d}K, \qquad J_i = \frac{1}{16\pi} \int_{S_\infty} \star \mathrm{d}m_i \tag{1.88}$$

where $K = \xi - \Omega_i m_i$ is the spacetime contains a black hole, if not, $K = \xi$. The charge

contained in the spacetime is defined by,

$$Q_I \equiv \frac{1}{8\pi}\int_{S_\infty} g_{IJ} \star F^J. \tag{1.89}$$

Then we introduce the globally defined potentials,

$$d\Phi^I_\xi = i_\xi F^I \quad \text{and} \quad d\Phi^I_{m_i} = i_{m_i} F^I. \tag{1.90}$$

Then let $G^I = \star F^I$, and so from the Maxwell equations and the symmetry conditions we can define the two forms Θ_I,

$$\Theta_I = g_{IJ} i_\xi G^J + -\frac{1}{2} C_{IJK} F^J \Phi^K. \tag{1.91}$$

Since $\mathcal{L}_{m_i}\Theta_I = 0$ and $d\Theta_I = 0$ one can define,

$$dU_{Ii} = i_{m_i}\Theta_I + \frac{1}{2} C_{IJK} d\Phi^J_i \Phi^K_H. \tag{1.92}$$

Then in the absence of black holes, the first law of soliton mechanics is,

$$M = \frac{1}{2}\sum_{[C]} \Psi[C] q[C] \quad \delta M = \sum_{[C]} \Psi[C]\delta q[C]. \tag{1.93}$$

where

$$q[C] = \frac{1}{4\pi}\int_C F \quad \text{and} \quad \Psi[C] = \pi v^i U_i \tag{1.94}$$

where $[C]$ is the basis for the 2-cycles, since it could be that two 2-cycles are homologous, we only want to count the ones that are not homologous. If a black hole is present then there will be the usual contributions as in (1.85) plus contributions from

disc topology surfaces ([D]) that extend from the horizon. We have,

$$\delta M = \frac{\kappa}{8\pi}\delta A + \Omega_i \delta J_i + \Phi_H^I \delta Q_I + \sum_{[C]} \Psi[C]\delta q[C] + \frac{1}{2}\sum_{[D]} \mathcal{Q}_I[D]\delta\Phi^I[D] \tag{1.95}$$

where $\Phi^I[D] = v_i \Phi_i^I$ and,

$$\mathcal{Q}_I[D] = \frac{1}{4}\int_D \left(\Theta_I + \frac{1}{2}C_{IJK}F^J\Phi_H^K\right). \tag{1.96}$$

The central idea of Chapter 6 is to apply and verify to various spacetimes the formula (1.95). We find regularity of the spacetime metric is essential for this to hold.

1.1.6 Linearized gravity

In this section we briefly review how to linearize EFEs[5]. We will first review the treatment for a flat background as this will help us motivate the perturbation theory for the Schwarzschild background.

It will prove helpful to review the definition of a Lie derivative. Let ϕ_t be a one parameter family of diffeomorphisms parametrized by t and let $\phi_{-t}^* = [\phi^{-1}]_t^*$ denote the pushforward induced by the inverse map. Then, if the vector ξ^μ is the generator of the diffeomorphism, the Lie derivative of a mixed rank tensor $T^\mu{}_\nu$ is defined as

$$\mathcal{L}_\xi T^\mu{}_\nu(p) = \lim_{t\to 0}\left\{\frac{\phi_{-t}^*[T^\mu{}_\nu(\phi_t(p))] - T^\mu{}_\nu(p)}{t}\right\} \tag{1.97}$$

Notice that in the limit that $t \to 0$, ϕ_t is an infinitesimal diffeomorphism with some generator ξ^μ. In coordinates this corresponds to an infinitesimal translation,

[5]This section closely follows [64]

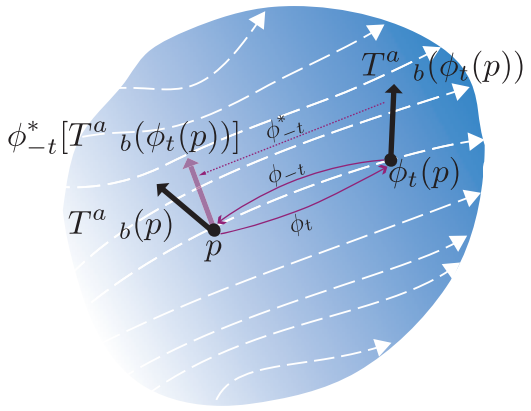

Figure 1.6: An illustration of the moving parts of the Lie derivative.

$\tilde{x}^\mu = x^\mu + \xi^\mu \delta t$. Proceeding with our goal of linearizing EFEs we write the metric as,

$$\tilde{g}_{\mu\nu} = g_{\mu\nu} + \lambda \delta\gamma_{\mu\nu} \qquad \Longrightarrow \qquad \delta\gamma_{\mu\nu} = \left.\frac{d\tilde{g}_{\mu\nu}}{d\lambda}\right|_{\lambda=0} \tag{1.98}$$

where it is assumed that $g_{\mu\nu}$ is a known solution and $\gamma_{\mu\nu}$ is a perturbation. Let us consider an infinitesimal diffeomorphism, ϕ_λ also parametrized by λ. Then we can define the perturbation as,

$$\delta\gamma'_{\mu\nu} = \left.\frac{d(\phi^*_\lambda \tilde{g}_{\mu\nu})}{d\lambda}\right|_{\lambda=0} = \delta\gamma_{\mu\nu} + \left.\frac{d(\phi^*_\lambda g_{\mu\nu})}{d\lambda}\right|_{\lambda=0} \tag{1.99}$$

The second equality follows from the linearity of ϕ^*_λ and that at linear order $\frac{d}{d\lambda}[\phi^*_\lambda(\lambda\gamma_{\mu\nu})] = \delta\gamma_{\mu\nu}$. Then by making the substitution $t = -\lambda$ in (1.97) we have,

$$\left.\frac{d(\phi^*_\lambda g_{\mu\nu})}{d\lambda}\right|_{\lambda=0} = -\mathcal{L}_\xi g_{\mu\nu} \tag{1.100}$$

Which finally gives us,

$$\delta\gamma'_{\mu\nu} = \delta\gamma_{\mu\nu} - \mathcal{L}_\xi g_{\mu\nu}. \tag{1.101}$$

The main purpose of the above exercise is to show that the decomposition of the metric

into a background spacetime and a perturbation is not unique due to the allowed infinitesimal changes of the coordinates (or gauge transformations); the freedom is given by (1.101). Below we will see how the linearized EFEs are invariant under this infinitesimal change of gauge.

With the thorny issue of gauge invariance addressed we are in a comfortable position to present the linearized EFEs. In this section we will show the treatment for when the background metric is flat, i.e., $\eta_{\mu\nu}$, backgrounds with curvature will be presented in subsequent chapters. In what follows, we will drop the λ and it will be understood that we are neglecting terms $\mathcal{O}(\delta^2)$ and higher. Then, our perturbation and its inverse (up to linear order) are given by,

$$\tilde{\eta}_{\mu\nu} = \eta_{\mu\nu} + \delta\gamma_{\mu\nu} \qquad\qquad \tilde{\eta}^{\mu\nu} = \eta^{\mu\nu} - \delta\gamma^{\mu\nu} \tag{1.102}$$

where the indices on $\delta\gamma_{\mu\nu}$ are raised by the unperturbed metric $\eta_{\mu\nu}$. The Christoffel symbols are

$$\delta\Gamma^{\sigma}_{\mu\nu} = \frac{1}{2}\eta^{\sigma\gamma}(\partial_\mu\delta\gamma_{\nu\gamma} + \partial_\nu\delta\gamma_{\mu\gamma} - \partial_\gamma\delta\gamma_{\mu\nu}) \tag{1.103}$$

and the Ricci tensor is

$$\begin{aligned}\delta R_{\mu\nu} &= \partial_\sigma\delta\Gamma^{\sigma}_{\mu\nu} - \partial_\mu\delta\Gamma^{\gamma}_{\nu\gamma} \\ &= \partial^\sigma\partial_{(\mu}\delta\gamma_{\nu)\sigma} - \frac{1}{2}\partial^\sigma\partial_\sigma\delta\gamma_{\mu\nu} - \frac{1}{2}\partial_\mu\partial_\nu\delta\gamma\end{aligned} \tag{1.104}$$

where $\delta\gamma = \delta\gamma^{\mu}_{\mu}$. Hence the linearized EFEs are given by

$$\delta G_{\mu\nu} = -\frac{1}{2}\partial^\sigma\partial_\sigma\delta\bar{\gamma}_{\mu\nu} + \partial^\sigma\partial_{(\mu}\delta\bar{\gamma}_{\nu)\sigma} - \frac{1}{2}\eta_{\mu\nu}\partial^\sigma\partial^\gamma\delta\bar{\gamma}_{\sigma\gamma} = 8\pi\delta T_{\mu\nu} \tag{1.105}$$

where $\delta G_{\mu\nu} = \delta R_{\mu\nu} - \frac{1}{2}\eta_{\mu\nu}\delta R$ is the Einstein tensor, $\delta\bar{\gamma}_{\mu\nu} = \delta\gamma_{\mu\nu} - \frac{1}{2}\eta_{\mu\nu}\delta\gamma$ and $\delta T_{\mu\nu}$

is the stress energy tensor. Note that under the gauge transformation (1.101), the linearized Einstein tensor in (1.105) does not change, i.e., it is gauge invariant. We can utilize this gauge invariance to simplify the form of the linearized EFEs. Note first that

$$\delta\bar{\gamma}'_{\mu\nu} = \delta\bar{\gamma}_{\mu\nu} - 2\partial_{(\mu}\xi_{\nu)} + \eta_{\mu\nu}\partial^{\sigma}\xi_{\sigma} \tag{1.106}$$

then, $\partial^{\nu}\delta\bar{\gamma}'_{\mu\nu} = \partial^{\nu}\delta\bar{\gamma}_{\mu\nu} - \partial^{\sigma}\partial_{\sigma}\xi_{\mu}$. If we chose ξ_{μ} such that, $\partial^{\nu}\delta\bar{\gamma}_{\mu\nu} = \partial^{\sigma}\partial_{\sigma}\xi_{\mu}$, then we have,

$$\partial^{\nu}\delta\bar{\gamma}'_{\mu\nu} = 0. \tag{1.107}$$

This is the analogue of the Lorentz gauge condition from electromagnetism. In the Lorentz gauge the linearized EFEs take the simple form,

$$\Box\delta\bar{\gamma}_{\mu\nu} = -16\pi\delta T_{\mu\nu} \tag{1.108}$$

where $\Box = \partial^{\mu}\partial_{\mu}$ and we have dropped the '$'$' since we will be exclusively in this gauge for all quantities.

Notice that the condition (1.107) does not entirely fix the gauge. We can do another gauge transformation, $\delta\gamma'_{\mu\nu} = \delta\gamma_{\mu\nu} - \partial_{\mu}\xi_{\nu} - \partial_{\nu}\xi_{\mu}$, as long as ξ_{μ} satisfies the condition,

$$\Box\xi_{\mu} = 0. \tag{1.109}$$

Imposing this condition on ξ_{μ} maintains the previous condition of $\partial^{\nu}\delta\gamma_{\mu\nu} = 0$. Further, in a spacetime where $\delta T_{\mu\nu} = 0$, it is possible[6] to spend this remaining gauge freedom to impose the conditions

$$\delta\gamma = 0, \qquad \delta\gamma_{0i} = 0 \qquad \text{for } i = 1, 2, 3 \qquad \text{and} \qquad \delta\gamma_{00} = 0. \tag{1.110}$$

[6]See Pg. 80 in [64] for more details.

This is the analogue of the radiation gauge from electromagnetism. Then, we may take the following anzatz for $\delta\gamma_{\mu\nu}$,

$$\delta\gamma_{\mu\nu} = H_{\mu\nu}\mathrm{e}^{ik_\sigma x^\sigma}, \tag{1.111}$$

where in general, $H_{\mu\nu}$ is a constant tensor field with 10 independent components. However their number can be significantly cut down. First, we see that for (1.111) to satisfy (1.108) with $\delta T_{\mu\nu} = 0$ we require $k^\sigma k_\sigma = 0$. Further, the gauge conditions (1.107) and (1.110) imply,

$$k^\mu H_{\mu\nu} = 0 \qquad H_{0\nu} = 0 \qquad H^\mu_\mu = 0. \tag{1.112}$$

Notice that both of the first two of these conditions imply, $H_{0\nu}k^\nu = 0$, hence, out of these 9 equations 8 are independent. Of the 10 independent components we are left with only 2 independent solutions. These two solutions are the two polarization modes of the recently discovered gravitational waves.

The above treatment was for perturbations to the Minkowski background. Any known background can be perturbed in a similar manner. Let us briefly consider the perturbations of a Schwarzschild background, we will follow the notation of [43]. A complete treatment of the development of the theory is given in Chapter 3. We begin with the metric expressed as,

$$ds^2 = g_{ab}dx^a dx^b + r^2\Omega_{AB}d\theta^A d\theta^B \tag{1.113}$$

where Ω_{AB} is the metric on the unit sphere, a, b run over r, t and A, B run over θ and ϕ. Then we add the perturbation to the metric, $p_{\mu\nu}$. Given that the spacetime is spherically symmetric we expand $p_{\mu\nu}$ in scalar, vector and tensor spherical harmonics.

These come in two varieties, odd and even. They are named this way based on their behaviour under a transformation $\mathbf{r} \to -\mathbf{r}$ where $\mathbf{r}$ is the coordinate position of a point on the sphere in an embedding in $\mathbb{R}^3$. If under this inversion the quantity transforms as $(-1)^l$ it is said to be even or polar, it it transforms as $(-1)^{l+1}$ it is said to be odd or azimuthal. We may then write the perturbations as shown in Table 1.2. Perturbations of Schwarzschild black holes also have the same gauge invariance

Even	Odd
$p_{ab} = \sum_{lm} h_{ab}^{lm}(t,r) Y^{lm}$	$p_{ab} = 0$
$p_{aB} = \sum_{lm} j_a^{lm} Y_B^{lm}$	$p_{aB} = \sum_{lm} h_a^{lm} X_B^{lm}$
$p_{AB} = r^2 \sum_{lm} \left(K^{lm} \Omega_{AB} Y^{lm} + G^{lm} Y_{AB}^{lm} \right)$	$p_{AB} = \sum_{lm} h_2^{lm} X_{AB}^{lm}$

Table 1.2: Odd and even parity perturbations

properties as that of Minkowski perturbations. This is remedied by working with gauge invariant quantities. Finding these gauge invariant quantities is facilitated by expanding the infinitesimal coordinate transformations also in spherical harmonics. For example, the gauge invariant variable for the odd perturbations is given by, $\tilde{h}_a = h_a - \frac{1}{2}\nabla_a h_2 + \frac{1}{r}\partial_a r h_2$. Inserting this perturbed metric into the linearized EFEs we arrive at a set of equations that are simplified by defining a master function which has dependence only on r and t. In terms of this master function, say ψ, the linear EFEs reduce to the following equation,

$$[\Box - V(r)]\,\psi = 0 \tag{1.114}$$

where $\Box = \nabla^a \nabla_a$ is the d'Alembertian for the r, t part and $V(r)$ is a potential. Such a master function exists for both odd and even perturbations with different potentials for each. All the information about the spacetime perturbations is encoded in ψ, once

(1.114) is solved the metric perturbations can be reconstructed from ψ.

1.1.7 The AdS_4 spacetime

While asymptotically flat spacetimes are probably the most important astrophysically and best represent isolated gravitational systems, theoretically asymptotically AdS spacetimes find many applications. Specially the AdS/CFT correspondence stemming from string theory and its offshoot the fluid/gravity correspondence which we will discuss below.

AdS space

Anti-de Sitter (AdS) is a spacetime with constant negative curvature. To gain an intuitive understanding of the AdS spacetime it is worthwhile to have a look at two examples of spaces (not spacetimes) with constant curvature. The first example is a space with constant positive curvature, a sphere, S^2. We can embed the sphere in $\mathbb{R}^3$ with metric,

$$ds^2 = dX^2 + dY^2 + dZ^2 \tag{1.115}$$

where the sphere is defined by the constraint,

$$X^2 + Y^2 + Z^2 = L^2, \tag{1.116}$$

we can parametrize this sphere by our familiar spherical coordinates, $X = L\sin\theta\cos\phi$, $Y = L\sin\theta\sin\phi$ and $Z = L\cos\theta$. This induces the usual metric on the sphere,

$$ds^2 = L^2(d\theta^2 + \sin^2\theta d\phi^2) \tag{1.117}$$

This sphere has a constant positive scalar curvature of $R = \frac{2}{L^2}$. Now let us consider the second example of constant negative curvature, a hyperbolic space, H^2 [50]. Rather than embedding this into the Euclidean space $\mathbb{R}^3$, we will embed it in the 2+1 Minkowski space, $\mathbb{R}^{2,1}$, with metric,

$$ds^2 = -dZ^2 + dX^2 + dY^2 \tag{1.118}$$

and the constraint is now,

$$-Z^2 + X^2 + Y^2 = -L^2. \tag{1.119}$$

Then in an analogous manner to the sphere we introduce coordinates, $X = L\sinh\rho\cos\phi$, $Y = L\sinh\rho\sin\phi$ and $Z = L\cosh\phi$, which induces the metric for the hyperbolic space,

$$ds^2 = L^2(d\rho^2 + \sinh^2\rho d\phi^2). \tag{1.120}$$

This space has a constant negative curvature of

$$R = -\frac{2}{L^2}. \tag{1.121}$$

There is a specific reason to embed this surface into a Minkowski rather than Euclidean "ambient space". The Euclidean metric distance is invariant under $SO(3)$ transformations, i.e., rotations. So when we embed the sphere into $\mathbb{R}^3$ rotations map points on the sphere to other points on the sphere. On the other hand, the Minkowski metric is invariant under $SO(2,1)$ transformations, i.e., Lorentz transformations or hyperbolic rotations. So when the hyperbolic space is embedded in $\mathbb{R}^{2,1}$, Lorentz transformations map points on the hyperbolic space to other points on the hyperbolic

space, this is shown in Figure 1.7, where the green surface is the embedding of the surface, ξ is hyperbolic rotation from A to A' in the XZ plane. Notice that if we had considered the case where constraint (1.119) is embedded in $\mathbb{R}^3$ we would get a two sheeted hyperboloid and transformations in $SO(3)$ would have removed points from this surface [50].

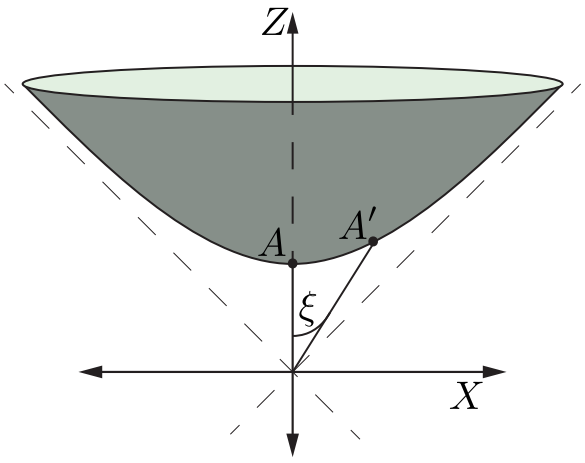

Figure 1.7: Hyperbolic space embedded in a Minkowski spacetime $\mathbb{R}^{2,1}$.

Now we are in a good position to consider a spacetime of constant negative curvature. Specifically a 4-dimensional one, hence we will begin with a five dimensional Minkowski spacetime, where the one extra dimension is time-like,

$$ds_5^2 = -du^2 - dv^2 + dx^2 + dy^2 + dz^2. \tag{1.122}$$

Next we embed the following hyperboloid,

$$-u^2 - v^2 + x^2 + y^2 + z^2 = -L^2 \tag{1.123}$$

and introduce coordinates,

$$u = L\cosh(\rho)\sin(t') \qquad v = L\cosh(\rho)\cos(t')$$
$$x = L\sinh(\rho)\cos\theta \qquad y = L\sinh(\rho)\sin\theta\cos\phi$$
$$z = L\sinh(\rho)\sin\theta\sin\phi$$

which induces the following metric on the hyperboloid;

$$ds^2 = L^2[-\cosh^2(\rho)dt'^2 + d\rho^2 + \sinh^2(\rho)d\Omega_2^2]. \tag{1.124}$$

It is important to note that this particular embedding leads to closed time-like curves given the periodic nature of t' ($\sin t'$ and $\cos t'$ for u and v). This is not an intrinsic property of the spacetime, only of the embedding. Thus, we "unwrap" the periodic coordinate t' by passing to the universal cover and time is taken to run from $-\infty < t' < \infty$. We introduce the following transformation $\cosh(\rho) = 1/\cos(\chi)$, which transforms the metric too,

$$ds^2 = \frac{L^2}{\cos^2\chi}\left[-(dt')^2 + d\chi^2 + \sin^2\chi d\Omega_2^2\right] \tag{1.125}$$

where $0 \leq \chi < \pi/2$. Figure 1.8 shows the Penrose diagram for the AdS spacetime with some time-like and null geodesics. Each point on the diagram is a two-sphere except the left dotted line which is a point at the origin. An interesting feature of AdS is that spatial infinity is a time-like surface rather than just a point. This allows null geodesics to reach infinity and come back to their origin in a finite amount of time, as shown by straight diagonal lines in the diagram below. The same is true for timelike geodesics which are shown by the curves.

On (1.124) we can do the further transformation $t' = t/L$ and $\sinh\rho = r/L$, to

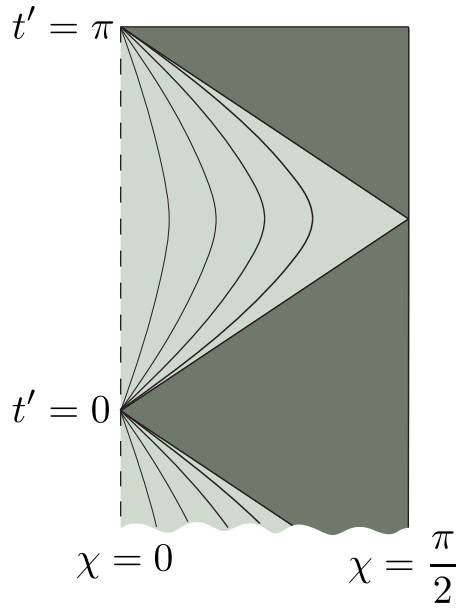

Figure 1.8: Penrose diagram for the AdS spacetime with some time-like and null geodesics.

bring the metric into static coordinates,

$$ds^2 = -\left(1 + \frac{r^2}{L^2}\right) dt^2 + \frac{1}{1 + \frac{r^2}{L^2}} dr^2 + r^2 d\Omega_2^2. \tag{1.126}$$

This is the AdS_4 spacetime, it belongs to a family of maximally symmetric spacetimes, i.e., it is both homogeneous and isotropic. The other two spacetimes in this family are the familiar Minkowski background and the de Sitter spacetime (constant positive curvature). AdS_4 is a solution to the vacuum EFEs with a cosmological constant that is negative,

$$R_{\mu\nu} = \Lambda g_{\mu\nu}, \tag{1.127}$$

which sets $\Lambda = -3/L^2$.

AdS_4 black hole and its timelike boundary

Constructing a black hole that is asymptotically AdS is fairly straightforward, the metric is given by,

$$ds^2 = -f(r)dt^2 + \frac{1}{f(r)}dr^2 + r^2 d\Omega_2^2 \quad \text{with} \quad f(r) = 1 - \frac{2M}{r} + \frac{r^2}{L^2}. \tag{1.128}$$

Notice that as $L \to \infty$, or equivalently $\Lambda \to 0$, we recover the Schwarzschild black hole and if $M \to 0$ we arrive at the AdS_4 spacetime.

An interesting feature of AdS black holes is that rather than having a point at spatial infinity we now have a timelike surface, this is the same as in pure AdS spacetimes, as shown in the spacetime diagram Figure 1.9. We see that null rays emanating from past null infinity can bounce from this timelike surface and fall into the black hole, this is shown by the black arrows in Figure 1.9.

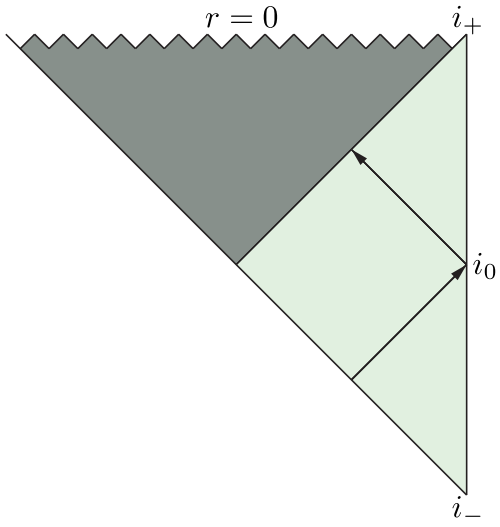

Figure 1.9: A spacetime diagram of an AdS black hole. Notice that spacelike infinity, i_0, is a timelike surface rather than a point. The arrows on this spacetime represent a nullray that bounces back from this surface.

By treating this timelike surface as a boundary of the spacetime, we can use the Hamilton Jacobi methods of [8], that are outlined in Section 1.1.3, to find the surface

stress energy tensor on a constant-r surface as $r \to \infty$. The procedure to do so is relatively straightforward but there is need of a few modifications.

Firstly since the spacetime contains a timelike Killing field, the contribution from the integrals on the spacelike surfaces in (1.49) vanishes. Further since we are now considering EFEs with a cosmological constant we need to modify R to $R-2\Lambda$. Finally we also need to add a "counter term", S_{ct}. This is done in order to cancel divergences that typically appear in the stress tensor when taking the $r \to \infty$ limit. Motivation for finding such a boundary stress tensor arose from the AdS/CFT duality, wherein, the gravitational action of the bulk is equivalent with the quantum effective action of the boundary CFT, and the $r \to \infty$ divergences correspond to ultraviolet divergences of quantum field theory [65] [10] [34] [32]. In [5] a well-defined meaning was given to energy and momentum in AdS by the counter terms, S_{ct}, which gave the desired features both for the bulk and also the boundary CFT. The procedure followed in [5] can be explained in the following manner: as we had discussed in Section 1.1.3, it is always possible to add a term, S_{ct}, as long as it is only a function of the boundary metric, $\gamma_{\mu\nu}$, i.e., $S_{ct} = S_{ct}(\gamma_{\mu\nu})$. Then the action becomes,

$$S[g] = \frac{1}{16\pi}\int_V (R - 2\Lambda)\sqrt{-g}d^4x - \frac{1}{8\pi}\int_{\partial V_r}\Theta\sqrt{-\gamma}d^3x + \frac{1}{8\pi}S_{ct}(\gamma_{\mu\nu}) \tag{1.129}$$

where ∂V_r is the constant-r boundary. The functional form of $S_{ct}(\gamma_{\mu\nu})$ that is needed to cancel divergences in AdS_4 has been elucidated in [5]; writing $S_{ct} = \int_{\partial V_r} L_{ct}$ it is found that,

$$L_{ct} = -\frac{2}{L}\sqrt{-\gamma}\left(1 - \frac{L^2}{4}\,{}^3R\right) \tag{1.130}$$

where ${}^3R$ is the scalar curvature of the metric $\gamma_{\mu\nu}$, which then gives for the stress tensor,

$$T^{\mu\nu} = \frac{1}{8\pi}\left(\Theta^{\mu\nu} - \Theta\gamma^{\mu\nu} - \frac{2}{L}\gamma^{\mu\nu} - {}^3G^{\mu\nu}L\right) \tag{1.131}$$

where ${}^3G^{\mu\nu}$ is the Einstein tensor of the metric $\gamma_{\mu\nu}$.

We can compute (1.131) for the metric (1.128). If we write the metric in an ADM-like decomposition, we have,

$$ds^2 = N^2 dr^2 + \gamma_{\mu\nu}(dx^\mu + N^\mu dr)(dx^\nu + N^\nu dr) \tag{1.132}$$

then, the lapse is $N = f(r)^{-1/2}$, $\gamma_{tt} = -N^{-2}$, $\gamma_{AB} = r^2\Omega_{AB}$ where Ω_{AB} is the metric on a unit sphere and A, B run over θ, ϕ, and clearly, the shift $N^\mu = 0$. Then the non-zero components of the stress tensor as $r \to \infty$ are given by [4],

$$8\pi T_{tt} = \frac{2M}{rL} + \mathcal{O}\left(\frac{1}{r^2}\right) \tag{1.133}$$

$$8\pi T_{\theta\theta} = \frac{ML}{r} + \mathcal{O}\left(\frac{1}{r^2}\right) \tag{1.134}$$

Notice that these components vanish, to get a finite result we apply a "holographic renormalization" procedure where the normalized stress tensor, $\mathbf{T}$ is given by,

$$\mathbf{T}_{\mu\nu} = \lim_{r\to\infty} \frac{r}{L}(8\pi)T_{\mu\nu}. \tag{1.135}$$

We apply a similar normalization to the metric,

$$\boldsymbol{\gamma}_{\mu\nu} = \lim_{r\to\infty} \frac{r^2}{L^2}\gamma_{\mu\nu}. \tag{1.136}$$

Further we point out that this stress tensor has a vanishing trace, $\mathbf{T} = \mathbf{T}_{\mu\nu}\boldsymbol{\gamma}^{\mu\nu} \to 0$ as $r \to 0$.

1.1.8 Relativistic fluids and the fluid/gravity duality

In this section we review non-relativistic and relativistic fluids. We first demonstrate perfect fluids and then show how we can model dissipation effects which depend on first order derivatives of the fluid flow. Then we show how in AdS spacetimes the fluid/gravity duality manifests itself in four dimensional black brane solutions.

Relativistic and non-relativistic fluids

The simplest relativistic fluid one can construct is a perfect fluid, such called since it is assumed that there are no dissipative effects like viscosity. The fluid is completely characterized by its flow field, $u^\mu(x^\sigma)$, pressure $p(x^\sigma)$ and energy density $\rho(x^\sigma)$. From these characteristic properties one can construct its energy momentum tensor,

$$T_{\mu\nu} = \rho u_\mu u_\nu + p\Delta_{\mu\nu} \tag{1.137}$$

where $\Delta_{\mu\nu} = g_{\mu\nu} + u_\mu u_\nu$ is a projection operator. We take this to be a timelike fluid and hence $u^\mu u_\nu = -1$. The equations of motion of this fluid are given by,

$$\nabla^\mu T_{\mu\nu} = 0. \tag{1.138}$$

If we take the spacetime to be Minkowski then $g_{\mu\nu} = \eta_{\mu\nu}$ and $\nabla_\mu = \partial_\mu$, hence the equations of motion now are, $\partial^\mu T_{\mu\nu} = 0$. If we take these equations and project them in parallel and perpendicular directions to u^μ we get the following equations [64];

$$u^\mu \partial_\mu \rho + (\rho + p)\partial^\nu u_\nu = 0 \tag{1.139}$$

$$(\rho + p)u^\mu \partial_\mu u_\nu + \Delta_{\mu\nu}\partial^\mu p = 0. \tag{1.140}$$

We see then, in the non-relativistic limit; $p \ll \rho, u^\mu = (1, \vec{u})$ and $u\ dp/dt \ll |\vec{\nabla} p|$, (1.139) and (1.140) give the continuity equation,

$$\frac{\partial \rho}{\partial t} = -\nabla \cdot (\rho \vec{u}) \tag{1.141}$$

and the Euler equation;

$$-\nabla p = \rho \left(\frac{\partial \vec{u}}{\partial t} + (\vec{u} \cdot \nabla)\vec{u} \right). \tag{1.142}$$

Above was the treatment for fluids without any mechanisms that lead to heat dissipation but the fluids we see in the real world tend to have mechanisms through which they dissipate energy. One such effect is friction, specifically kinetic friction that occurs when there is any type of motion that generates a shear. To take a simple analogy of shear consider sliding a book over a very smooth surface (possibly with very tiny spherical grains spread across the surface), there is negligible friction between the surface and the book. Now consider sliding it over a surface which offers more resistance, say a rubber sheet, then one would experience a shearing effect on the book, the bottom cover will tend to lag behind, the spine would tilt, the pages would slightly slide on top of each other and a resistive force would be felt at the top cover (where force is applied) in order to maintain a constant velocity.

There is a similar effect for fluids. In Figure 1.10 we see a fluid between two plates, the bottom plate is stationary and the top plate is slowly moving with a constant velocity. As we move down the y-axis from the top plate the velocity decreases, hence creating a velocity gradient, $\partial u_x/\partial y$. There is friction between the different layers of the fluid and a force is felt at the top plate opposite to the direction of the motion. This type of force is felt all along the fluid and creates a stress, it is called the shear

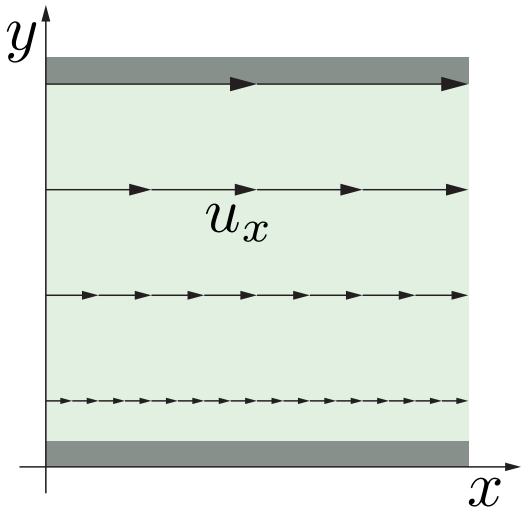

Figure 1.10: Shear stress caused by a fluid in between a stationary plate (bottom) and moving plate (top)

stress, τ. It is proportional to the gradient in the y direction [20],

$$\tau(y) = \frac{F}{A} = \eta \frac{\partial u_x(y)}{\partial y} \tag{1.143}$$

with the constant of proportionality being the shear viscosity η, and A is the area of the plate. We want to now model the effect of viscosity in the Euler equation (1.140). Since the effects of the viscosity arise from the first spatial derivative, we consider the tensor,

$$\sigma_{ij} = \partial_i u_j + \partial_j u_i - \frac{2}{3}\delta_{ij}\partial_k v^k. \tag{1.144}$$

Then the Euler equation (1.139) becomes (in index notation) [20],

$$\rho\left(\frac{\partial u_j}{\partial t} + u^k \partial_k u_j\right) = -\partial_j p + \eta \partial^i \sigma_{ij} + \zeta \partial_j \partial^k u_k \tag{1.145}$$

where ζ is the bulk viscosity, it measures the the friction that is caused by shear-free expansions and contractions of the fluid. Equation (1.145) is popularly known as the Navier-Stokes equation (without the external force term) [20].

Since we will mainly be dealing with relativistic fluids, we need to generalize the effects of viscosity to the relativistic stress tensor and the relativistic equations of motion. We accomplish this by splitting the stress tensor, $T_{\mu\nu}$ of the fluid into a perfect fluid part, $T^{\text{perf}}_{\mu\nu}$, given by (1.137), and a viscous part, $T^{\text{visc}}_{\mu\nu}$,

$$T^{\mu\nu} = T^{\text{perf}}_{\mu\nu} + T^{\text{visc}}_{\mu\nu}. \tag{1.146}$$

We know from our previous discussions that viscous effects depend on the first derivatives of the velocity, but in the relativistic case we have four velocities rather just spatial velocities. Hence, we can use the projection operator $\Delta_{\mu\nu}$ to define a relativistic analogue of σ_{ij},

$$\sigma_{\mu\nu} = 2\nabla_{<\mu}u_{\nu>} \tag{1.147}$$

where,

$$\nabla_{<\mu}u_{\nu>} = \Delta_{\mu\sigma}\Delta_{\nu\gamma}\nabla^{(\sigma}u^{\gamma)} - \frac{1}{3}\Delta_{\mu\nu}\Delta_{\sigma\gamma}\nabla^{\sigma}u^{\gamma}. \tag{1.148}$$

The analogue of the bulk viscosity term is $\Delta_{\mu\nu}\nabla_{\gamma}u^{\gamma}$. Combining these two terms we construct $T^{\text{visc}}_{\mu\nu}$ as,

$$T^{\text{visc}}_{\mu\nu} = -\eta\sigma_{\mu\nu} - \zeta\Delta_{\mu\nu}\nabla_{\gamma}u^{\gamma}. \tag{1.149}$$

Then the equations of motion,

$$\nabla^{\mu}(T^{\text{perf}}_{\mu\nu} + T^{\text{visc}}_{\mu\nu}) = 0 \tag{1.150}$$

are the relativistic analogue of (1.145).

The fluid/gravity duality

The motivation for the fluid/gravity correspondence comes from the discovery of the AdS/CFT correspondence by Juan Maldacena in the late 90s [41]. The AdS here means Anti-de Sitter spacetime and the CFT means a conformal field theory.

The AdS/CFT correspondence, it is popularly known, arises in the context of string theory. Broadly speaking it relates a gravitational theory in a particular spacetime (the bulk) to a non-gravitational conformal field theory on its boundary. The particular example from which it arose is of type IIB string theory which is asymptotically $AdS_5 \times S^5$ and a $\mathcal{N} = 4$ SYM gauge theory on the boundary, which describes strongly coupled systems like quarks, for example [2]. Although the AdS/CFT correspondence (also gauge/gravity correspondence) provides a motivation for fluid/gravity duality it is not required for it.

This is not the first instance where a connection has been between spacetime and fluid-like behaviour. There is a good amount of similarity between black holes and fluid-like phenomena. As early as the 70's due to Hawking's famous result on black holes thermodynamics and Hawking radiation [29], fluid analogues with sonic horizons were motivated to check for Hawking radiation [61]. The higher dimensional black string solution develops the famous Gregory-Laflamme instability which bears a striking similarity to the Rayleigh-Plateau instability of fluid droplets [9] [25]. Finally there is also the celebrated Membrane paradigm where the horizon of a black hole is modelled to have fluid like properties like viscosity and conductivity [14] [60].

For the fluid/gravity program, mainly we will see that for a AdS Schwarzschild black hole geometry in the bulk a stress tensor on its boundary can be calculated through the induced boundary metric. Then it can be shown that the EFE in the bulk imply the fluid equations for this boundary stress tensor.

In the following we shall demonstrate how the fluid/gravity duality arises for solutions of EFEs called black branes. The treatment here follows closely the work done in [63], which is an application of the techniques developed in [6]. Specifically we will be interested in the uniform AdS_4 black brane solution with cosmological constant, $\Lambda = 3$. The metric is,

$$ds^2 = 2dvdr - r^2 f(br)dv^2 + r^2 dx^i dx^i \tag{1.151}$$

with $f(r) = 1 - 1/r^3$ and $b = 3/(4\pi T)$, where T is the Hawking temperature of the black hole. Consider then the velocity,

$$u^\mu = (1, 0, 0) \quad \text{and} \quad u_\mu = (-1, 0, 0). \tag{1.152}$$

And also, the projection operator,

$$P_{\mu\nu} = \eta_{\mu\nu} + u_\mu u_\nu \tag{1.153}$$

where μ, ν run over all the indices except r, this makes u_μ a boundary velocity on surfaces on constant r. In terms on this velocity we can write the metric as,

$$ds^2 = -2u_\mu dx^\mu dr - r^2 f(br) u_\mu u_\nu dx^\mu dx^\nu + r^2 P_{\mu\nu} dx^\mu dx^\nu. \tag{1.154}$$

This form of the metric makes the velocity of the dual fluid manifest. Then consider the following form of the velocity, u^μ,

$$u^0 = \frac{1}{\sqrt{1 - \vec{\beta}^2}} \qquad u^i = \frac{\beta^i}{\sqrt{1 - \vec{\beta}^2}}. \tag{1.155}$$

The next step is to find perturbations of this metric that satisfy the EFE which will prove to be useful when perturbing the metric.

Now we perturb the metric in a specific manner, the first step is to change b and β to slowly varying functions of x^μ, i.e., $b(x^\mu)$ and $\beta(x^\mu)$ and say, we call the metric with this change, $g^{(0)}$. Of course, $g^{(0)}(r, b(x^\mu), \beta(x^\mu))$ no longer solves the EFE. Also, let us do a coordinate change $x^\mu \to \epsilon x^\mu$, where ϵ helps to clarify the perturbation procedure and will later be changed to unity. To see how, note that the power of ϵ will match the order of derivatives of β and b w.r.t. x^μ. The idea is to expand the solution g to EFE in powers of ϵ;

$$g = g^{(0)} + \epsilon g^{(1)} + \epsilon^2 g^{(2)} + \mathcal{O}(\epsilon^3). \tag{1.156}$$

Then the same is done for $\beta(x^\mu)$ and $b(x^\mu)$;

$$\beta^i = (\beta^{(0)})^i + \epsilon(\beta^{(1)})^i + \epsilon^2(\beta^{(2)})^i + \mathcal{O}(\epsilon^3) \tag{1.157}$$

$$b = b^{(0)} + \epsilon b^{(1)} + \epsilon^2 b^{(2)} + +\mathcal{O}(\epsilon^3). \tag{1.158}$$

Further, the following gauges are chosen;

$$g_{rr} = 0 \qquad g_{r\mu} \propto u_\mu \qquad (g^{(0)})^{\mu\nu} g^{(n>0)}_{\mu\nu} = 2g^{(n)}_{rv} + \frac{1}{r^2} g^{(n)}_{ii}. \tag{1.159}$$

Next say the solution up to certain order $m \leq n-1$ has been found. Which means that equations (1.156), (1.157) and (1.158) are known up to the coefficients of order ϵ^m. Then one more order is added and the metric is inserted into the EFE. Orders with ϵ^m cancel and the coefficient of ϵ^n gives,

$$H\left[g^{(0)}\left(r, (\beta^{(0)})^i, b^{(0)}\right)\right] g^{(n)}(r, x^\mu) = s_n \tag{1.160}$$

where the H is a second order differential operator with only an r dependence and its exact form depends only on the values of $(\beta^{(0)})^i$ and $b^{(0)}$ at x^μ. The right hand side of the equation, s_n, is a source term and arises from orders less than n.

Applying the above procedure for the case of AdS_4, we have the most general form of the metric to n^{th} order as,

$$\begin{aligned} g^{(n)} =& \frac{k_n}{r^2} u_\mu u_\nu dx^\mu dx^\nu - 2h_n u_\mu dx^\mu dr - r^2 h_n P_{\mu\nu} dx^\mu dx^\nu \\ & - \frac{2}{r}(j_n)_\nu u_\mu dx^\mu dx^\nu + r^2 (\alpha_n)_{\mu\nu} dx^\mu dx^\nu \end{aligned}$$

where the k, h, j, α have the dependence,

$$k_n(r, u_\mu(x), b(x)),\ h_n(r, u_\mu(x), b(x)),\ j_n^\mu(r, u_\mu(x), b(x)),$$
$$a_n^{\mu\nu}(r, u_\mu(x), b(x))$$

and contain derivatives upto n of $\beta^i(x^\mu)$ and $b(x^\mu)$. Further, it is sufficient to solve the EFE at a single point, $x^\mu = 0$ is chosen with coordinates such that, $b(0) = 1$ and $\beta_i(0) = 0$. This is done by going to a coordinate system in which we can set an arbitrary velocity to zero and an arbitrary $b^{(0)}$ to unity at $x^\mu = 0$. This can then used to write down the metric about any point, details can be found in [6]. This simplifies the above n^{th} order metric to;

$$\begin{aligned} g^{(n)}|_{x^\mu=0} =& \frac{k_n(r)}{r^2} dv^2 + 2h_n(r) dv dr - r^2 h_n(r) dx^i dx^i \\ & + \frac{2}{r} j_n^i(r) dv dx^i + r^2 \alpha^{ij}(r) dx^i dx^j. \end{aligned}$$

Then the equations (1.160) at n^{th} order become;

$$\begin{aligned}
W_{rr}^{(n)} = 0 \quad &\Rightarrow \quad \frac{1}{r^4}\frac{d}{dr}(r^4 h_n'(r)) = S_h^{(n)}(r) \\
r^4 f(r) W_{rr}^{(n)} - W_{ii}^{(n)} = 0 \quad &\Rightarrow \quad \frac{d}{dr}\left(\frac{-2}{r}k_n(r) + (1-4r^3)h_n(r)\right) = S_k^{(n)}(r) \\
W_{ri}^{(n)} = 0 \quad &\Rightarrow \quad \frac{r}{2}\frac{d}{dr}\left(\frac{1}{r^2}\frac{d}{dr}\vec{j_n}(r)\right) = \vec{S_j}^{(n)}(r) \\
W_{ij}^{(n)} - \frac{1}{2}\delta_{ij}W_{ii}^{(n)} = 0 \quad &\Rightarrow \quad \frac{d}{dr}\left(-\frac{1}{2}r^4 f(r)\frac{d}{dr}\alpha_n^{ij}(r)\right) = \mathbf{S}_\alpha^{(n)}(r)
\end{aligned}$$

where W_{IJ} is the Einstein's equations written as,

$$W_{IJ} \equiv R_{IJ} + 3g_{IJ} = 0. \tag{1.161}$$

The other set of equations arising from $W_{rv} = W_{vv} = W_{vi} = 0$ are called the constraint equations and do not contain $g^{(n)}$. These equations obey,

$$\partial_\mu T^{\mu\nu} = 0 \tag{1.162}$$

where $T^{\mu\nu}$ is the boundary stress tensor which is dual to the fluid, computed in the same manner as (1.131). We point out that since the boundary is at $r \to \infty$, the conservation equations (1.162) are conformally invariant [2]. Conformal invariance is defined as follows: let there be a field ψ which satisfies some equations $\mathcal{H}[\psi, g_{\mu\nu}] = 0$. Say we change the metric by a conformal factor, $g_{\mu\nu} = e^{2\phi}\tilde{g}_{\mu\nu}$. The equations $\mathcal{H}$ then are said to be conformally invariant iff $\mathcal{H}[\tilde{\psi}, \tilde{g}_{\mu\nu}] = 0$ for $\psi = e^{s\phi}\tilde{\psi}$ where $s \in \mathbb{R}$ is the conformal weight. It has been shown [39] that the conservation equations $\nabla^\mu T_{\mu\nu}$ are

conformally invariant if,

$$T^{\mu}{}_{\mu} = 0 \quad \text{and} \quad s = -(d+2) \tag{1.163}$$

here d is the spacetime dimension of the fluid.

This is the central essence of how the fluid/gravity duality arises. The core idea is that the constraint equations of EFEs end up being equivalent to the conservation equations of the fluid. Notice that this is done for black branes. In the introduction it was mentioned that for spherical black hole perturbations we get a nice simplification of the linearized EFEs as a wave equation. We will see in Chapter 3, for AdS black hole perturbations this wave equation can be interpreted as the fluid conservation equation.

1.2 Overview

In this section we give a summary of the manuscripts.

1.2.1 Master equation as a radial constraint

In Section 1.1.6 we showed how perturbations to Schwarzschild black holes can be succinctly encoded in a master function ψ which satisfies the master equation (1.114). We can analogously perturb the AdS black holes also, and find similar master functions and a master equation. AdS space has the interesting feature that its spatial infinity is actually a timelike surface. In Section 1.1.8 we had demonstrated how, for a black brane solution, on this surface we can find a stress tensor which can be interpreted as the stress tensor of a fluid. Further in the bulk the constraints to the EFEs were dual to the conservation equations of the fluid. A similar duality also exists for black hole

solutions [4], [45]. Previous studies of the fluid/gravity duality for linear perturbations of spherically symmetric black holes relied on a frequency domain mode expansion of ψ.

In our work below, we emphasised that given a constant-r foliation on the space-time there always exists constraint equations on such a surface due to the Gauss-Codazzi equations. Further these conservation equations can be written as the conservation equations of a Brown-York stress tensor. We showed that if we consider these conservation equations on all constant-r surfaces, (not just the one at infinity), then we arrive precisely at the master equation (1.114). Hence we make a direct connection between conservation equations in one less dimensions of space and standard perturbation theory of black holes in the bulk.

An advantage of our approach is that we always work in the time domain and make no assumption on the form of ψ. We then continue on, and express the viscosity, velocity, energy and other fluid parameters in terms of the master function and find that all the time dependence for the fluid parameters arises from ψ. With expressing all fluid quantities in terms of ψ we set the stage for a more general duality between gravitational perturbations in the bulk and fluid quantities in the boundary.

1.2.2 Non-Newtonian fluids in the fluid/gravity duality (in progress)

This is a work in progress and in Chapter 4 we report on some preliminary results. In this section we provide the motivation for the study.

In Section 1.2.1 it was mentioned that one of the results we obtained were expressions for the fluid parameters in terms of the master function at any constant-r surface. Recall that this is more general than previous work that had been done strictly in the frequency domain [4], [45]. Amongst these fluid parameters is the shear viscosity η.

Usually the fluid is assumed to be Newtonian which means that the viscosity is constant. But in everyday life we frequently encounter fluids which are non-Newtonian, i.e., their viscosities are not necessarily constant through out the flow. A common example of such a fluid is "oobleck" which is a suspension of cornstarch particles in water, it is a shear thickening fluid, its viscosity increases with increased stress. In contrast consider ketchup which is a shear thinning fluid, its viscosity decreases with increased stress.

We find that our results from our study in Chapter 3 accommodate, under certain conditions, non-Newtonian fluids. Our preliminary results show that at late times in the evolution of a bulk perturbation we recover the constant viscosity, but at intermediate times we see non-Newtonian behaviour. In Chapter 4 we will provide all the relevant details.

1.2.3 Deformation of horizons during a merger

Above we had mentioned how LIGO's result [1] confirms the existence of gravitational radiation. It also provides strong evidence for the existence of black holes and black hole mergers. We carried out a study of a very specific type of merger called an extreme mass ratio (EMR) merger. EMR mergers have $\mu/M \to 0$, where μ is the mass of the small black hole and M is the mass of the larger black hole. Further we assume that this is a head-on merger and the particle falls along the $z-$axis which is the axis of symmetry.

The assumption, $\mu/M \to 0$ allows us to model the small black hole as a point particle moving along a radial trajectory in the geometry of the large Schwarzschild black hole. Since the particle is small its gravitational field can be modelled by a perturbation. Such a problem was first studied by Zerilli [66]. The treatment is

similar to Section 1.2.1, except that now the master equation has a source term,

$$[\Box - V(r)]\,\psi = S(r,t) \tag{1.164}$$

and only the even perturbations are excited due to the axisymmetry of the problem. Roughly speaking, the source term $S(r,t)$ is constructed from a spherical harmonics expansion of the stress tensor of the point particle. The master equation (1.164) is then integrated numerically with time symmetric initial data using a robust algorithm [42] [40]. We are particularly interested in how the event and apparent horizons deform as the merger proceeds. Hence, the quantity extracted from the numerical integration is $\psi(v) = \psi|_{\mathcal{H}_1}$ where $\mathcal{H}_1$ is the horizon and v is from ingoing coordinates.

Remarkably just from $\psi(v)$ we can compute both how the event horizon and apparent horizon deform. The deformation of the event horizon is constructed by calculating how the null generators forming the horizon of the large black hole are perturbed by the gravitational field of the particle. Since the event horizon is teleological in nature, we consider the null generators at the end of the merger and integrate them back in time. It is found that generators in the vicinity of the large black hole at early times join the event horizon. As these null generators join the horizons they cross each other forming caustics, which is prominent feature of all mergers.

The apparent horizon deformation is computed by slicing the spacetime into surfaces Σ_t of constant Schwarzschild time t. Since we know that for Schwarzschild black holes the event horizon and apparent horizon coincide we assume that the apparent horizon during the merger is a perturbation of the Schwarzschild apparent horizon at $r = 2M$. We then solve for the perturbation $\delta h(\theta)$ such that $\tau = r - 2M - \delta h(\theta) = 0$ is the scalar function defining the perturbed apparent horizon, S. We solve for $\delta h(\theta)$

by requiring that the outgoing null geodesics, which when projected onto Σ_t are normal to S, have vanishing expansion. We find a behaviour that at first seems counter intuitive, the apparent horizon surface appears to move inwards becoming concave outwards as the particle crosses the event horizon. Further thought shows that this behaviour can be understood in the following manner: as the particle gets closer its gravitational fields attracts null geodesics towards it, this causes an increase in the expansion of the outgoing null geodesics, hence the geodesics inside the $r = 2M$ that have a negative expansion increase to zero thus moving the zero expansion surface inwards. Thus we see that even by using simple linear perturbation theory we can capture the key features of an EMR merger.

1.2.4 Soliton Mechanics

In Section 1.1.4 we had discussed how small changes to the mass, spin, and charge of a four-dimensional black hole satisfy the first law of black hole thermodynamics (1.84). Then in Section 1.1.5 we showed how this law is generalized for five-dimensional Einstein-Maxwell spacetimes that have a non-trivial topology, specifically spacetimes that contain solitons. Thus we arrived at the first law of soliton mechanics, (1.95). In Chapter 6 we apply the first law of soliton mechanics to three different spacetimes. Also, this is where the techniques involving rod structure discussed in Section 1.1.2 are utilized.

The first spacetime is a single charged, non-supersymmetric gravitational soliton. This spacetime is constructed from the Chong-Cvetic-Lu-Pope (CCLP) class of solutions [11] in five-dimensional minimal gauged supergravity. These type of five-dimensional solutions are motivated by AdS/CFT duality which was discussed above, since on the boundary this corresponds to a four-dimensional non-gravitational CFT.

For our purposes though we consider the asymptotically flat case. The CCLP solutions are characterized by four non-trivial parameters, the charge, the mass and two angular momentum parameters that are independent. For a specific choice of these parameters one can "pinch off" a soliton, thus no black hole is present, but there is mass and angular momentum [12] [27]. The second example is a supersymmetric asymptotically flat spacetime containing two solitons. The solution is described as one that has a metric which takes a canonical form of a timelike fibration over a hyperKähler base space [22]. Similar to the previous example, the parameters of the solution can be fixed by solving "bubble equations" to arrive at two solitons. The final example we consider is an asymptotically flat dipole ring [16]. This is a spacetime which contains a horizon with topology $S^1 \times S^2$. If Σ is a spacelike slice then we have $\Sigma \cong \mathbb{R}^4 \# (S^2 \times D^2)$, hence we get disk contributions in the generalized first law for soliton mechanics.

In a nutshell, with these three examples we show the extra terms that arise in the first law (1.95) as a result of the non-trivial spacetime topology. For the case of the black ring we show the terms in the first law are needed to get the correct variational law for δM. These terms are needed since the black ring has non-trivial topology in its exterior, i.e., a disk. Further we demonstrate for spacetimes that contain only solitons the presence of conserved charges M and J even in the absence of horizons.

Chapter 2

Co-authorship Statement

Table 2.1 below summarizes the contribution of all authors.

	Master equation as a radial constraint	Non-Newtonian fluids in the fluid/gravity duality (in progress)	Deformation of horizons during a merger	Soliton Mechanics
Design and identification of the research proposal	IB	UH	IB	HK
Practical aspects of the research	UH	UH	UH	HK, SG and UH
Data analysis and numerics	UH	UH	UH	SG and UH
Manuscript preparation	UH with edits from IB and HK	UH	UH with edits from IB	HK and SG with minor edits by UH
Status	Published: PhysRevD.93.123001	In progress	Posted (arXiv:1705.01510) soon to be submitted	Published :PhysRevD.94.124029

Table 2.1: Contributions of the different authors. The initials are, Dr. Ivan Booth (IB), Dr. Hari Kunduri (HK), Sharmila Gunasekaran (SG), Uzair Hussain (UH).

Chapter 3

Master equation as a radial constraint

Master equation as a radial constraint

Uzair Hussain,* Ivan Booth,† and Hari K. Kunduri‡

Department of Mathematics and Statistics,

Memorial University of Newfoundland St John's NL A1C 4P5, Canada

(Dated: September 21, 2017)

Abstract

We revisit the problem of perturbations of Schwarzschild-AdS$_4$ black holes by using a combination of the Martel-Poisson formalism for perturbations of four-dimensional spherically symmetric spacetimes [1] and the Kodama-Ishibashi formalism [2]. We clarify the relationship between both formalisms and express the Brown-York-Balasubramanian-Krauss boundary stress-energy tensor, $\bar{T}_{\mu\nu}$, on a finite-r surface purely in terms of the even and odd master functions. Then, on these surfaces we find that the spacelike components of the conservation equation $\bar{\mathcal{D}}^{\mu}\bar{T}_{\mu\nu} = 0$ are equivalent to the wave equations for the master functions. The renormalized stress-energy tensor at the boundary $\frac{r}{L}\lim_{r\to\infty}\bar{T}_{\mu\nu}$ is calculated directly in terms of the master functions.

* uh1681@mun.ca

† ibooth@mun.ca

‡ hkkunduri@mun.ca

I. INTRODUCTION

The linear perturbation theory of Schwarzschild spacetimes has been applied to a wide range of physical scenarios such as the prediction of gravitational radiation, stability analysis, studying binary systems, and the scattering and absorption of gravitational radiation [3]. Since its inception by Regge and Wheeler [4] as a tool for studying the stability of Schwarzschild black holes, the perturbation formalism has received steady enhancements. Early fundamental contributions were made by Zerilli [5], Vishweshwara [6] and Chandrasekhar [7]. Although powerful, the equations were limited to particular gauge choices under infinitesimal coordinate transformations: the well-known Regge-Wheeler, and Zerilli gauges. This lack of gauge invariance was remedied by Moncrief in [8] where the equations were presented in a gauge invariant formalism. Further upgrades to a coordinate independent formalism were made by Gerlach and Sengupta [9].

More recently, there have been two further generalizations which incoporate gauge invariance and coordinate independence. Martel and Poisson developed a particularly robust and practical four-dimensional formalism in [1] which also included the linear effect of matter sources. Meanwhile, in [2] Kodama and Ishibashi generalized to perturbations of any maximally symmetric black hole in spacetime dimensions $d \geq 4$.

In the current work we apply the formalisms developed in these two papers to study aspects of the AdS/CFT correspondence. We are especially interested in the body of work flowing from the calculation of the effective shear viscosity of the gauge theory in the strongly coupled regime at finite temperature [10]. The marrow of that calculation was the observation that an interacting quantum field theory under local thermal equilibrium can be effectively described in terms of fluid dynamics [11]. In this regime the AdS/CFT correspondence can be viewed as a fluid/gravity correspondence

by looking at long wavelength fluctuations about equilibrium (see [12] and [13] and references therein).

In this regime the fields on both sides of the duality are classical and so it can be established independently without recourse to more general arguments. Directly from general relativity, one may identify the Brown-York-Balasubramanian-Krauss (BYBK) stress-energy tensor [14] induced at timelike infinity with the stress-energy tensor of a near-ideal fluid. In such a setting one may compare the perturbations of black holes/branes with corresponding perturbations of the fluid velocity, energy, and pressure.

For five-dimensional AdS_5 black-brane spacetimes, a systematic procedure to study this correspondence was developed by Bhattacharyya et. al. [11]. The approach begins by writing an equilibrium brane solution coordinate-boosted to the proper velocity of the boundary fluid. One then perturbatively solves the Einstein equations order-by-order over the background metric in terms of derivatives of the boundary fluid velocity and temperature. In analogy to the (3+1) formulation of general relativity, the Einstein equations can be decomposed into constraints on (timelike) constant coordinate-radius surfaces along with radial evolution equations.

Now, even away from infinity, one can calculate a quasilocal BYBK stress-energy tensor on each surface of constant coordinate-radius. A crux of the calculation is that the diffeomorphism-constraint equation on each constant-radius surface is identical with the conservation of the induced stress-energy tensor along that surface[1]. Meanwhile the radial evolution equation ensures that such surfaces link together to form a coherent spacetime.

In [11] this formalism was worked out for AdS_5 black branes up to second order

[1] The conservation law follows directly from the Gauss-Codazzi equations. From the geometric perspective it is an identity which holds on any timelike surface.

in derivative expansion. Since the behaviour of 2+1 dimensional fluids is different, especially in terms of the behaviour of turbulence, Raamsdonk in [15], applied the same methods to AdS_4 black branes again up to second order in derivatives.

In this current paper we will be concerned with how the fluid/gravity duality arises for large[2] spherical AdS_4 black holes. Some work has already been done in this area. For example a connection between the bulk dynamics of the spherical black hole and the boundary fluid has been made in terms of the quasinormal modes (QNMs) of the black hole which were first calculated in [23]. In [17] the QNMs of the perturbations expanded in even spherical harmonics were computed using a Robin boundary condition. The authors showed that there were low lying modes which, for large black holes, corresponded precisely to the modes of a linearly perturbed fluid on $\mathbb{R} \times S^2$, the boundary manifold under said Robin boundary conditions. For general boundary conditions the fluid/gravity duality in terms of the boundary BYBK stress-energy tensor is presented in [18] (and further considered in [19]) for both even and odd spherical harmonics.

Our goal is to understand how the well-developed perturbation theory of spherical black holes in AdS_4 is connected to the dynamics of the fluid. In particular we are interested in understanding the role of the master function on the fluid dynamics side: one of the most remarkable features of the perturbative formalism is that allowed perturbations of the spacetime are determined by a scalar master function which obeys an inhomogeneous wave equation [1, 2]. The whole system of Einstein's equations can be characterized by this master variable along with equations that relate it back to the components of the metric perturbation.

We will show that this master equation is equivalent to the conservation of the

[2] Recall that only black holes whose mass is large relative to the radius of cosmological curvature are thermodynamically stable[16]. Black branes are all large but spherical Schwarzschild-AdS black holes can be either large or small.

quasilocal BYBK stress-energy tensor on finite-r surfaces. This can be thought of as a (non-trivial) extension of the result from the black-brane formalism [11], where the radial constraint equation was shown to be equivalent to the conservation equation of the induced stress-energy tensor and the rest were radial evolution equations. Here, in the spherical case, we show that if we rewrite the metric perturbations in term of the master function then the conservation of the induced stress-energy is equivalent to the master equation. This can be contrasted to the work of [20], in which it was shown that prescribing a Lorenzian metric on a constant-r surface could be used to determine the bulk black brane spacetime metric in the long wavelength regime.

We also show how the form of the BYBK stress-energy tensor is greatly simplified when expressed in terms of the master variable. We provide formulas for the energy, pressure, velocity, viscosity, and vorticity in terms of the master variable both in the bulk and at the boundary. This enables us to express the quantities in the time domain rather than the frequency domain. Lastly, we go to the frequency domain to demonstrate how the fluid at the boundary arises for large black holes.

The paper is organized as follows. Section II reviews standard perturbation theory for spherical black holes in AdS_4. Section III considers the stress-energy tensor induced on finite-r surfaces and shows that the conservation equations are equivalent to the master equations derived in the previous section. Section IV shows how properties of the fluid (e.g. energy, pressure) can be identified in terms of the master function. We discuss some open problems in Section V.

II. PERTURBATIONS OF ADS$_4$ BLACK HOLES

The Schwarzschild AdS$_4$ black hole is a solution to Einstein's equations with a negative cosmological constant $\Lambda < 0$,

$$R_{\alpha\beta} = \Lambda g_{\alpha\beta} \tag{1}$$

and the metric exterior to the event horizon is given by

$$ds^2 = -f(r)dt^2 + \frac{1}{f(r)}dr^2 + r^2(d\theta^2 + \sin^2\theta d\phi), \tag{2}$$

with, $f(r) = 1 - \frac{2M}{r} + \frac{r^2}{L^2}$ and $L = \sqrt{\frac{-3}{\Lambda}}$. The metric is stationary and spherically symmetric, with $-\infty < t < \infty$, $0 < \theta < \pi$, $0 < \phi < 2\pi$ and $r > r_+$ where r_+ is the largest root of $f(r)$. The spacetime is asymptotically AdS$_4$ with length scale L. Following [1], and given the spherical symmetry of the spacetime, the metric is expressed as,

$${}^4g_{\alpha\beta}dX^\alpha dX^\beta = g_{ab}dx^a dx^b + r^2\Omega_{AB}d\theta^A d\theta^B. \tag{3}$$

Here, ${}^4g_{\alpha\beta}$ is the full 4-dimensional metric, g_{ab} is the metric on the 2-dimensional submanifold $\mathcal{M}^2$, consisting of the orbits of spherical symmetry which in Schwarzschild coordinates is the spatio-temporal or '(r,t)' part. Lastly, Ω_{AB} are the components of the metric of a unit sphere, S^2. The 4-dimensional coordinates are expressed as X^α, the coordinates on $\mathcal{M}^2$ are expressed as x^a and the coordinates on the sphere are expressed as θ^A. Note that, $\{\alpha, \beta\}$ run over all coordinates, lower-case Latin indices run over r and t, and upper case Latin indices run over θ and ϕ. The covariant derivative compatible with g_{ab} will be written as ∇_a and the covariant derivative compatible with Ω_{AB} will be written as D_A. Again following [1] we will introduce the one-form r_a,

$$r_a = \frac{\partial r}{\partial x^a} \tag{4}$$

which is $r_a = (0, 1)$ in Schwarzschild coordinates.

A. Odd Perturbations

We may now perturb the black hole given by adding a perturbation, $p_{\alpha\beta}$. We shall expand this perturbation in terms of odd spherical harmonics, X_A and X_{AB}. Their precise definition can be found the Appendix. In what follows we closely follow [1] until (13). The perturbation is written as ${}^4g_{AB} = r^2\Omega_{AB} + p_{AB}$ and ${}^4g_{aB} = p_{aB}$, where,

$$p_{aB} = \sum_{lm} h_a^{lm} X_B^{lm} \ , \qquad p_{AB} = \sum_{lm} h_2^{lm} X_{AB}^{lm} \tag{5}$$

where h_a and h_2 are functions of x^a. Infinitesimal gauge transformations will also be expanded in terms of odd harmonics,

$$e_A = \sum_{lm} e^{lm} X_A^{lm} \tag{6}$$

with e^{lm} as a function of x^a. Under such gauge transformations we have, dropping the lm indices, the following gauge invariant variables,

$$\tilde{h}_a = h_a - \frac{1}{2}\nabla_a h_2 + \frac{1}{r} r_a h_2. \tag{7}$$

All gauge invariant quantities will have the '~' symbol hereafter. Using the linearized Einstein's equations we find that the whole system is characterized by the following equation,

$$(\Box - V_{odd})\tilde{\Xi}_{RW} = 0 \tag{8}$$

where $\Box$ is the d' Alembertian on $\mathcal{M}^2$, $\tilde{\Xi}_{RW}$ is the well known Regge-Wheeler master function and,

$$V_{odd} = \frac{\lambda}{r^2} - \frac{6M}{r^3} \tag{9}$$

for $\lambda = l(l+1)$. Further, in Schwarzschild coordinates, one may reconstruct the metric perturbations from the following equations,

$$\tilde{h}_t = f \int \partial_r \left(r \tilde{\Xi}_{RW} \right) dt' \quad \text{and} \tag{10}$$

$$\tilde{h}_r = \frac{r}{f} \tilde{\Xi}_{RW}. \tag{11}$$

Note that this system is underdetermined and so one needs to pick a gauge to fully reconstruct the perturbation. We will work in the Regge-Wheeler gauge with $h_2 = 0$.

One can also define an alternate master variable, the Cunningham-Moncrief-Price (CMP) function $\tilde{\Psi}$,

$$\frac{\mu}{2r} \tilde{\Psi} = \left(\partial_r \tilde{h}_t - \partial_t \tilde{h}_r - \frac{2}{r} \tilde{h}_t \right) \tag{12}$$

where $\mu = (l-1)(l+2)$. This is related to Ξ_{RW} by

$$\tilde{\Xi}_{RW} = \frac{1}{2} \partial_t \tilde{\Psi}. \tag{13}$$

Interestingly, $\tilde{\Psi}$ satisfies the same master equation, (8), as $\tilde{\Xi}_{RW}$.

We can compare the above results with those from the formalism of [2] by noting the following relationships between their notation and the one used here. Comparing the metric perturbations we find

$$h_a \leftrightarrow -r f_a \qquad \text{and} \qquad h_2 \leftrightarrow \frac{2r^2}{k_V} H_T \tag{14}$$

which leads to the following relationship for the gauge invariant variables

$$\tilde{h}_a \leftrightarrow -r F_a. \tag{15}$$

The master function in [2] is defined by

$$r F^a = \epsilon^{ab} \partial_b (r \tilde{\Psi}_{KI}). \tag{16}$$

Comparing (16) with (10) and (11) it can be deduced that

$$-2 \tilde{\Psi}_{KI} = \tilde{\Psi}. \tag{17}$$

So the master function used in [2] is essentially the same as that of CMP.

B. Even Perturbations

Following the same scheme as for the odd perturbations and [1], we write the perturbation $p_{\alpha\beta}$ as, ${}^4g_{ab} = g_{ab} + p_{ab}$, ${}^4g_{AB} = r^2\Omega_{AB} + p_{AB}$ and ${}^4g_{aB} = p_{aB}$. Now the perturbations will be expanded in even harmonics, Y^{lm}, Y^{lm}_A, Y^{lm}_{AB}, and $\Omega_{AB}Y^{lm}$. The definitions of these can be found in the Appendix. Then the perturbations are

$$p_{ab} = \sum_{lm} h^{lm}_{ab} Y^{lm}, \tag{18}$$

$$p_{aB} = \sum_{lm} j^{lm}_a Y^{lm}_B \quad \text{and} \tag{19}$$

$$p_{AB} = r^2 \sum_{lm} \left(K^{lm}\Omega_{AB}Y^{lm} + G^{lm}Y^{lm}_{AB} \right) \tag{20}$$

where h^{lm}_{ab}, j^{lm}_a, K^{lm} and G^{lm} are functions of x^a. Infinitesimal gauge transformations are expanded in terms of the even harmonics

$$e_a = \sum_{lm} e^{lm}_a Y^{lm} \qquad \text{and} \qquad e_A = \sum_{lm} e^{lm} Y^{lm}_A \tag{21}$$

with e^{lm}_a and e^{lm} as functions of x^a. Under such gauge transformations we have, dropping the lm indices, the following gauge invariant variables,

$$\tilde{h}_{ab} := h_{ab} - \nabla_a \varepsilon_b - \nabla_b \varepsilon_a \tag{22}$$

$$\tilde{K} := K + \frac{1}{2}\lambda G - \frac{2}{r} r^a \varepsilon_a \tag{23}$$

for,

$$\varepsilon_a := j_a - \frac{1}{2} r^2 \nabla_a G. \tag{24}$$

We now proceed using the master function from [2], since in [1] the treatment is for asymptotically flat rather than asymptotically AdS black holes. We can make this

switch by noting how the notation of the two compare:

$$h_{ab} \leftrightarrow f_{ab} \ , \quad j_a \leftrightarrow -\frac{1}{k} r f_a \ , \tag{25}$$

$$K \leftrightarrow 2H_L \quad \text{and} \quad G \leftrightarrow \frac{2}{k^2} H_T \tag{26}$$

which leads to relationships for the gauge invariant variables,

$$\varepsilon_a \leftrightarrow -X_a \ , \quad \tilde{h}_{ab} \leftrightarrow F_{ab} \quad \text{and} \quad \tilde{K} \leftrightarrow 2F. \tag{27}$$

Then in terms of the functions X,Y, and Z from [2] we have,

$$\tilde{h}_{tt} = -\frac{f}{2}\left(X - Y\right) \ , \quad \tilde{h}_{rr} = -\frac{1}{2f}\left(X - Y\right), \tag{28}$$

$$\tilde{h}_{rt} = \frac{1}{f} Z \quad \text{and} \quad \tilde{K} = -\frac{X + Y}{2}. \tag{29}$$

The master function is defined as;

$$\Phi(t, r) = \frac{2\tilde{Z} - r(X + Y)}{H} \tag{30}$$

where $Z = -\partial_t \tilde{Z}$, and the following equations hold:

$$X = \frac{1}{r}\left(-\frac{r^2}{f}\partial_t^2 \tilde{\Phi} - \frac{P_X}{16H^2}\tilde{\Phi} + \frac{Q_X}{4H} r \partial_r \tilde{\Phi}\right), \tag{31}$$

$$Y = \frac{1}{r}\left(\frac{r^2}{f}\partial_t^2 \tilde{\Phi} - \frac{P_Y}{16H^2}\tilde{\Phi} + \frac{Q_Y}{4H} r \partial_r \tilde{\Phi}\right) \quad \text{and} \tag{32}$$

$$Z = -\frac{P_Z}{4H}\partial_t \tilde{\Phi} + f r \partial_r \partial_t \tilde{\Phi}, \tag{33}$$

where

$$H := \mu + \frac{6M}{r} \tag{34}$$

and P_X, P_Y, Q_X, Q_Y and P_Z are all functions of r as defined in [2]. The master function satisfies the following wave equation:

$$(\Box - V_{even})\tilde{\Phi} = 0 \tag{35}$$

where,

$$V_{even} = \frac{1}{H^2}\Bigg[\mu^2\left(\frac{\mu+2}{r^2}+\frac{6M}{r^3}\right)+\frac{36M^2}{r^4}\left(\mu+\frac{2M}{r}\right) + 72\frac{M^2}{r^2L^2}\Bigg]. \tag{36}$$

III. STRESS-ENERGY TENSOR

In this section we will show how the conservation of the induced quasilocal stress-energy tensor on a finite-r surface is equivalent to the master equation, for both the odd and even perturbations. The formula for the stress-energy tensor is as in the usual Brown-York [21] treatment with Balasubramanian-Krauss counterterms added to regulate the $r \to \infty$ divergences for AdS [14]:

$$\bar{T}_{\mu\nu} := \kappa^{-2}\bar{\mathcal{T}}_{\mu\nu} = \bar{K}_{\mu\nu} - \bar{K}\bar{\gamma}_{\mu\nu} - 2\sqrt{-\frac{\Lambda}{3}}\bar{\gamma}_{\mu\nu} + \sqrt{-\frac{3}{\Lambda}}\,{}^3\bar{G}_{\mu\nu}, \tag{37}$$

where the indices $\{\mu,\nu\}$ run over all coordinates but r, κ^{-2} is a constant, $\bar{\gamma}_{\mu\nu}$ is the metric on the finite-r 3-surface, $\bar{K}_{\mu\nu}$ is the extrinsic curvature and $\bar{K} = \bar{\gamma}^{\mu\nu}\bar{K}_{\mu\nu}$ is its trace, and ${}^3\bar{G}$ is the Einstein tensor for $\bar{\gamma}_{\mu\nu}$. The bar notation is there to remind us that the quantity includes a perturbation, e.g, $\bar{A}_{\mu\nu} = A_{\mu\nu} + \delta A_{\mu\nu}$.

A. Stress-energy tensor for static AdS_4 black holes

In this section we calculate the stress-energy tensor for the static black hole, i.e., without perturbations. We use Schwarzschild coordinates with the normal vector,

$$n_\alpha = \frac{1}{\sqrt{f}}\delta^r_\alpha. \tag{38}$$

The metric on the timelike slice has components $\gamma_{tt} = -f(r), \gamma_{AB} = r^2\Omega_{AB}$ Using the following formula for the extrinsic curvature,

$$K_{\alpha\beta} = -\nabla_\alpha n_\beta - n_\alpha n^\gamma \nabla_\gamma n_\beta \tag{39}$$

the non-vanishing components are,

$$K_{tt} = \frac{\sqrt{f}f'}{2} \quad \text{and} \quad K_{AB} = -\sqrt{f}r\Omega_{AB} \tag{40}$$

with trace

$$K = -\frac{f'}{2\sqrt{f}} - \frac{2\sqrt{f}}{r}. \tag{41}$$

After including the counter terms shown in (37) the non-vanishing components of the stress-energy tensor are

$$T_{tt} = \frac{1}{r^2}\left(L + \frac{2r^2}{L} - 2r\sqrt{f}\right) f = \tau_1 f \quad \text{and} \tag{42}$$

$$T_{AB} = \left(\frac{f'}{2\sqrt{f}} + \frac{\sqrt{f}}{r} - \frac{2}{L}\right) r^2\Omega_{AB} = \tau_2 r^2 \Omega_{AB} \tag{43}$$

which defines the functions τ_1, τ_2.

B. Conservation of odd stress-energy tensor

In this section we will calculate the the odd perturbation of the stress-energy tensor and demonstrate the equality of the conservation equation and the odd master equation (8). To calculate the perturbation note that since we are taking traces with $\bar{\gamma}^{\mu\nu} = \gamma^{\mu\nu} - \delta\gamma^{\mu\nu}$, the trace of an unperturbed quantity will pick up a perturbation, for e.g., $\bar{A} = \gamma^{\mu\nu}A_{\mu\nu} - \delta\gamma^{\mu\nu}A_{\mu\nu}$. The expression for the odd perturbation to the stress-energy tensor in a general gauge is,

$$\begin{aligned}\delta T_{tA} =& \frac{\sqrt{f}}{2}\left(\partial_t\tilde{h}_r - \partial_r\tilde{h}_t + \frac{2}{r}\tilde{h}_t\right) X_A \\ &+ \frac{L\mu}{2r^2}\tilde{h}_t X_A + \tau_2 h_t X_A \quad \text{and}\end{aligned} \tag{44}$$

$$\delta T_{AB} = \left(\sqrt{f}\tilde{h}_r - \frac{L}{f}\partial_t\tilde{h}_t\right) X_{AB} + \tau_2 h_2 X_{AB}. \tag{45}$$

These terms cannot be written purely in terms of the gauge independent $\tilde{h}_a$ (7) and so the quasilocal stress-energy is gauge dependent. However, this dependence does not effect the conservation equations: they hold for all gauges.

This invariance allows us to freely choose a gauge. We choose the Regge Wheeler gauge $h_2 = 0$, $\tilde{h}_t = h_t$ and $\tilde{h}_r = h_r$ and use (10) and (11) to express the stress-energy tensor in terms of Ξ_{RW}. Now, we invoke the conservation equations

$$\tilde{\mathcal{Q}}_\nu := \bar{\mathcal{D}}^\mu \bar{T}_{\mu\nu} = 0. \tag{46}$$

Here the $\bar{\mathcal{D}}$ is the covariant derivative compatible with $\bar{\gamma}_{\mu\nu}$, the bar on $\mathcal{D}$ indicates that the Christoffel symbol contains a perturbation. The index is raised with metric plus its perturbation, $\tilde{\gamma}_{\mu\nu} = \gamma_{\mu\nu} + \delta\gamma_{\mu\nu}$. Keeping only the linear terms we find that the $\nu = t$ equation of (46) is trivially satisfied, whereas the $\nu = A$ equations result in

$$(\Box - V_{odd})\,\tilde{\Xi}_{RW} X_A = 0 \tag{47}$$

which is equivalent to the Regge-Wheeler master equation (8). If the substitution above is done in terms of the CMP function $\tilde{\Psi}$ by using the relationship (13) instead of the Regge Wheeler function all components of (46) are trivally satisfied. This is because the relationship, (13), between the CMP function and the Regge Wheeler function assumes that the master equation is satisfied.

C. Conservation of even stress-energy tensor

As mentioned in the beginning of the previous section, we must keep the subtleties of the trace in mind when using (37) to calculate the even perturbation of the stress-energy tensor. Since the expression is lengthy we have included it in the Appendix.

We use the gauge condition $G = j_t = j_r = 0$ and, in analogy with the odd case, we invoke the conservation equations (46). Keeping only the linear terms we find that

the $\nu = t$ component of (46) gives,

$$\left[\left(\frac{\sqrt{f}}{r} - \frac{f'}{2\sqrt{f}}\right)\partial_t K - \frac{\lambda\sqrt{f}}{2r^2}h_{tr} - \frac{f\sqrt{f}}{r}\partial_t h_{rr} + \sqrt{f}\partial_r\partial_t K\right]Y = 0 \tag{48}$$

which is the same as the tr component of the Einstein equations. Using (48) and (28)−(33), it can be shown that the $\nu = A$ components yield:

$$(\Box - V_{even})\,\tilde{\Phi}_{even}Y_A = 0 \tag{49}$$

which is equivalent to the even master equation, (35).

IV. FLUID REPRESENTATION

In this section we show how the stress-energy tensor, along with its perturbation, can be expressed in a fluid form, determined entirely from the master function. This allows us to connect fluid properties like energy, velocity, viscosity, and vorticity with gravitational quantities of the bulk. We will make this connection both at finite-r surfaces and at infinity.

To begin, we briefly review the fluid stress-energy tensor (we closely follow [18]). For perfect fluids we have

$$T_{\mu\nu} = \mathcal{E}u_\mu u_\nu + \mathcal{P}\Delta_{\mu\nu} \tag{50}$$

where, $\mathcal{E}$ is the energy density, $\mathcal{P}$ is the pressure, and $\Delta_{\mu\nu} = u_\mu u_\nu + \gamma_{\mu\nu}$. As $r \to \infty$ the trace of this stress tensor vanishes however at finite-r this is not generally the case. Instead we have,

$$\mathcal{P} = \frac{1}{2}\left(T + \mathcal{E}\right) \tag{51}$$

where T is the trace of (50). To include the effects of dissipation the stress-energy

tensor may be written as

$$\bar{T}_{\mu\nu} = \bar{\mathcal{E}} u_\mu u_\nu + \bar{\mathcal{P}} \bar{\Delta}_{\mu\nu} + \Pi_{\mu\nu}. \tag{52}$$

We have added a '$-$' over quantities to show that there may be linear perturbations to the metric, energy and pressure. Note that now (51) is also modified to include perturbations,

$$\bar{\mathcal{P}} = \frac{1}{2}\left(\bar{T} + \bar{\mathcal{E}}\right) \tag{53}$$

and we will be working in the Landau frame,

$$\bar{T}_{\mu\nu} u^\nu = -\bar{\mathcal{E}} u_\mu. \tag{54}$$

The quantity $\Pi_{\mu\nu}$ is transverse to the velocity and captures the viscous effects of the fluids and can be expanded in terms of the derivatives of the velocity:

$$\Pi_{\mu\nu} = \Pi^{(1)}_{\mu\nu} + \Pi^{(2)}_{\mu\nu} + \dots \tag{55}$$

where the superscripts denote the order of the derivative of u_μ. We will only be interested in the first order,

$$\Pi^{(1)}_{\mu\nu} = -\eta\sigma_{\mu\nu} - \zeta \bar{\Delta}_{\mu\nu} \bar{\mathcal{D}}_\gamma u^\gamma \tag{56}$$

with η as the shear viscosity and ζ is the bulk viscosity which we will take to be zero. This leaves us with $-\eta\sigma_{\mu\nu}$ for

$$\sigma_{\mu\nu} = 2\bar{\mathcal{D}}_{<\mu} u_{\nu>} \tag{57}$$

and

$$\bar{\mathcal{D}}_{<\mu} u_{\nu>} = \bar{\Delta}_{\mu\sigma} \bar{\Delta}_{\nu\gamma} \bar{\mathcal{D}}^{(\sigma} u^{\gamma)} - \frac{1}{2} \bar{\mathcal{D}}_{\mu\nu} \bar{\Delta}_{\sigma\gamma} \bar{\mathcal{D}}^\sigma u^\gamma. \tag{58}$$

Hence, $\sigma_{\mu\nu}$ is the transverse, symmetric, and traceless part of $\Pi^{(1)}_{\mu\nu}$. We will also make use of the following formula for the anti-symmetric vorticity tensor:

$$\bar{\omega}_{\mu\nu} = \bar{\Delta}_{\mu\sigma} \bar{\Delta}_{\nu\gamma} \bar{\mathcal{D}}^{[\sigma} u^{\gamma]} \tag{59}$$

It was shown in [18] that the vorticity of the fluid vanishes at infinity when even perturbations were used. Below, we confirm that this result continues to hold on finite-r surfaces.

A. Fluid representation of the static stress-energy tensor

We can quite easily get the fluid representation for the static case by using the Landau condition (54) with (42) and (43) as the stress-energy tensor. By taking $\mu = t$ in (54) we find the energy density to be

$$\mathcal{E} = \tau_1 \,. \tag{60}$$

The trace is given by, $T = 2\tau_2 - \tau_1$. Thus, by using (51) we find the pressure to be

$$\mathcal{P} = \tau_2 \,. \tag{61}$$

Finally, by taking the $\mu = A$ in (54) we have

$$u_A = 0 \tag{62}$$

and $u_t = -\sqrt{f}$ by requiring that $u^\mu u_\mu = -1$.

B. Fluid representation of the odd stress-energy tensor

To find the fluid representation with odd perturbations we use the CMP function (12). The form of the CMP function is particularly useful in simplifying the odd perturbations to the stress-energy tensor. In the gauge choice $h_2 = 0$, in terms of Ψ we have

$$\delta T_{tA} = \left(A\Psi + B\partial_{r^*}\Psi\right) X_A \quad \text{and} \tag{63}$$

$$\delta T_{AB} = \partial_t \left(C\Psi + D\partial_{r^*}\Psi\right) X_{AB} \tag{64}$$

where A, B, C and D are functions of r and are defined in the Appendix. Notice that we have removed the '$\sim$' symbol from Ψ to emphasize that a gauge choice has been made and one can only use equations (10) and (11) to get the metric components h_t and h_r, and not the gauge invariant quantities, $\tilde{h}_t$ and $\tilde{h}_r$. We can get the fluid representation of the odd stress-energy tensor by using the Landau frame (54) which allows us to find the energy density and the velocity of the fluid. The requirement for the fluid to be timelike gives

$$u_t = -\sqrt{f}\,. \tag{65}$$

The energy density is the same as the static case:

$$\mathcal{E} = \tau_1 \tag{66}$$

and since the trace of the stress-energy tensor is the same as the static case, the pressure is the same as (61). The spatial components of the velocity are $u_A = U_{odd} X_A$, where:

$$U_{odd} = -\chi \left[\left(A - \frac{f}{2}\tau_2 \right) \Psi + \left(B - \frac{r}{2}\tau_2 \right) \partial_{r^*} \Psi \right] \tag{67}$$

with

$$\chi = \frac{1}{\sqrt{f}\,(\mathcal{E} + \mathcal{P})}\,. \tag{68}$$

The shear tensor of this velocity field is $\sigma_{AB} = \Sigma_{odd} X_{AB}$ where

$$\Sigma_{odd} = 2U_{odd} - \sqrt{f}\Psi - \frac{r}{\sqrt{f}}\partial_{r^*}\Psi\,. \tag{69}$$

Since there are no perturbations to the energy and pressure, and we take $h_2 = 0$, we get

$$\Pi^{(1)}_{AB} = \delta T_{AB}. \tag{70}$$

Further since both σ_{AB} and δT_{AB} are proportional to X_{AB}, we can find the viscosity

$$\eta_{odd} = -\Sigma^{-1}_{odd}\partial_t \left(C\Psi + D\partial_{r^*}\Psi \right). \tag{71}$$

Finally, it was found in [18] that the odd vorticity is non-vanishing at the boundary. We find that on any finite-r surface the vorticity is

$$\omega_{AB} = U_{odd}\mathring{X}_{AB} \tag{72}$$

where $\mathring{X}_{AB}$ is an anti-symmetric tensor defined in the Appendix.

C. Fluid representation of the even stress-energy tensor

To find the fluid representation with even perturbations we proceed by using the gauge condition $G = j_t = j_r = 0$ and use (28)−(33) to write the stress-energy tensor in terms of Φ:

$$\delta T_{tt} = \left(E_1\Phi + E_2\partial_{r^*}\Phi + E_3\partial_t^2\Phi\right)Y, \tag{73}$$

$$\delta T_{tA} = \partial_t(F_1\partial_{r^*}\Phi + F_2\Phi)Y_A \quad \text{and} \tag{74}$$

$$\begin{aligned}\delta T_{AB} = &\left[G_1\Phi + G_2\partial_{r^*}\Phi + \partial_t^2(G_3\partial_{r^*}\Phi + G_4\Phi)\right]\Omega_{AB}Y \\ &+ \left(G_5\Phi + G_6\partial_{r^*}\Phi + G_7\partial_t^2\Phi\right)Y_{AB}\end{aligned} \tag{75}$$

where the E's, F's and G's are functions of r and are defined in the appendix. Note that we have again removed the '$\sim$' symbol, emphasizing that equations (28)−(33) may only be used to find h_{ab} and K, and not $\tilde{h}_{ab}$ and $\tilde{K}$. Continuing like we did for the odd case, we use the Landau condition to find the energy density and velocity. Requiring the fluid velocity be timelike gives,

$$u_t = -\sqrt{f} + \frac{1}{2\sqrt{f}}h_{tt}Y. \tag{76}$$

The perturbation to the energy density $\delta\mathcal{E}$ is given by:

$$\delta\mathcal{E} = \frac{1}{f}\left(E_1 + \frac{1}{2}f\tau_1 rV_{even}\right)\Phi + \frac{1}{f}\left(E_2 - \frac{\tau_1 Q_-}{8H}\right)\partial_{r^*}\Phi. \tag{77}$$

The spatial components of the velocity are $u_A = U_{even} Y_A$, where

$$U_{even} = -\chi \partial_t \left(F_1 \partial_{r^*} \Phi + F_2 \Phi \right). \tag{78}$$

The shear tensor of this velocity field is $\sigma_{AB} = \Sigma_{even} Y_{AB}$ where

$$\Sigma_{even} = 2 U_{even}. \tag{79}$$

To find the viscosity we recall that $\Pi^{(1)}_{AB}$ is a trace-free tensor on the sphere. So we expect that, $\Pi^{(1)}_{AB} = (\ldots) Y_{AB}$. To show this note that since the energy, trace, and hence the pressure have perturbations, we have

$$\Pi^{(1)}_{AB} = \delta T_{AB} - \mathcal{P} \delta \gamma_{AB} - \delta \mathcal{P} \gamma_{AB} \tag{80}$$

using (53) and the perturbation to the energy (77) it can be shown that

$$\Pi^{(1)}_{AB} = \delta T_{AB} - \frac{1}{2} \Omega_{AB} \delta T_{FG} \Omega^{FG} \tag{81}$$

which is the trace-free part of (75). Now, given that the shear tensor is also proportional to Y_{AB}, we may use (81) to find the viscosity

$$\eta_{even} = -\Sigma^{-1} \left(G_5 \Phi + G_6 \partial_{r^*} \Phi + G_7 \partial_t^2 \Phi \right). \tag{82}$$

We also found that the vorticity of the even perturbations vanishes, in agreement with results at infinity of [18].

D. Fluid Representation on boundary

In this section we show how we can take the above fluid representation of the fluid on finite-r surfaces to the surface where $r \to \infty$. Taking this limit we have the

following normalization factors:

$$\bar{\mathbf{T}}_{\mu\nu} = \lim_{r\to\infty} \frac{r}{L}\bar{T}_{\mu\nu}, \qquad \bar{\boldsymbol{\gamma}}_{\mu\nu} = \lim_{r\to\infty} \frac{L^2}{r^2}\bar{\gamma}_{\mu\nu},$$
$$\mathbf{u}_\mu = \lim_{r\to\infty} \frac{L}{r}u_\mu, \qquad \boldsymbol{\eta} = \lim_{r\to\infty} \frac{r^2}{L^2}\eta \text{ and}$$
$$\bar{\boldsymbol{\mathcal{E}}} = \lim_{r\to\infty} \frac{r^3}{L^3}\mathcal{E}.$$

This allows us to write down formulas for the fluid quantities at the boundary in terms of the odd and and even master functions at infinity. The stress-energy tensor at the boundary for the odd case is:

$$\delta\mathbf{T}_{tA} = \frac{1}{2L^2}\left(M\Psi_\infty + \frac{1}{2}\mu L^2\partial_{r^*}\Psi_\infty\right)X_A \tag{83}$$

$$\delta\mathbf{T}_{AB} = -\frac{1}{2}L^2\partial_{r^*}\dot{\Psi}_\infty X_{AB} \tag{84}$$

where $\Psi_\infty := \Psi(t, r=\infty)$, $\partial_{r^*}\Psi_\infty = \partial_{r^*}\Psi(t, r=\infty)$ and $\partial_{r^*}\dot{\Psi}_\infty := \partial_t\partial_{r^*}\Psi(t, r=\infty)$. The components of the velocity for the odd case are

$$\mathbf{u}_t = -1 \quad \text{and} \quad \mathbf{u}_A = -\frac{\mu L^2}{12M}\partial_{r^*}\Psi_\infty X_A\,. \tag{85}$$

Finally the viscosity for the odd case is,

$$\boldsymbol{\eta}_{odd} = -\frac{3ML^2\partial_{r^*}\dot{\Psi}_\infty}{\mu L^2\partial_{r^*}\Psi_\infty + 6M\Psi_\infty}. \tag{86}$$

Similarly for the even case we have the stress-energy tensor at infinity:

$$\delta\mathbf{T}_{tt} = \left[\left(\frac{\mu\lambda}{4L^2} + \frac{18M^2}{L^4\mu}\right)\Phi_\infty - \frac{3M}{L^2}\partial_{r^*}\Phi_\infty\right]Y \tag{87}$$

$$\delta\mathbf{T}_{tA} = -\frac{\mu}{4}\dot{\Phi}_\infty Y_A \tag{88}$$

$$\begin{aligned}\delta\mathbf{T}_{AB} = &\left[\left(\frac{\mu\lambda}{8} + \frac{3M^2}{L^2\mu}\right)\Phi_\infty - \frac{1}{2}M\partial_{r^*}\Phi_\infty\right]\Omega_{AB}Y \\ &+ \left[\left(\frac{\lambda}{4} + \frac{18M^2}{\mu^2L^2}\right)\Phi_\infty - \frac{3M}{\mu}\partial_{r^*}\Phi_\infty + \frac{L^2}{2}\ddot{\Phi}_\infty\right]Y_{AB}.\end{aligned} \tag{89}$$

The perturbation to the energy for the even case is

$$\delta\boldsymbol{\mathcal{E}} = \left(\frac{\mu\lambda}{4L^2} + \frac{18M^2}{L^4\mu}\right)\Phi_\infty - \frac{3M}{L^2}\partial_{r^*}\Phi_\infty. \tag{90}$$

The velocity for the even case is

$$\mathbf{u}_t = -1 \quad \text{and} \quad \mathbf{u}_A = \frac{L^2\mu}{12M}\dot{\Phi}_\infty Y_A \tag{91}$$

and finally the viscosity for the even case is,

$$\boldsymbol{\eta}_{even} = -\frac{6M}{L^2\mu\dot{\Phi}_\infty}\left[\left(\frac{\lambda}{4} + \frac{18M^2}{\mu^2L^2}\right)\Phi_\infty - \frac{3M}{\mu}\partial_{r^*}\Phi_\infty + \frac{L^2}{2}\ddot{\Phi}_\infty\right]. \tag{92}$$

When we go to the frequency domain we find that expressions (83)−(92) agree with those presented in [18].

V. CONCLUSION

As a result of a number of studies over the past few years, the fluid/gravity correspondence has come to be understood in a precise sense in particular for the brane (non-compact flat horizon) case. The aim of the present work was to explore the emergence of the duality from the viewpoint of standard perturbation theory. The dynamics of perturbations of spherical AdS black holes and their corresponding fluid interpretation were analyzed within the robust classical framework that describes perturbations of spherically symmetric black hole spacetimes. A key feature of this formalism is that it is covariant on the orbits of spherical symmetry (i.e. in the (t, r) coordinates). This allows one to avoid explicitly working in the frequency domain.

From this perspective an important question is: under what conditions do the gravitational perturbations have an equivalent description as a near-equilibrium fluid? This is certainly possible for large ($M \gg L$) black holes if the fluid is taken to live at timelike infinity on $\mathbb{R} \times S^2$. However even on surfaces of finite-r some fluid-like

behaviours remain. For example, the conservation of the quasilocal BYBK stress-energy tensor follows from a geometric identity that holds on all surfaces irrespective of the size of the black hole. Thus on any such surface the stress-energy tensor can be viewed as arising from some kind of matter that obeys conservation laws. Further, one can always write the stress-energy tensor in a fluid-like form. The real question then is: under what circumstances does that interpretation make sense so that the stress-energy evolves in the same way as that of a fluid?

In an effort to better understand the emergence of fluid behaviour we have reformulated as much of the problem as possible in terms of the well-developed perturbation theory of spherical spacetimes. We have seen that components of the stress-energy can be rewritten in terms of the master functions and the conservation laws are equivalent to the master equations. Various fluid quantities can then also be written in terms of the master function. In particular one can show that the expressions for viscosity match those found [18] when one restricts to the frequency domain and sends $r \to \infty$.

A natural further investigation would perform a numerical integration for the master function along the lines of [22]. Doing this for a range of parameters and studying the BYBK stress-energy tensor on surfaces of increasingly large r would allow one to study the emergence of "fluidness". More precisely one could determine the circumstances under which the identifications from Section IV produce a genuinely physical fluid.

As an example of non-fluid behaviour, note that even in the frequency domain one does not get a real viscosity for all QNMs. This emerges only for the case of low-lying modes [17]. Taking the odd viscosity as an example,

$$\boldsymbol{\eta}_{odd} = -\frac{3ML^2\partial_{r^*}\dot{\Psi}_\infty}{\mu L^2\partial_{r^*}\Psi_\infty + 6M\Psi_\infty} \tag{93}$$

for the boundary condition $\Psi_\infty = 0$ and assume $\Psi = R(r)e^{-i\omega t}$ then $\partial_{r^*}\Psi_\infty = K_1 e^{-i\omega t}$

and $\partial_{r^*}\dot{\Psi}_\infty = -i\omega K_1 e^{-i\omega t}$. Hence, in the frequency domain

$$\boldsymbol{\eta}_{odd} = i\omega\frac{3M}{\mu}. \tag{94}$$

If ω has a real part (for large black holes this frequency is purely imaginary [23],[18]) the viscosity is imaginary and so the identification of the BYBK stress-energy as that of a fluid fails.

We have made an initial attempt to implement this numerical integration. Unfortunately while our code ran well for small black holes, it developed numerical difficulties precisely during the transition to large black holes (where the required resolution at large r became impossibly fine). Similar problems were previously encountered in [24]. We will return to those issues in the future, but for now settle for having established the foundation from which those studies may proceed.

ACKNOWLEDGMENTS

UH is partially funded by a fellowship from the School of Graduate Studies at Memorial University and the National Science and Engineering Research Council of Canada (NSERC). IB and HK are supported respectively by NSERC Discovery Grants grants 261429-2013 and 418537-2012.

VI. APPENDIX

A. Odd and even stress-energy tensor

The even stress-energy tensor in terms of the metric perturbations in a general gauge is given by:

$$\begin{aligned}\delta T_{tt} =& \left(\frac{3\sqrt{f}}{r} - \frac{L}{r^2} - \frac{2}{L}\right) f^2 \tilde{h}_{rr} Y + \frac{\mu f L}{2r^2}\tilde{K}Y \\ & - f\sqrt{f}\partial_r \tilde{K} Y - 2\tau_1 \partial_t \varepsilon_t Y \\ & + \left[\left(\frac{L}{r^2} + \frac{2}{L} - \frac{3\sqrt{f}}{r}\right) f' + \frac{\mu f L}{r^3} + \frac{2f\sqrt{f}}{r^2} - \frac{\sqrt{f}\lambda}{r^2}\right] f\varepsilon_r Y \end{aligned} \tag{95}$$

$$\begin{aligned}\delta T_{tA} =& \left[\frac{1}{2}\sqrt{f}\tilde{h}_{tr} - \frac{1}{2}L\partial_t \tilde{K} + \frac{1}{2}\tau_2 r^2 \partial_t G \right. \\ & \left. + \left(\sqrt{f} - \frac{Lf}{r}\right)\partial_t \varepsilon_r - \tau_1 \varepsilon_t\right] Y_A \end{aligned} \tag{96}$$

$$\begin{aligned}\delta T_{AB} =& \left\{ \left(\frac{1}{4}Lf\lambda - \frac{3}{4}f'\sqrt{f}r^2 - \frac{1}{2}f^{3/2}r\right)\tilde{h}_{rr} \right. \\ & - \frac{1}{2}f^{3/2}r^2\partial_r \tilde{h}_{rr} + \frac{r^2}{\sqrt{f}}\partial_t \tilde{h}_{tr} - \frac{1}{2}\tau_2 r^2 \lambda G \\ & + \tau_2 r^2 \tilde{K} + \left[\left(\frac{1}{2}\sqrt{f} - \frac{1}{4}Lf'\right)\lambda + f(r^2\tau_2)'\right]\varepsilon_r \\ & \left. + \left(\frac{r^2}{\sqrt{f}} - Lr\right)\partial_t^2 \varepsilon_r + \frac{1}{2}\sqrt{f}r^2\partial_r \tilde{K} - \frac{1}{2}\frac{Lr^2}{f}\partial_t^2 \tilde{K}\right\}\Omega_{AB} Y \\ & + \left[\frac{1}{2}Lf\tilde{h}_{rr} + \tau_2 r^2 G + \left(\sqrt{f} - \frac{1}{2}Lf'\right)\varepsilon_r\right] Y_{AB} \end{aligned} \tag{97}$$

The radial functions defined for the odd stress-energy tensor are given by:

$$A = \frac{f}{2}\left(\frac{L\mu}{2r^2} + \tau_2\right) - \frac{\sqrt{f}\mu}{4r}, \qquad B = \frac{r}{2}\left(\frac{L\mu}{2r^2} + \tau_2\right), \tag{98}$$

$$C = \frac{r}{2\sqrt{f}} - \frac{L}{2} \quad \text{and} \quad D = -\frac{Lr}{2f}. \tag{99}$$

The radial functions for the even stress-energy tensor are given by the functions:

$$E_1 = \left(\frac{\sqrt{f}}{2} - \frac{L}{2r} - \frac{r}{L}\right) V_{even} f + \left(\sqrt{f} + \frac{L\mu}{2r}\right) \frac{f P_+}{32 H^2 r^2} - \frac{f\sqrt{f} P'_+}{32 H^2 r} + \frac{f\sqrt{f} P_+ H'}{16 H^3 r} \tag{100}$$

$$E_2 = \frac{L\mu f}{2r^2} + \left(-\frac{3\sqrt{f}}{r} + \frac{2}{L} + \frac{L}{r^2}\right) \frac{Q_-}{8H} - \frac{\sqrt{f} P_+}{32 H^2 r} \tag{101}$$

$$E_3 = - r\tau_1 \tag{102}$$

along with

$$F_1 = \frac{1}{2}\left(\frac{r}{\sqrt{f}} - L\right) \tag{103}$$

$$F_2 = - \frac{L P_+}{64 H^2 r} - \frac{P_Z}{8\sqrt{f} H} \tag{104}$$

and

$$G_1 = \left(\frac{\sqrt{f}}{2} - \frac{2r}{L} + \frac{f'r}{2\sqrt{f}} - \frac{\sqrt{f}H'r}{H}\right)\frac{P_+}{32H^2} + \frac{Q_-V_{even}r^2}{16\sqrt{f}H} + \left(\frac{L\lambda r}{8} - \frac{f'r^3}{8\sqrt{f}}\right)V_{even} - \frac{V'_{even}\sqrt{f}r^3}{4} + \frac{\sqrt{f}r}{2}\frac{P'_+}{32H^2} \tag{105}$$

$$G_2 = \left(r\sqrt{f} - \frac{L\lambda}{2} - \frac{r^2f'}{2\sqrt{f}} - \frac{\sqrt{f}H'r^2}{H}\right)\frac{Q_-}{16fH} + \frac{rP_+}{64\sqrt{f}H^2} - \frac{V_{even}r^3}{4\sqrt{f}} + r^2\tau_2 + \frac{Q'_-r^2}{16\sqrt{f}H} \tag{106}$$

$$G_3 = \frac{r^2}{2f}\left(\frac{r}{\sqrt{f}} - L\right) \tag{107}$$

$$G_4 = \frac{1}{f\sqrt{f}}\left(\frac{f'r^3}{4} + \frac{r^2Q_-}{16H} - \frac{P_Zr^2}{4H}\right) + \frac{1}{f}\left(\frac{L\lambda r}{4} - \frac{LP_+r}{64H^2}\right) - \frac{r^2}{2\sqrt{f}} \tag{108}$$

$$G_5 = \frac{rLV_{even}}{4} \tag{109}$$

$$G_6 = -\frac{LQ_-}{16fH} \tag{110}$$

$$G_7 = \frac{rL}{2f} \tag{111}$$

where $P_+ = P_X + P_Y$ and $Q_- = Q_X - Q_Y$.

B. Even Harmonics

This section closely follows [1], we include it here for completeness. For the even scalar sector we have the usual spherical harmonic functions $Y^{lm}(\theta, \phi)$ which satisfy the equation $[\Omega^{AB}D_AD_B + l(l+1)]Y^{lm} = 0$. The even vector harmonics are defined as:

$$Y^{lm}_A := D_AY^{lm}, \tag{112}$$

they satisfy the following orthogonality relations:

$$\int \bar{Y}^A_{lm} Y^{l'm'}_A \, d\Omega = l(l+1)\, \delta_{ll'} \delta_{mm'} \tag{113}$$

the bar indicates complex conjugation and $d\Omega := \sin\theta \, d\theta d\phi$ is the area element on the unit sphere. The tensor harmonics are $\Omega_{AB} Y^{lm}$ and

$$Y^{lm}_{AB} := \Big[D_A D_B + \frac{1}{2} l(l+1) \Omega_{AB} \Big] Y^{lm} \tag{114}$$

they satisfy the following orthogonality relations:

$$\int \bar{Y}^{AB}_{lm} Y^{l'm'}_{AB} \, d\Omega = \frac{1}{2}(l-1)l(l+1)(l+2)\, \delta_{ll'} \delta_{mm'} \tag{115}$$

and are traceless:

$$\Omega^{AB} Y^{lm}_{AB} = 0 \tag{116}$$

C. Odd Harmonics

This section also closely follows [1]. The odd scalar sector is empty since the scalar functions $Y(\theta, \phi)$ are even. The odd vector harmonics are defined as:

$$X^{lm}_A := -\varepsilon_A{}^B D_B Y^{lm}. \tag{117}$$

they satisfy the following orthogonality relations:

$$\int \bar{X}^A_{lm} X^{l'm'}_A \, d\Omega = l(l+1)\, \delta_{ll'} \delta_{mm'}, \tag{118}$$

the bar indicates complex conjugation and $d\Omega := \sin\theta \, d\theta d\phi$ is the area element on the unit sphere. The tensor harmonics are:

$$X^{lm}_{AB} := -\frac{1}{2} \big(\varepsilon_A{}^C D_B + \varepsilon_B{}^C D_A \big) D_C Y^{lm}. \tag{119}$$

they satisfy the following orthogonality relations:

$$\int \bar{X}^{AB}_{lm} X^{l'm'}_{AB}\, d\Omega = \frac{1}{2}(l-1)l(l+1)(l+2)\,\delta_{ll'}\delta_{mm'}. \tag{120}$$

and are traceless:

$$\Omega^{AB} X^{lm}_{AB} = 0 \tag{121}$$

We will also find it useful to define the following anti-symmetric tensor,

$$\mathring{X}_{AB} = D_{[A} X_{B]} \tag{122}$$

The odd and even vector harmonics are orthogonal:

$$\int \bar{Y}^{A}_{lm} X^{l'm'}_{A}\, d\Omega = 0, \tag{123}$$

as are the tensor harmonics:

$$\int \bar{Y}^{AB}_{lm} X^{l'm'}_{AB}\, d\Omega = 0. \tag{124}$$

---

[1] Karl Martel and Eric Poisson, "Gravitational perturbations of the Schwarzschild spacetime: A Practical covariant and gauge-invariant formalism," Phys. Rev. **D71**, 104003 (2005), arXiv:gr-qc/0502028 [gr-qc].

[2] Hideo Kodama and Akihiro Ishibashi, "A Master equation for gravitational perturbations of maximally symmetric black holes in higher dimensions," Prog. Theor. Phys. **110**, 701–722 (2003), arXiv:hep-th/0305147 [hep-th].

[3] V. P. Frolov and I. D. Novikov, eds., *Black hole physics: Basic concepts and new developments* (1998).

[4] Tullio Regge and John A. Wheeler, "Stability of a Schwarzschild singularity," Phys. Rev. **108**, 1063–1069 (1957).

[5] F. J. Zerilli, "Gravitational field of a particle falling in a schwarzschild geometry analyzed in tensor harmonics," Phys. Rev. **D2**, 2141–2160 (1970).

[6] C. V. Vishveshwara, "Stability of the schwarzschild metric," Phys. Rev. **D1**, 2870–2879 (1970).

[7] Subrahmanyan Chandrasekhar, *The mathematical theory of black holes* (1985).

[8] V. Moncrief, "Gravitational perturbations of spherically symmetric systems. I. The exterior problem." Annals Phys. **88**, 323–342 (1974).

[9] U. H. Gerlach and U. K. Sengupta, "Gauge invariant coupled gravitational, acoustical, and electromagnetic modes on most general spherical space-times," Phys. Rev. **D22**, 1300–1312 (1980).

[10] G. Policastro, Dan T. Son, and Andrei O. Starinets, "The Shear viscosity of strongly coupled N=4 supersymmetric Yang-Mills plasma," Phys. Rev. Lett. **87**, 081601 (2001), arXiv:hep-th/0104066 [hep-th].

[11] Sayantani Bhattacharyya, Veronika E Hubeny, Shiraz Minwalla, and Mukund Rangamani, "Nonlinear Fluid Dynamics from Gravity," JHEP **02**, 045 (2008), arXiv:0712.2456 [hep-th].

[12] Veronika E. Hubeny, Shiraz Minwalla, and Mukund Rangamani, "The fluid/gravity correspondence," in *Black holes in higher dimensions* (2012) pp. 348–383, [,817(2011)], arXiv:1107.5780 [hep-th].

[13] Mukund Rangamani, "Gravity and Hydrodynamics: Lectures on the fluid-gravity correspondence," *Strings, Supergravity and Gauge Theories. Proceedings, CERN Winter School, CERN, Geneva, Switzerland, February 9-13 2009*, Class. Quant. Grav. **26**, 224003 (2009), arXiv:0905.4352 [hep-th].

[14] Vijay Balasubramanian and Per Kraus, "A Stress tensor for Anti-de Sitter gravity," Commun. Math. Phys. **208**, 413–428 (1999), arXiv:hep-th/9902121 [hep-th].

[15] Mark Van Raamsdonk, "Black Hole Dynamics From Atmospheric Science," JHEP **05**, 106 (2008), arXiv:0802.3224 [hep-th].

[16] S. W. Hawking and Don N. Page, "Thermodynamics of Black Holes in anti-De Sitter Space," Commun. Math. Phys. **87**, 577 (1983).

[17] Georgios Michalogiorgakis and Silviu S. Pufu, "Low-lying gravitational modes in the scalar sector of the global AdS(4) black hole," JHEP **02**, 023 (2007), arXiv:hep-th/0612065 [hep-th].

[18] Ioannis Bakas, "Energy-momentum/Cotton tensor duality for AdS(4) black holes," JHEP **01**, 003 (2009), arXiv:0809.4852 [hep-th].

[19] Aida Ahmadzadegan, *Perturbation of Large Anti-deSitter Black Holes and AdS/CFT Correspondence*, Master's thesis, Memorial University of Newfoundland (2011).

[20] Daniel Brattan, Joan Camps, R. Loganayagam, and Mukund Rangamani, "CFT dual of the AdS Dirichlet problem : Fluid/Gravity on cut-off surfaces," JHEP **12**, 090 (2011), arXiv:1106.2577 [hep-th].

[21] J. David Brown and James W. York, Jr., "Quasilocal energy and conserved charges derived from the gravitational action," Phys. Rev. **D47**, 1407–1419 (1993), arXiv:gr-qc/9209012 [gr-qc].

[22] Bin Wang, C. Molina, and Elcio Abdalla, "Evolving of a massless scalar field in Reissner-Nordstrom Anti-de Sitter space-times," Phys. Rev. **D63**, 084001 (2001), arXiv:hep-th/0005143 [hep-th].

[23] Vitor Cardoso and Jose P. S. Lemos, "Quasinormal modes of Schwarzschild anti-de Sitter black holes: Electromagnetic and gravitational perturbations," Phys. Rev. **D64**, 084017 (2001), arXiv:gr-qc/0105103 [gr-qc].

[24] Jaqueline Morgan, Vitor Cardoso, Alex S. Miranda, C. Molina, and Vilson T. Zanchin, "Gravitational quasinormal modes of AdS black branes in d spacetime dimensions,"

JHEP **09**, 117 (2009), arXiv:0907.5011 [hep-th].

Chapter 4

Non-Newtonian fluids in the fluid/gravity duality (in progress)

Non-Newtonian fluids in the fluid/gravity duality

(Work in progress)

Department of Mathematics and Statistics,

Memorial University of Newfoundland St John's NL A1C 4P5, Canada

(Dated: September 21, 2017)

Abstract

For perturbations of AdS_4 black holes in the frequency domain of the master function there are certain "hydrodynamic frequencies", ω_{hydro}, which solve the master equation for large black holes. When considering this frequency as the only one present in the solution the stress tensor at $r \to \infty$ can be written in the form of a Newtonian fluid, i.e, as a fluid with a constant viscosity. In this note we show that a non-Newtonian (NN) fluid is one where the viscosity is no longer a constant but can be a function of other fluid parameters, like the shear. We demonstrate that such a NN fluid can arise when analysing the perturbations in the time domain as opposed to the frequency domain.

I. INTRODUCTION

It was demonstrated in [1] how the fluid/gravity duality manifests itself in the language of standard perturbation theory of spherically symmetric black holes. Specifically it was shown that there is an equivalence between the Zerilli-Regge-Wheeler master equations in the time domain and the conservation equations for the Brown-York stress tensor [2] on all constant-r surfaces. The work was motivated by previous studies for spherical black holes that had established the duality in the context of quasinormal modes of the master equation [3] [4]. For odd perturbations, which will be the subject of this note, we have specific quasinormal modes called hydrodynamic modes, ω_{hydro}, that are slow decaying and do not oscillate (purely imaginary). These hydrodynamic modes are thus called because they correspond to a Newtonian fluid on the $r \to \infty$ boundary.

In this note we perform a numerical time domain evolution for the master equation for the odd perturbations and use the results of [1] to argue how a non-Newtonian fluid may arise on a constant-r Dirichlet surface. The rest of this introduction defines NN-fluids and recalls some relevant results from [1] for the odd perturbations, in Section II we outline the numerical method used and in Section III provide the results.

A. NN fluids

In this section we briefly review how non-Newtonian fluids are modelled, it frequently draws upon [5]. Consider first Newtonian fluids. Let u^i be the velocity vector of a non-relativistic fluid on 3-dimensional flat Euclidean space. We may define the traceless "rate of deformation tensor" or traceless shear tensor as,

$$\sigma_{ij} = 2\partial_{(i}u_{j)} - \frac{2}{3}\delta_{ij}\partial^k u_k \tag{1}$$

Then if τ_{ij} is the shear stress, the two are related by,

$$\tau_{ij} = \eta\sigma_{ij} \tag{2}$$

where the constant of proportionality is the viscosity. For non-Newtonian fluids η is no longer a constant and may be a function of other fluid parameters. For example in Nature we see fluids that have a shear dependent viscosity. These can be modelled by defining $\dot{\gamma}^2 = \sigma_{ij}\sigma^{ij}/2$, and letting $\eta = \eta(\dot{\gamma})$. Then,

$$\frac{\partial\eta}{\partial\dot{\gamma}} > 0 \implies \text{shear-thickening} \qquad \frac{\partial\eta}{\partial\dot{\gamma}} < 0 \implies \text{shear-thinning.} \tag{3}$$

We commonly encounter non-Newtonian fluids in everyday life, ketchup is a non-Newtonian, shear-thinning fluid, "Oobleck" which is a suspension of corn starch particles in water is a shear-thickening fluid.

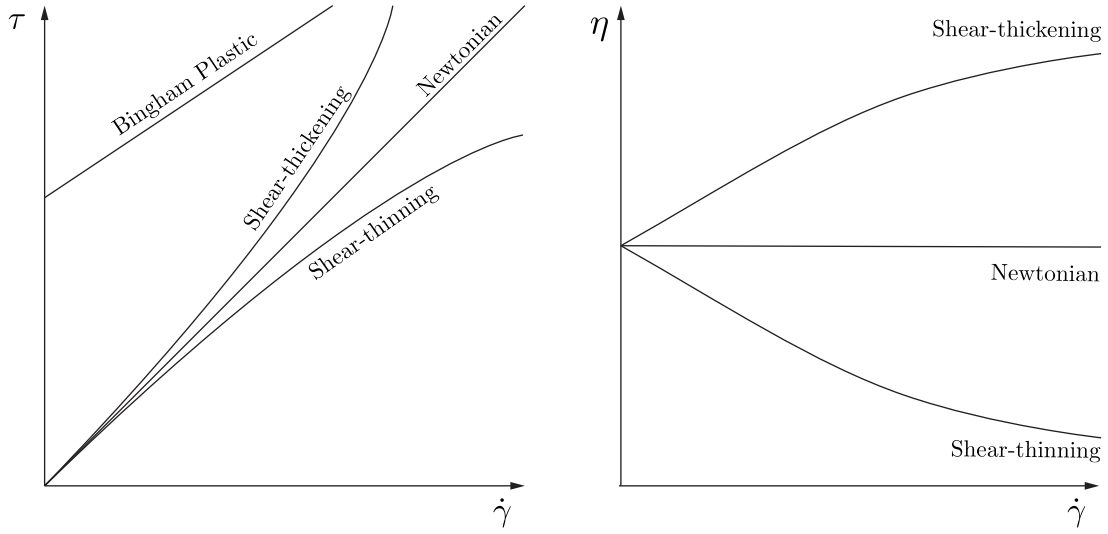

FIG. 1. A typical plot of τ vs. $\dot{\gamma}$ (left) and η vs. $\dot{\gamma}$ (right) , showing the different types of fluids.

There are other non-Newtonian behaviours, for example, viscoplastic fluids behave as solids under low stress, $\tau < \tau_c$, and as fluids when the stress is increased, $\tau > \tau_c$. A

simple example of viscoplastic fluids are Bingham plastics which behave as Newtonian fluids for $\tau > \tau_c$. Simple examples are mayonnaise and mustard. These fluids can hold peaks or ridges on their surface when behaving as a solid under low stress.

There also exist time dependent non-Newtonian fluids. Thixotropic fluids are such that if a constant shear, $\dot{\gamma}_0$ is applied the stress τ decreases monotonically as a function of time. In contrast, Rheopectic fluids are such that if a constant shear, $\dot{\gamma}_0$ is applied the stress τ increases monotonically as a function of time. In Figure 1 we have a typical plot of τ vs. $\dot{\gamma}$, and from (3) we see that the slope of the graph is the viscosity which is constant for the Newtonian fluid. In general, any deviation from this straight line implies a non-Newtonian fluid.

B. Viscosity in the fluid/gravity duality

Previously in [1] we had derived formulas relating the master function of black hole perturbations and fluid parameters. If we assume Dirichlet boundary conditions on a constant-r surface, r_C and consider only the odd perturbations, we can write the velocity and shear tensor as,

$$u_A^{odd} = \sum_l U^l_{odd} X^l_A \quad \sigma_{AB} = \sum_l \Sigma^l_{odd} X^l_{AB} \tag{4}$$

where X^l_A and X^l_{AB} are the l^{th} mode vector and tensor spherical harmonics respectively (we use $m = 0$ harmonics for simplicity), $A, B, \ldots$ run over θ,ϕ, and

$$U^l_{odd} = U^l_c \partial_{r^*} \Psi^l \quad \Sigma^l_{odd} = \Sigma^l_c \partial_{r^*} \Psi^l \tag{5}$$

where U^l_c and Σ^l_c are functions of r fixed at $r = r_c$ and can be read off from [1], and Ψ^l is the odd master function for the l^{th} mode. Finally the viscosity for the l^{th} mode perturbation can be written as,

$$\eta^l_{odd} = \eta^l_c \frac{\partial_t \Sigma^l_{odd}}{\Sigma^l_{odd}} \tag{6}$$

where $\eta_c = Lr_c/(2f(r_c)\Sigma_c^l)$ where L is the AdS length and $f(r) = 1 - 2M/r + r^2/L^2$. From (6) we can see how non-Newtonian behaviour may arise. We get the Newtonian case from a frequency domain expansion of the master function, $\Psi(t,r) = R(r)e^{-i\omega t}$. Then for each l mode we have a frequency $\omega^l_{\rm hydro}$ which solves the master equation. For odd perturbations $\omega^l_{\rm hydro}$ is imaginary [6–8]. Thus, we see that inserting the frequency domain solution with $\omega = \omega^l_{\rm hydro}$ into (6) we get a constant viscosity, i.e, a Newtonian fluid.

Now, if instead we were to integrate the master equation in the time domain and insert it into the viscosity equation (6), it is likely that we would get a different behaviour. Although for the fluid interpretation to still make sense we need to impose the condition that, $\eta^l_{odd} > 0$. Finally notice that Σ^l_{odd} is not identical to $\dot\gamma$. To get a better analogue of $\dot\gamma$ we need to calculate $\sigma_{AB}\sigma^{AB}$. We define the average shear as,

$$\langle\dot\gamma^l\rangle = \Sigma_c\partial_{r^*}\Psi|_{r_c}\left(\int X^{AB}X_{AB}d\Omega\right)^{1/2} = (\mu\lambda/2)^{1/2}\,\Sigma^l_{odd} \tag{7}$$

where we have taken the average over the sphere and, $\mu = (l-1)(l+2)$ and $\lambda = l(l+1)$. Thus we see that $\Sigma^l \propto \langle\dot\gamma^l\rangle$ and hence provides a good measure of the average shear.

II. NUMERICAL INTEGRATION OF Ψ

In this section we describe the algorithm used to integrate the master equation for the odd perturbations,

$$(\Box - V^l_{odd})\Psi^l = 0 \quad \text{where} \quad V_{odd} = \frac{\lambda}{r^2} - \frac{6M}{r^3} \tag{8}$$

and $\Box = \nabla^a\nabla_a$ where ∇_a is the covariant derivative compatible with g_{ab} where $a, b, \ldots$, run over r, t. We use algorithm employed in [9–11]. In double null coordinates (u, v) the master equation can be written as,

$$-4\partial_u\partial_v\Psi^l = fV^l_{odd}\Psi^l \tag{9}$$

which can be discretized as (we will omit the l indices wherever there is no confusion),

$$\left[1-\frac{\Delta^2}{16}V(S)\right]\Psi(N)=$$
$$\Psi(E)+\Psi(W)-\Psi(S)-\frac{\Delta^2}{16}\left[V(S)\Psi(S)+V(E)\Psi(E)+V(W)\Psi(W)\right] \tag{10}$$

The points N, S, W and E are defined as, $N=(u+\Delta,v+\Delta), W=(u+\Delta,v), E=(u,v+\Delta)$ and $S=(u,v)$. The local error is of the order of $O(\Delta^4)$.

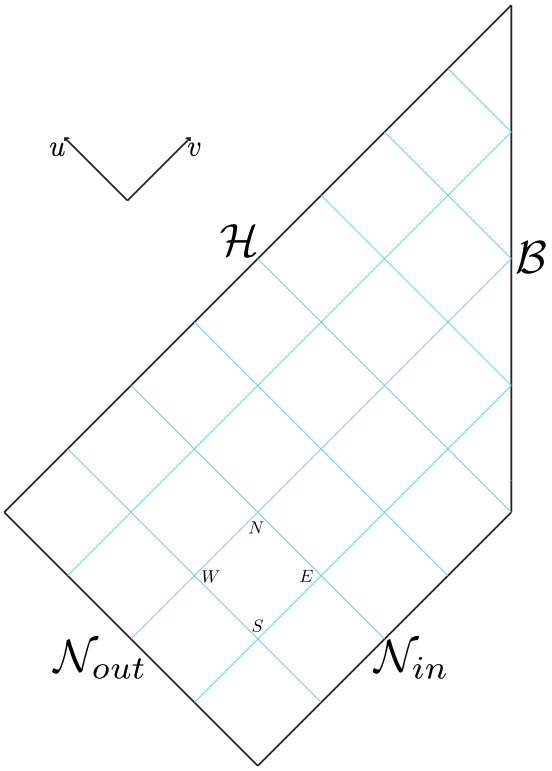

FIG. 2. Domain for numerical integration, the surface $\mathcal{H}$ approximates the horizon, $\mathcal{B}$ is the constant-r_c boundary and, $\mathcal{N}_{in}$ and $\mathcal{N}_{out}$ are two null surfaces for initial data.

We take the AdS length to be $L=1$ and the size of the black hole to be $r_h=10.0$. The domain is shown in Figure 2, the surface $\mathcal{H}$ approximates the event horizon and is given by, $u_{\mathcal{H}}=-2r^*(\hat{r}_h)$ where r^* is the tortoise coordinate and $\hat{r}_h=(1+10^{-5})r_h$. The boundary surface $\mathcal{B}$ is given by $r_c^*=10^{-3}$, we fix $r^*(r)$ such that as $r\to\infty$,

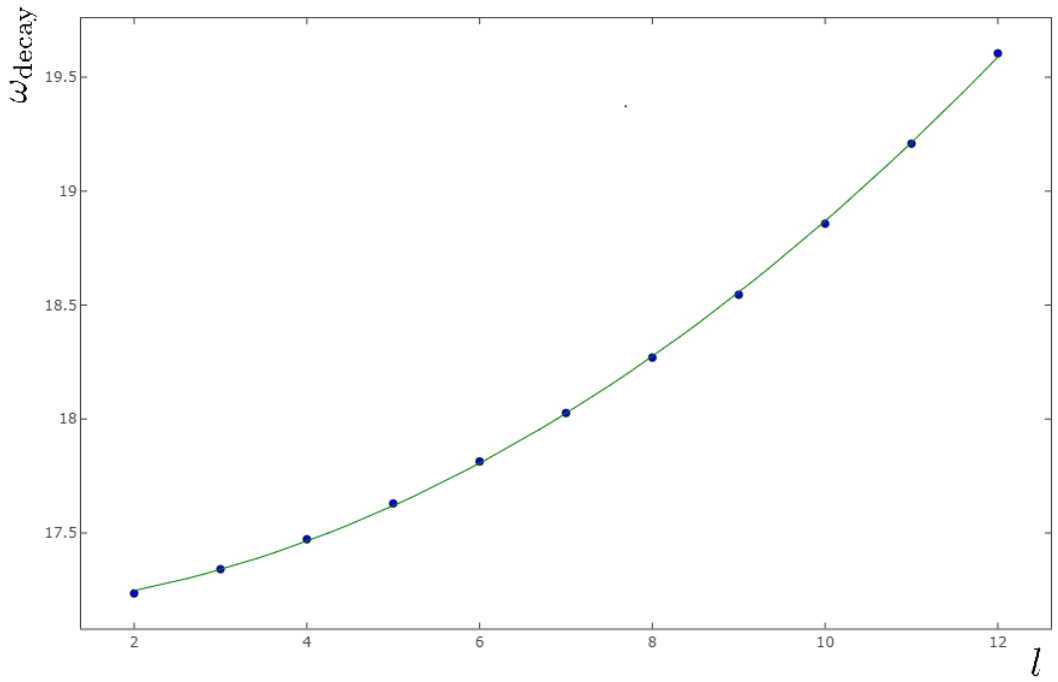

FIG. 3. These are the decay frequencies (blue dots) as a function of l obtained from a linear fit on $\ln(\psi|_{\mathcal{B}})$. Although this is not the same value as ω_{hydro} it still has the same quadratic dependence as shown by the quadratic fit (green curve).

$r^* \to 0$. The surfaces, $\mathcal{N}_{in}$ and $\mathcal{N}_{out}$ are given by $u_{in} = -[r^*(\hat{r}_h) + r_c^*]$ and $v_{out} = 0$ respectively. The initial data is a Gaussian pulse, with $\sigma = 0.01(r^*(r_c^* - \hat{r}_h))$, on the surface $\mathcal{N}_{in}$, we take the boundary conditions, $\Psi = 0$ on $\mathcal{B}$ and $\mathcal{N}_{out}$.

In Figure 4 we show $\Psi(v)$ extracted on the surface $\mathcal{H}$. The y-axis is a log scale, the darker lines are lower l modes with the darkest line being $l = 2$, and the lightest one is $l = 12$. Notice the purely decaying modes which is consistent with quasinormal modes, also, the higher l modes decay faster which is also consistent with quasinormal modes [6–8].

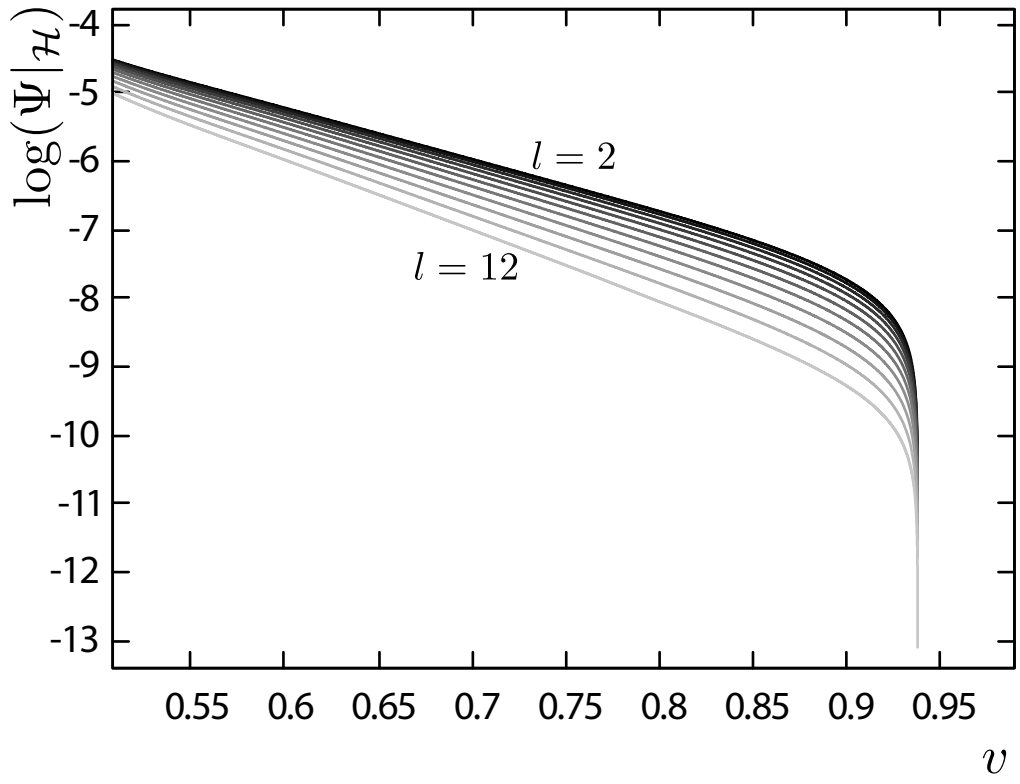

FIG. 4. Plot of Ψ vs v extracted at the horizon for black hole with $r_h = 10$. The y-axis is a logscale. The darker lines are low l modes with the darkest one being the $l = 2$ the lighter lines are higher modes with the lightest one being $l = 12$.

III. RESULTS AND OUTLOOK

In Figure 5 we have a plot of the viscosity η vs. the shear Σ for various l modes from $l = 2$ to $l = 12$. It is clear from this plot that we have non-Newtonian fluid behaviour. Specifically we see that for the most part the behaviour is shear thickening, as shear increases the viscosity also increases. We see tiny bit of shear thinning behaviour for low shears, $\Sigma < 0.06$. As this is a decaying perturbation low shears correspond to late times and high shears to early times as shown in Figure 7. In Figure 6 we have a plot of the viscosity η vs. the time v. We see that for early times, when the shear is

high, the viscosity is higher. Then as the shear decays we see the viscosity decrease, with a small period of increase, which is due to the shear thinning behaviour seen in Figure 5. Finally at late times we see the viscosity approach a constant value, and we get Newtonian behaviour. In Figure. 7 we have a plot of $\log(\Sigma)$ vs. v, we see that at late times the shear decays exponentially with an almost constant decay constant. We point out that in Figure. 6 we start to see noise at $v > 0.25$ this is because now we are dealing with very small quantities and then taking second order derivatives of numerical data to calculate the viscosity from (6), that being said we do start to see an approach to constant viscosity before the noise develops.

In this preliminary work our aim was to explore whether the fluid/gravity duality can be generalized to include non-Newtonian fluids, especially if we work in the time domain rather than the frequency domain. We know from previous results that the duality is established in the frequency domain for certain quasinormal modes ω_{hydro}, which for odd perturbations are the slowly decaying ones. These modes correspond to a constant viscosity at the boundary. This is consistent with our findings of a constant viscosity at late times in Figure 6. At late times when we expect that all the fast decaying modes have died out we are left with the slow ones which correspond to a Newtonian fluid. The work remaining in this study is to analyse the even perturbations in the time domain and verify if similar results also hold. The procedure for the even modes will proceed in an almost identical manner, although the terms involved are significantly more tedious as compared to the odd case.

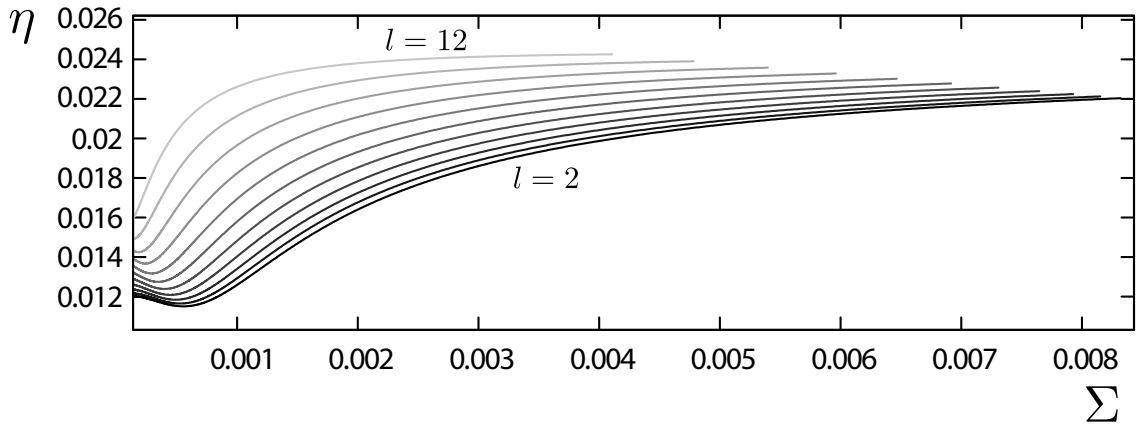

FIG. 5. Plot of the viscosity η vs Σ the shear evaluated on $\mathcal{B}$. The darker lines are low l modes with the darkest one being the $l = 2$ the lighter lines are higher modes with the lightest one being $l = 12$. Notice that the viscosity changes with the shear, for low viscosities there is a small amount shear thining behaviour but the majority of the behaviour is shear thickening.

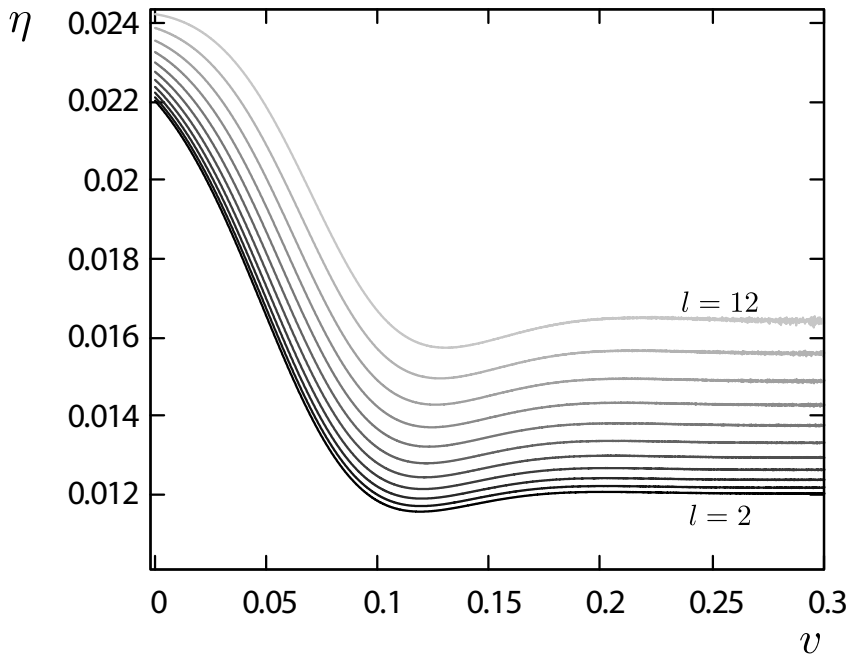

FIG. 6. Plot of η vs v evaluated on $\mathcal{B}$, the darker lines are low l modes with the darkest one being the $l = 2$ the lighter lines are higher modes with the lightest one being $l = 12$. Notice that at late times the the viscosity becomes constant and we get Newtonian behaviour.

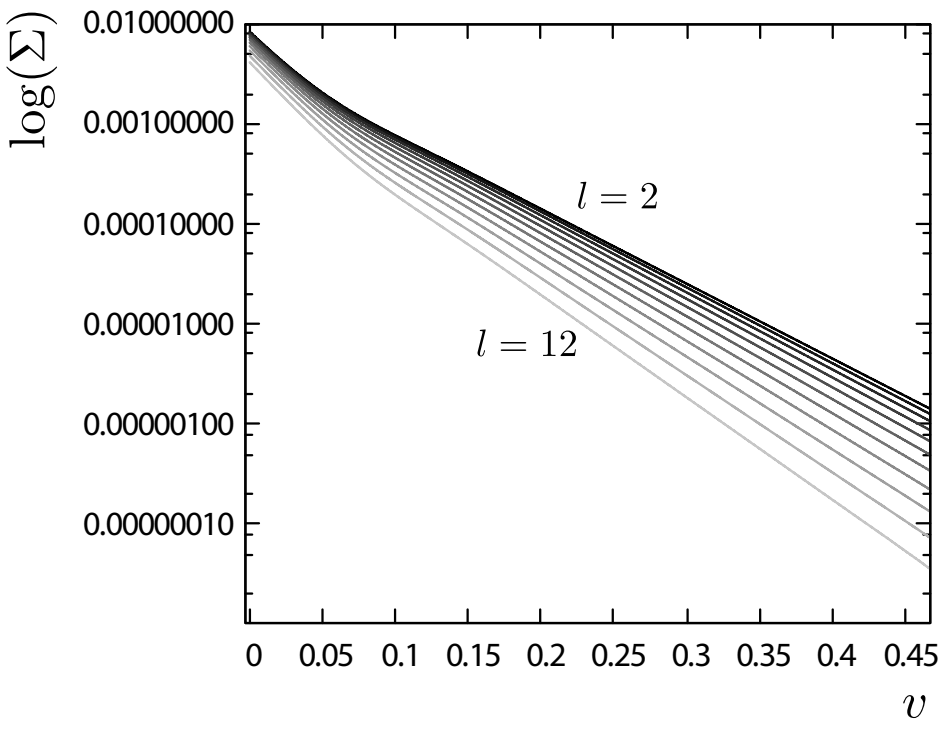

FIG. 7. Plot of Σ vs v evaluated on $\mathcal{B}$, the darker lines are low l modes with the darkest one being the $l = 2$ the lighter lines are higher modes with the lightest one being $l = 12$. Notice that at late times the the shear decays with a constant decay constant.

[1] U. Hussain, I. Booth, and H. K. Kunduri, "Master equation as a radial constraint," *Phys. Rev.*, vol. D93, no. 12, p. 123001, 2016.

[2] V. Balasubramanian and P. Kraus, "A Stress tensor for Anti-de Sitter gravity," *Commun. Math. Phys.*, vol. 208, pp. 413–428, 1999.

[3] I. Bakas, "Energy-momentum/Cotton tensor duality for AdS(4) black holes," *JHEP*, vol. 01, p. 003, 2009.

[4] G. Michalogiorgakis and S. S. Pufu, "Low-lying gravitational modes in the scalar sector of the global AdS(4) black hole," *JHEP*, vol. 02, p. 023, 2007.

[5] F. Irgens, *Rheology and Non-Newtonian Fluids*. Springer, 2014 ed., 7 2013.

[6] V. Cardoso and J. P. S. Lemos, "Quasinormal modes of Schwarzschild anti-de Sitter black holes: Electromagnetic and gravitational perturbations," *Phys. Rev.*, vol. D64, p. 084017, 2001.

[7] V. Cardoso, R. Konoplya, and J. P. S. Lemos, "Quasinormal frequencies of Schwarzschild black holes in anti-de Sitter space-times: A Complete study on the asymptotic behavior," *Phys. Rev.*, vol. D68, p. 044024, 2003.

[8] I. G. Moss and J. P. Norman, "Gravitational quasinormal modes for anti-de Sitter black holes," *Class. Quant. Grav.*, vol. 19, pp. 2323–2332, 2002.

[9] J.-M. Zhu, B. Wang, and E. Abdalla, "Object picture of quasinormal ringing on the background of small Schwarzschild anti-de Sitter black holes," *Phys. Rev.*, vol. D63, p. 124004, 2001.

[10] B. Wang, C.-Y. Lin, and C. Molina, "Quasinormal behavior of massless scalar field perturbation in Reissner-Nordstrom anti-de Sitter spacetimes," *Phys. Rev.*, vol. D70, p. 064025, 2004.

[11] B. Wang, C. Molina, and E. Abdalla, "Evolving of a massless scalar field in Reissner-Nordstrom Anti-de Sitter space-times," *Phys. Rev.*, vol. D63, p. 084001, 2001.

Chapter 5

Deformation of horizons during a merger

Deformation of horizons during a merger

Uzair Hussain* and Ivan Booth†

Department of Mathematics and Statistics,

Memorial University of Newfoundland St John's NL A1C 4P5, Canada

(Dated: September 21, 2017)

Abstract

We model an extreme mass ratio merger (EMR) as a point particle radially plunging into a large Schwarzschild black hole. We assume that the mass of the point particle, μ, is much smaller than the black hole mass M. Under this assumption we can employ the Zerilli formalism modified to include a source term which arises from the energy-momentum tensor of the small object. We solve the Zerilli equation by numerically evolving initial data. Then, we ray trace the null geodesics of the event horizon from after the merger backward in time to extract the geometry of the perturbed event horizon. Further, we take advantage of the axisymmetry of the setup to locate the apparent horizon and study its geometry.

* uh1681@mun.ca

† ibooth@mun.ca

I. INTRODUCTION

From the gravitational radiation observed by LIGO's interferometers we now have strong evidence pointing towards the existence of binary black hole systems and their inevitable mergers [1]. To predict the waveforms of the radiation emitted by these mergers complex simulations are executed on super computers using state-of-art algorithms. These simulations can accommodate a wide range of the possible parameters of the binary system, for e.g., initial spins, spin orientations, mass ratios, initial separation and velocities, etc.

In a very specific type of merger the calculations can be handled by much simpler methods. This happens when we consider the head-on merger of two non-spinning black holes which have an extreme mass ratio (EMR). This means that the mass, μ, of one of the black holes is much smaller than the mass, M, of the other, i.e. $\mu/M \to 0$. This allows to us to model the smaller black hole as a point particle with mass μ. Hence, the problem is reduced to the radial in-fall of a point particle into a Schwarzschild black hole.

This approach to the problem was pioneered by Zerilli [2] and has since been studied extensively [3–5]. At the heart of the solution is the assumption that the gravitational field produced by the particle drops off rapidly and so only perturbs the surrounding geometry. Further, there is no back-reaction on the particle and thus it follows a geodesic in the spacetime of the large Schwarzschild black hole. Under these assumptions Einstein's equations can be linearized.

Here we will be particularly interested in how, in this perturbed spacetime, the event and apparent horizons of the large black hole are deformed by the stress-energy tensor of the point particle. As we will see below, for the deformation of the event horizon a prominent role is played by caustics, which are points where null rays in

the vicinity of the large black hole's horizon cross each other and join the horizon. Recently, similar results have been shown in [6]. There the strategy was to take the limit $M \to \infty$ and model the large black hole as a Rindler-type planar horizon accelerating towards the small black hole, which is assumed to be Schwarzschild. Then as the small black hole approaches, the null generators of the planar horizon are deflected towards the small black hole due to its Schwarzschild geometry and as such the deformation of the planar event horizon and the smaller hole's event horizon can be computed. Another study that shows a similar deformation of the event horizon is [7], where the approach is the one we take; to approximate the small black hole as a point particle and solve for the perturbed geometry. In [7] the influence of the particle is treated as an impulse in the frequency domain of the perturbations.

By contrast, in this study we will do a direct numerical evolution, in the time domain, of Brill-Linquist type initial data for binary black holes. For the apparent horizon, we obtain a result that is at first counter-intuitive: the apparent horizon appears to recede away from the approaching particle. However a little consideration shows that this isn't so strange. Intuitively, as the particle gets closer there are null geodesics inside the black hole, close to the horizon, which get pulled outwards by the particle's gravitational field. Hence the zero expansion surface moves inwards. This type of behaviour is also seen when examining the marginally outer trapped surfaces (MOTSs) in slices of initial data for arbitrary mass ratio head-on collisions [8].

The paper is organized as follows. Section II reviews the perturbation formalism for the radial in-fall of a point particle, Section III outlines the numerical method used to evolve the initial data, Section IV shows how the event and apparent horizons are deformed, and finally we conclude with Section V.

II. PERTURBATIONS BY RADIALLY IN-FALLING POINT PARTICLE

We assume the particle creates a small disturbance in the spacetime which can be modelled by standard perturbation theory methods. We use the approach of Zerilli [2] with the Moncrief wavefunction [9] and express the metric as $\tilde{g}_{\mu\nu} = g_{\mu\nu} + p_{\mu\nu}$, where $g_{\mu\nu}$ is the Schwarzschild metric and $p_{\mu\nu}$ is the perturbation. Given the spherical symmetry of the Schwarzchild spacetime, $p_{\mu\nu}$ can be expanded in terms of odd and even modes with indices l and m arising from the spherical harmonics. If we assume the particle falls along the z-axis, then we can see that the problem is axisymmetric and only even modes are excited [3]. We write the perturbation as

$$\delta g^{l0}_{\mu\nu} dx^\mu dx^\nu = Y^{l0}(\theta) \left(f H_0^{l0} dt^2 + 2 H_1^{l0} dt dr + \frac{1}{f} H_2^{l0} dr^2 + r^2 K^{l0} d\Omega^2 \right) \tag{1}$$

where we have taken $m = 0$ again because of axisymmetry, $f(r) = 1 - 2M/r$ and H_0, H_1, H_2 and K are functions of r and t. We will omit the $l0$ where there is no confusion. We work in the Regge-Wheeler gauge and Schwarzschild coordinates.

When we invoke Einstein's equations up to linear order in $p_{\mu\nu}$, we find that the equations can be decoupled into one inhomogeneous wave equation,

$$\left[-\frac{\partial^2}{\partial t^2} + \frac{\partial^2}{\partial r^{*2}} - V(r) \right] \psi(r,t) = S(r,t) \tag{2}$$

where $r^* = r + 2M \ln(r/2M - 1)$ is the tortoise coordinate,

$$\psi(r,t) = \frac{r}{\lambda + 1} \left\{ K + \frac{f}{\Lambda} \left[H_2 - r \frac{\partial}{\partial r} K \right] \right\} \tag{3}$$

is the Zerilli-Moncrief function,

$$V(r) = \frac{2f}{r^2 \lambda^2} \left[\lambda^2 (\Lambda + 1) + \frac{9M^2}{r^2} \left(\Lambda - \frac{2M}{r} \right) \right] \tag{4}$$

is the even potential with $\lambda = (l+2)(l-1)/2$ and $\Lambda = \lambda + \frac{3M}{r}$, and

$$S(r,t) = \frac{2}{l(l+1)\Lambda}\Bigg\{ r^2 f\left[f^2\frac{\partial}{\partial r}Q^{tt} - \frac{\partial}{\partial r}Q^{rr}\right] \tag{5}$$

$$- \frac{f^2}{\Lambda r}\left[\lambda(\lambda-1)r^2 + (4\lambda-9)Mr + 15M^2\right]Q^{tt} + r(\Lambda - f)Q^{rr}\Bigg\} \tag{6}$$

is the source term for radial infall. The tensor Q^{ab} where a, b run over r, t is given by,

$$Q^{ab} = 8\pi \int T^{ab} Y^*(\theta,\phi) d\Omega \tag{7}$$

where $T^{ab} = \mu \int u^a u^b \delta^4(x^\nu - x_p^\nu(\tau))\sqrt{-g}d\tau$, is the stress tensor of the particle, μ is the mass of the particle, τ is the proper time along the particle's trajectory, $x_p(\tau)$, and the four vector of the particle is,

$$u^\nu = (\tilde{E}/f, -(\tilde{E}^2 - f)^{1/2}, 0, 0) \tag{8}$$

where $\tilde{E}$ is the conserved energy. Further we have,

$$Q^{ab} = \mu\frac{8\pi}{r^2}\frac{u^a u^b}{u^t}\delta(r - r_p(t))Y^*(\theta(t),\phi(t))\,. \tag{9}$$

Here $Y^*(\theta(t),\phi(t))$ means that the spherical harmonic is evaluated along the trajectory of the particle. Inserting (9) into (5) we have,

$$S(r,t) = 16\pi\frac{\sqrt{(2l+1)/4\pi}}{l(l+1)}\frac{\mu}{\tilde{E}}\frac{f^3}{\Lambda}\left\{\delta'(r - r_p(t)) - \left[\frac{(\lambda+1)r - 3M}{r^2 f} - \frac{6M\tilde{E}^2}{\Lambda r^2 f}\right]\delta(r - r_p(t))\right\} \tag{10}$$

where $r_p(t)$ is the trajectory of the particle and $Y^{*l0}(0) = \sqrt{(2l+1)/4\pi}$. The equation for the trajectory starting from rest is,

$$\frac{t}{2M} = \tilde{E}\sqrt{1 - \frac{r}{r_0}}\sqrt{\frac{r}{2M}}\frac{r_0}{2M} + 2\text{arctanh}\left(\frac{\sqrt{\frac{2M}{r} - \frac{2M}{r_0}}}{\tilde{E}}\right) + \tilde{E}\left(1 + \frac{4M}{r_0}\right)\left(\frac{r_0}{2M}\right)^{3/2}\arctan\left(\sqrt{\frac{r_0}{r} - 1}\right) \tag{11}$$

where r_0 is the initial position of the particle and $\tilde{E} = \sqrt{1 - \frac{2M}{r_0}}$.

III. NUMERICAL METHOD

We use the numerical method of Lousto and Price [5] with the modification by Martel and Poisson [3]. The method is a finite difference algorithm on a staggered grid with a step size $\Delta = \Delta r^*/4M = \Delta t/2M \approx 0.009$ over a domain bounded by two null hypersurfaces, $\mathcal{H}_1$ and $\mathcal{H}_2$, and one spacelike surface Σ_0. $\mathcal{H}_1$ approximates the event horizon and is given by, $u = t_f - r_p^*(t_f)$ where t_f is determined by (11) with $r_p(t_f)/2M = 1.00001$. $\mathcal{H}_2$ is a null hypersurface which approximates future null infinity and is chosen to be, $v/2M = (t + r^*)/2M \approx 1500$. Finally Σ_0 is the $t = 0$ surface which is the moment of time symmetry for the initial data.

After discretizing the domain we encounter two kinds of cells, as shown in FIG. 1; ones that do not contain the particle trajectory (Type I) and ones that that do (Type II). For Type I cells we do not have a contribution from the source term, $S(r, t)$. So we may discretize (2) with the following formula,

$$\psi_N = -\psi_S + (\psi_W + \psi_E)\left(1 - \frac{\Delta^2}{2}V_S\right) \tag{12}$$

where $S = (r_S^*, t_S)$ is the base point, $W = (r_S^* - \Delta, t_S + \Delta)$, $E = (r_S^* + \Delta, t_S + \Delta)$ and $N = (r_S^*, t_S + 2\Delta)$. This scheme is accurate to $\mathcal{O}(\Delta^4)$.

For Type II cells there is a contribution from the source term and (2) now takes the form[1]

$$\begin{aligned}\psi_N = &-\psi_S\left[1 + \frac{V_S}{4}(A_2 - A_3)\right] + \psi_E\left[1 - \frac{V_S}{4}(A_3 + A_4)\right] \\ &+ \psi_W\left[1 - \frac{V_S}{4}(A_1 + A_3)\right] - \frac{1}{4}\left(1 - \frac{V_b}{4}A_3\right)\int\int dAS(r,t)\end{aligned} \tag{13}$$

where the A_i's are the areas illustrated in right panel of FIG. 1 and $\int\int dAS(r,t)$ is

[1] There is a typo in [3] for equations (13) and (14), see [4].

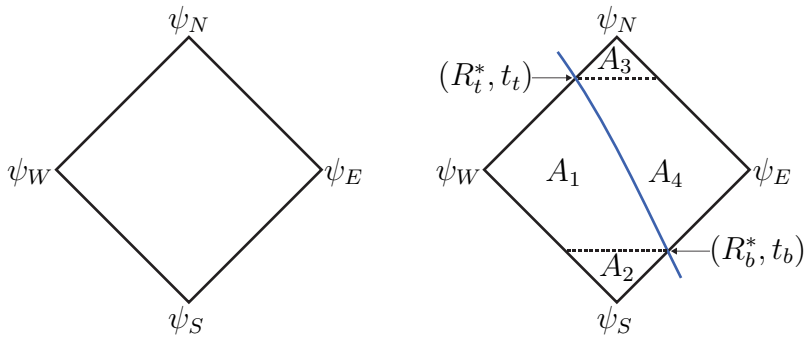

FIG. 1. These are the two types of cells that arise when discretizing the domain. The left one (Type I) does not contain the particle and hence we do not need to integrate over a source term. The right one (Type II) contains the particle and hence we have to integrate over the delta function source.

the integration of the source term over the cell,

$$\int\int dAS(r,t) = -\kappa \int_{t_b}^{t_t} dt \frac{f(t)}{\Lambda(t)^2}\frac{1}{r_p(t)}\left[\frac{6M}{r_p(t)}(1-\tilde{E}^2)+\lambda(\lambda+1)-\frac{3M^2}{r_p(t)^2}+4\lambda\frac{M}{r_p(t)}\right] \pm \kappa\left\{\frac{f(t_b)}{\Lambda(t_b)}[1\mp \dot{r}_p^*(t_b)]^{-1}+\frac{f(t_t)}{\Lambda(t_t)}[1\pm \dot{r}_p^*(t_t)]^{-1}\right\} \tag{14}$$

where, $l(l+1)\tilde{E}\kappa = 16\pi\mu\sqrt{(2l+1/(4\pi)}$, $\dot{r}_p^*(t) = -\sqrt{\tilde{E}^2 - f(t)}/\tilde{E}$, $f(t) = f(r_p(t))$, $\Lambda(t) = \Lambda(r_p(t))$, t_b (t_t) is the time when the particle enters (leaves) the cell. Further, in the expression on the second line, the upper (lower) sign for the first term (function of t_b) is used when the particle enters the cell on the right (left) of r_S^*. For the second term (function of t_t) the upper (lower) sign is used when the particle leaves the cell on the right (left) of r_S^*. The initial data at $t = 0$ is constructed from the Brill-Lindquist [10] solution and is therefore conformally flat. It has been analysed in detail in [3, 5, 11], and is given by,

$$H_2 = K = 2\mu\frac{\sqrt{4\pi/(2l+1)}}{(1+M/2\bar{r}_0)(1+M/2\bar{r})}\frac{\bar{r}_<^l}{\bar{r}_>^{l+1}} \tag{15}$$

where $\bar{r} = r(1+\sqrt{f})^2/4$ is the isotropic radius, and $\bar{r}_<(\bar{r}_>)$ is the smaller (greater) of $\bar{r}$

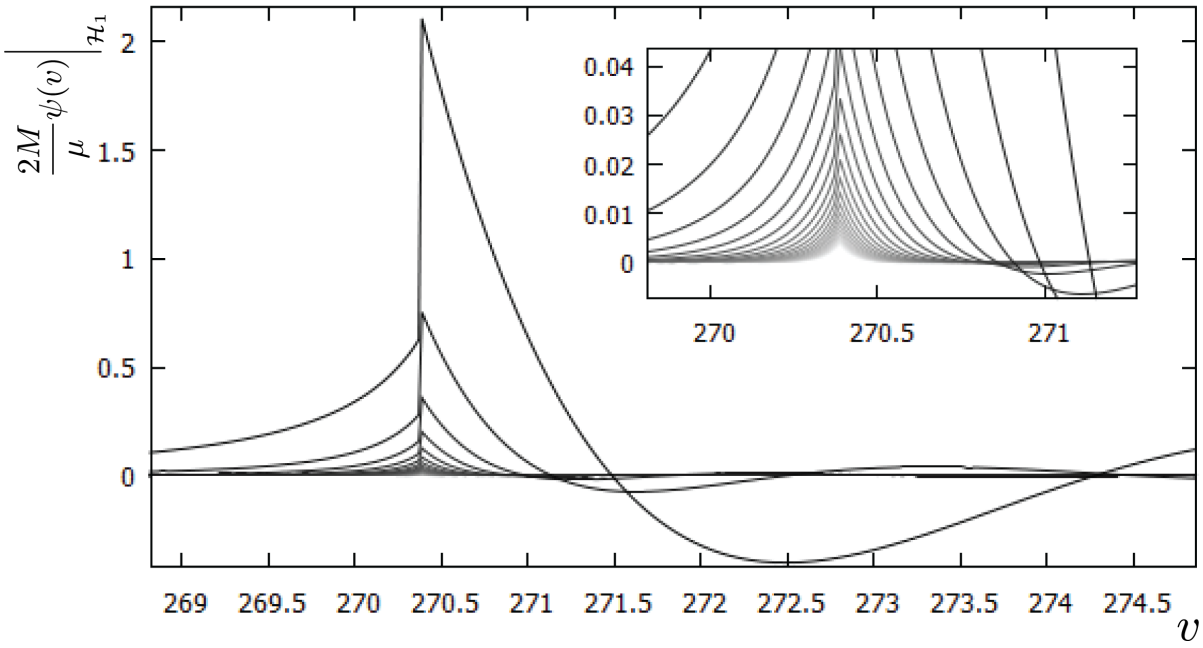

FIG. 2. Waveforms, $\psi(v)$ extracted at $\mathcal{H}_1$ for $l = 2$ to $l = 25$. The lower the amplitude the higher the value of l. The inset is zoomed in at the time when the particle meets the event horizon.

and $\bar{r}_0$. Note that with this choice of initial data, when we evolve from the Σ_0 surface, we have not specified what the ψ_S points will be. We circumvent this problem by doing a Taylor expansion, $\psi(-\Delta, r^*) = \psi(\Delta, r^*) - 2\Delta\partial_t\psi(t_0, r^*) + \mathcal{O}(\Delta^3)$, since the data is time symmetric we can take $\psi(-\Delta, r^*) = \psi(\Delta, r^*)$. Since we will be interested in the horizon deformations, we will extract ψ on the $\mathcal{H}_1$ surface. FIG. 2 shows the waveforms, $\psi(v)$, for $l = 2$ to $l = 25$ extracted on the surface $\mathcal{H}_1$ as a function of the ingoing coordinate v with $r_0/2M = 30$. This choice of r_0 makes $\tilde{E} \approx 1$. Notice that for large l we get a smaller amplitude. Hence, we introduce a cutoff, $l_{\rm cut}$, at $l_{\rm cut} = 25$.

IV. HORIZONS DEFORMATION

A. Event Horizon

To find the deformation of the event horizon we use a method similar to the one employed in [7], which calculates how each null generator of the horizon gets perturbed from its usual Schwarzschild position. For another method which locates the whole event horizon as a null surface, see [12]. Consider the null generators of the event horizon of the static Schwarzschild spacetime in Kruskal-Szekeres coordinates,

$$\frac{d^2X^\mu}{dV^2} = -\hat{\Gamma}^\mu_{\sigma\gamma}\frac{dX^\sigma}{dV}\frac{dX^\gamma}{dV} + g\frac{dX^\mu}{dV} \tag{16}$$

where $X^0 = V, X^1 = U = 0, X^3 = \theta, X^4 = \phi$, $\hat{\Gamma}^\mu_{\sigma\gamma}$ denotes the Christoffel symbols in the Kruskal-Szekeres coordinates and we have kept the non-affine parameter g; for the static case we have $g = 0$. In our case of interest there is a perturbation present and so we add a perturbative term to each of the X^i where i runs over U and θ. We have then, $X^i \to X^i + \delta X^i$. Also, the Christoffel symbols will be perturbed, $\hat{\Gamma}^\mu_{\sigma\gamma} \to \hat{\Gamma}^\mu_{\sigma\gamma} + \delta\hat{\Gamma}^\mu_{\sigma\gamma}$. Inserting this *ansatz* into (16) and appropriately evaluating on the horizon we get for $i = \theta$;

$$\frac{d^2\delta\theta}{dV^2} = -\delta\hat{\Gamma}^\theta_{VV} \tag{17}$$

for δU we may use the null condition for the generators,

$$\frac{d\delta U}{dV} = e\kappa^2\delta g_{VV} \tag{18}$$

Switching to ingoing coordinates and expressing the perturbed quantities in terms of ψ, we can write (17) and (18) as,

$$\left(\frac{\partial}{\partial v} - \kappa\right)\frac{\partial\delta\theta^l}{\partial v} = \kappa\left(\frac{\partial}{\partial v} - \kappa\right)\frac{\partial\psi^l}{\partial v}\partial_\theta Y^l \tag{19}$$

$$\left(\frac{\partial}{\partial v}-\kappa\right)\delta r^l=-\frac{1}{2\kappa}\left(\frac{\partial}{\partial v}-\kappa\right)\frac{\partial\psi^l}{\partial v}Y^l \tag{20}$$

where l is the mode number for the spherical harmonics. The general solution is given by,

$$\delta\theta^l=\kappa\psi^l\partial_\theta Y^{l0}+\frac{1}{\kappa}\theta_0^l e^{\kappa v}+\theta_1^l \tag{21}$$

$$\delta r^l=-\frac{1}{4\kappa}\partial_v\psi^l Y^{l0}+R_0^l e^{kv} \tag{22}$$

where R_0^l,θ_0 and θ_1 are constants.

To find the horizon deformation we need to evolve the equations 'backwards in time'. We start from the null generator of a static black hole at $U=0$ and $V\to\infty$ and integrate backwards to extract the deformation of the horizon. Hence, we impose the requirement that $\delta\theta$ and δr vanish for $v\gg v_m$ where v_m is time when the particle and black hole meet. Since at late times the perturbation vanishes we choose $R_0^l=\theta_0=\theta_1=0$. For $v=v_m$, note that there is a discontinuity in ψ (cf. FIG. 2). To get a continuous deformation we choose:

$$R_0^l=-\frac{1}{4\kappa}\Delta\psi^l_{,v}e^{-kv}|_{v_-}Y^l \tag{23}$$

$$\theta_0^l=\kappa\Delta\psi^l_{,v}\partial_\theta Y^l e^{-kv}|_{v_-} \tag{24}$$

$$\theta_1^l=(\kappa\Delta\psi^l-\Delta\psi^l_{,v})\partial_\theta Y^l \tag{25}$$

where,

$$\Delta\psi^l=\psi^l|_{v_+}-\psi^l|_{v_-}\qquad\Delta\psi^l_{,v}=\psi^l_{,v}|_{v_+}-\psi^l_{,v}|_{v_-} \tag{26}$$

where $v_{+(-)}$ are the limits from the right (left) of v_m.

The effect of the monopole term, $l=0$, is calculated in the following manner; since the monopole term is isotropic, we use (18) for $v>v_m$ and arrive at,

$$\left(\frac{\partial}{\partial v}-\kappa\right)\delta r^0=-\frac{\mu}{2M} \tag{27}$$

which has a general solution $\delta r^0 = 2\mu + C_0 e^{\kappa v}$, where C_0 is a constant. For $v < v_m$ the right hand side of (27) will be zero and as such we have $\delta r^0 = C_0 e^{\kappa v}$. We fix $C_0 = 0$ for $v > v_m$ and for continuity at v_m we fix $C_0 = 2\mu e^{\kappa(v - v_m)}$ for $v < v_m$.

The contribution from the $l = 1$ mode to the deformation of the horizons can be removed by performing an infinitesimal gauge transformation to go into the singular gauge [13], as shown in Appendix A, where we see that although the perturbation is singular, there is no contribution to the deformation of the event horizon.

In FIG. 3 we see how the horizon deforms prior to v_m. The blue line is the event horizon and black dot illustrates the location of the particle. The green dots are null geodesics that are in the vicinity of the black hole. The mass of the large black hole is, $M = 1/2$ and the mass of the particle is $\mu = 0.025$. As the particle approaches the black hole, pairs of geodesics on either side of the axis symmetry form caustics as they cross over each other at $\theta = 0$ and join the horizon. In FIG. 4 we see the event horizon after the merger, the bump at $\theta = 0$ smooths out, the black hole enters its ringdown phase and settles back to an almost spherical shape.

B. Apparent Horizon

In this section we locate the apparent horizon[2] and see how it is deformed by the infalling particle. The method we use is a standard one [14, 15] modified for small perturbations from the background geometry. We foliate the spacetime into spacelike slices, Σ, with the normal vector,

$$\tilde{n}_\mu = \left(-\sqrt{f} + \frac{1}{2\sqrt{f}} p_{tt} \right) \delta^t_\mu \tag{28}$$

[2] Here we use apparent horizon in its colloquial sense as the outermost MOTS for the large black hole.

which is the Schwarzschild time with a normalization $\tilde{n}^\mu \tilde{n}_\mu = -1$. Let S be a closed two-dimensional surface in Σ and let $\tilde{s}^\mu$ be the spacelike normal to S, hence, $\tilde{s}^\mu \tilde{s}_\mu = 1$. For all points on S we have outward and inward pointing null geodesics whose tangents, denoted $\tilde{k}^\mu$ and $\tilde{l}^\mu$ respectively, can be written as,

$$\tilde{k}^\mu = \frac{1}{\sqrt{2}}\left(\tilde{n}^\mu + s^\mu\right) \quad \text{and} \quad \tilde{l}^\mu = \frac{1}{\sqrt{2}}\left(\tilde{n}^\mu - s^\mu\right) \tag{29}$$

Then the metric, $\tilde{m}_{\mu\nu}$, on S can be written as, $\tilde{m}_{\mu\nu} = \tilde{g}_{\mu\nu} + \tilde{k}_\mu \tilde{l}_\nu + \tilde{l}_\mu \tilde{k}_\nu$. Further, the expansion of the outgoing null rays is given by, $\Theta = \tilde{m}^{\mu\nu}\tilde{\nabla}_\mu \tilde{k_\nu}$. The apparent horizon is then defined to be a marginally outer trapped surface (MOTS) on which the expansion of the outward null geodesics vanishes, $\Theta = 0$.

We can define S as a level surface of some scalar function $\tilde{\tau}(x^i) = 0$, where the x^i are coordinates on Σ. In the axisymmetric case, using Schwarzschild coordinates, we write,

$$\tilde{\tau}(r, \theta) = r - \tilde{h}(\theta) \tag{30}$$

and a normal and tangent to S are

$$\tilde{m}_i = \partial_i \tilde{\tau} = (1, -\partial_\theta \tilde{h}, 0) \quad \text{and} \quad \tilde{u}^i = \partial_\theta x^i = (\partial_\theta \tilde{h}, 1, 0) \tag{31}$$

Then the condition for vanishing expansion can be written as

$$\partial_\theta^2 \tilde{h} = -(\tilde{X} + \tilde{s}^2 \tilde{Y}) - \frac{\tilde{s}}{\sqrt{\tilde{\gamma}^{(2)}}}(\tilde{P} + \tilde{s}^2 \tilde{Q}) \tag{32}$$

where,

$$\tilde{X} := \tilde{\Gamma}^A_{BC} \tilde{m}_A \tilde{u}^B \tilde{u}^C, \qquad \tilde{Y} := \tilde{\gamma}^{\phi\phi} \tilde{\Gamma}^A_{\phi\phi} \tilde{m}_A, \tag{33}$$

$$\tilde{P} := \tilde{K}_{AB} \tilde{u}^A \tilde{u}^B, \qquad \tilde{Q} := \tilde{\gamma}^{\phi\phi} \tilde{K}_{\phi\phi}, \tag{34}$$

$$\tilde{s}^2 := \tilde{\gamma}_{AB} \tilde{u}^A \tilde{u}^B, \tag{35}$$

$\tilde{\gamma}_{\mu\nu}$ is the induced metric on Σ, the indices A, B run over (r, θ), and $\tilde{\gamma}^{(2)}$ is the determinant of $\tilde{\gamma}_{AB}$. Since our approach is perturbative to linear order we will use

the *ansatz* $\tilde{h}(\theta) = 2M + \delta h(\theta)$ and keep terms linear in δ. Further evaluating $\psi(v)$ on $\mathcal{H}_1$, which allows us to switch to ingoing coordinates, (32) becomes,

$$\left(\partial_\theta^2 + \cot\theta\partial_\theta\right)\delta h - 2\delta h = -2\left[\partial_v^2\psi^l - (\lambda+2)\,\partial_v\psi^l\right]Y^l. \tag{36}$$

Notice that $(\partial_\theta^2 + \cot\theta\partial_\theta)$ is the Laplacian on the unit sphere. To solve (36) we assume that δh can be expanded in $(m = 0)$ spherical harmonics,

$$\delta h(\theta) = \sum_l a^l Y^{l0}(\theta), \tag{37}$$

inserting this into (36) we find,

$$a^l = \lambda^{-1}\partial_v^2\psi^l - \partial_v\psi^l. \tag{38}$$

Inserting (38) into (37) we can construct the deformation of the apparent horizon. This is shown as the magenta curve in FIG. 3. For early times, when the particle is far from the black hole the apparent horizon coincides with $r = 2M$. However note that as the particle gets closer, the zero expansion surface appears to move inwards, ultimately becoming concave outwards as the particle crosses the event horizon.

Intuitively this behaviour can be understood in the following way. As the particle approaches the black hole, it bends light rays towards it. In particular this increases the outward expansion of congruences of null geodesics inside the $r = 2M$ surface and thereby increases their (initially negative) expansion. Thus the new $\Theta = 0$ surface is inside the old $r = 2M$ surface. This recession does not violate the rule that apparent horizons cannot decrease in area [16–19]: our approximation is only first order and area change is a second order effect. To the order of accuracy of our approximation the area can't change.

That said, the apparent recession of the horizon as the particle approaches is robust and not a consequence of the approximation. A similar effect can be seen in the

analysis of the MOTSs in initial data for head-on collisions in a non-perturbative setting [8]. In a full analysis we expect that the apparent recession would be balanced by an overall increase in the area of the horizon and in [8] the total area does increase during the approach.

Finally we note that $v = 270.35$ is probably as far as we can expect our linear perturbation theory to return reasonable results for the apparent horizon. In our simulation $\mu/M = 0.05$ and so at $v = 270.35$ the apparent horizon of the small black hole (that we are modelling as a particle) is approaching that of the large black hole. Hence we are now in a region where the gravitational field that we have assumed to be small is becoming large. Indeed just after this point, our horizon finding methods fail and we suspect that this is a result of our approximations no longer holding. Identifying the location of an apparent horizon is strongly dependent on local features of the geometry. As such, once we lose control of those details in a region through which the horizon should pass, we can no longer locate it.

By contrast the highly non-local event horizon calculations are more robust. Problems in one small region only affect a few geodesics and so the global evolution is not seriously perturbed.

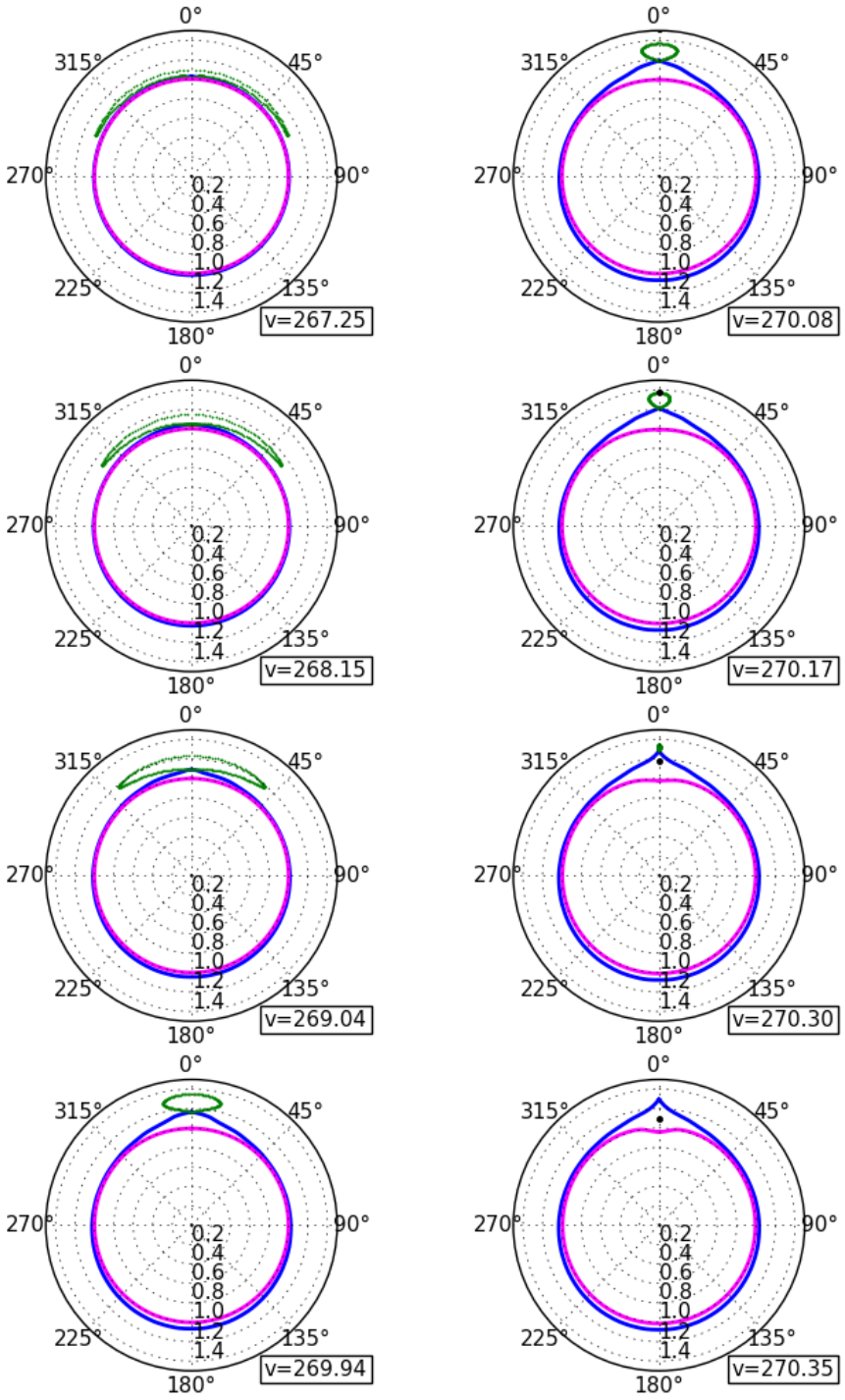

FIG. 3. A visualization of the deformation of the coordinate shapes of the event and apparent horizons when the mass of the incoming particle is $\mu = 0.025$. Time advances from the top left down the columns. The green dots are null geodesics that join the event horizon forming caustics at $\theta = 0$. The blue is the event horizon and the magenta is the apparent horizon.

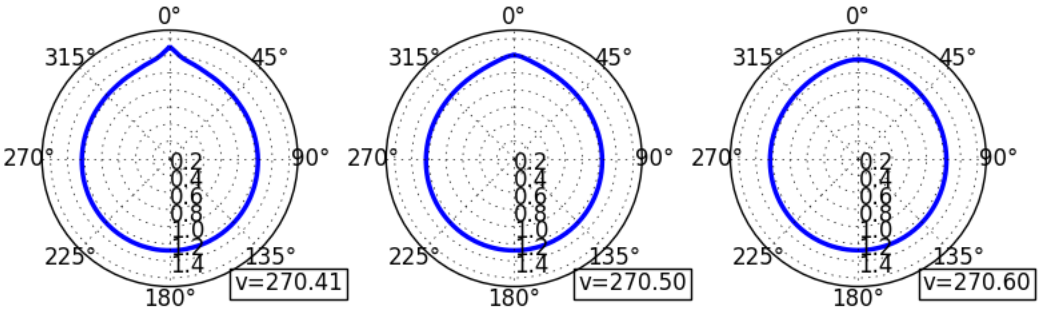

FIG. 4. After the merger the black hole returns to its spherical shape, although slightly larger because of the contribution from the mass of the particle.

V. DISCUSSION

In this paper we modelled an EMR merger by using perturbation techniques for Schwarzschild black holes. Specifically, we used the stress tensor of a point particle to model the gravitational field of a small black hole and used Zerilli's formalism to solve the linearized Einstein's equations. We then studied the deformation of the event and apparent horizons as the particle approaches the black hole (FIGS. 3 and 4).

Given the teleological nature of event horizons we used final post-merger boundary conditions and integrated backwards in time to get the full horizon. To ensure a smooth horizon evolution we fixed constants in (23) to (25), whereby we see that the discontinuity in the initial data plays a major role in the deformation of the event horizon. This discontinuity arises from doing a multipole expansion of the Brill-Lindquist type initial data [11]. Such a dependence on initial data for perturbations is lost when analysing solutions of (2) in the frequency domain. We also saw how there is a "bubble" of null rays that emerges between the particle and the black hole just before the merger, shown in green in FIG. 3. These are null rays that join the event horizon at the top of the black hole by crossing each other and forming caustics. This bubble of null rays and associated caustics are a standard feature of black hole mergers and commonly seen in full non-linear treatments. See [20] for an example.

For locating the apparent horizon we used a standard approach [15] simplified to the case of linear perturbations. Perhaps the most interesting observation was that as the particle makes its final approach to the black hole, the region of the apparent horizon facing the particle appears to recede away from it, ultimately becoming concave outwards in the diagrams. This apparently non-intuitive behaviour can be understood as resulting from null rays in the immediate vicinity of the unperturbed apparent horizon being attracted towards particle. Hence relative to the unperturbed

metric the apparent horizon moves inwards. At the same time we noted that the recession doesn't result in a decrease in the area of the horizon: in our first order expansion the area is invariant.

It is interesting to compare the quite different evolutions of the event versus apparent horizons. The event horizon is "attracted" towards the particle as one might naively expect, while the apparent horizon initially recedes. Further during the final approach the event horizon puckers to form a caustic cusp as new null generators join the horizon while the apparent horizon remains smooth (at least as long as our approximations continue to hold).

The appearance of caustics is not a consequence of our point source. For one we have noted that our cut-off of higher l modes "smears out" the particle and so despite our initial set-up we are not really dealing with a point source. However more generally caustics are a result of geodesic focussing and this does not require a point source. For example they are also seen in [6] where the smaller black hole has a Schwarzschild geometry and is not a point source, as well as in the full non-linear treatment of mergers with arbitrary initial parameters [20, 21].

The event horizon grows during the approach (thanks to its final boundary conditions) while the apparent horizon does not (thanks to the linear approximations). However this is realistic. During this physical process most of the mass change in the large black hole comes directly from the infalling particle. The event horizon grows "in anticipation" of the absorption however the apparent horizon should not substantially change in size until the particle actually is absorbed.

Overall we have found that for an EMR merger many key features can be captured by using standard perturbation methods. However some features escape us. Specifically any features related to the event and apparent horizon of the smaller black hole are lost, simply because we use a point particle approximation. Perhaps the

matched asymptotic methods suggested in [6] could be used to focus on the event horizon geometry of the smaller black hole. Further the appearance of a common apparent horizon [22–25] that is usually seen in arbitrary mass ratio mergers is also lost. This feature in principle could also be recovered by upgrading the particle to a Schwarzschild geometry rather than a point stress tensor.

ACKNOWLEDGMENTS

IB thanks Abhay Ashtekar and Aaron Zimmerman for a conversation at the 15th Canadian Conference on General Relativity and Relativistic Astrophysics which inspired this paper. UH would like to thank Hari Kunduri, Harald Pfeiffer and Aaron Zimmerman for their insights and suggestions. IB is supported by NSERC Discovery Grant 261429-2013. During the course of this research UH was partially funded by a fellowship from the School of Graduate Studies at Memorial University as well as stipends from NSERC Discovery Grants 261429-2013 and 418537-2012.

Appendix A: $l = 1$ perturbation

The solution to the $l = 1$ perturbation is given by [2][7],

$$H_0^{10} = \frac{\left[f_0(t) + (r^3/M)\ddot{f}_0(t)\right]}{3(r-2M)^2}\Theta(r - r_p(t)) \tag{A1}$$

$$H_1^{10} = -\frac{r\dot{f}_0(t)}{(r-2M)^2}\Theta(r - r_p(t)) \tag{A2}$$

$$H_2^{10} = \frac{f_0(t)}{(r-2M)^2}\Theta(r - r_p(t)) \tag{A3}$$

where $r_p(t)$ is the trajectory of the particle, Θ is the Heaviside function and,

$$f_0(t) = 8\pi\mu(r_p(t) - 2M)\sqrt{3/4\pi}. \tag{A4}$$

Then we perform a gauge transformation generated by the vector field ξ^μ whose non-zero covariant components are given by [2],

$$\xi_t = -\frac{r}{f}\sigma\dot{\rho}\Theta(r - r_p(t)) \quad \xi_r = \frac{1}{f^2}\rho\sigma\Theta(r - r_p(t)) \quad \xi_\theta = \frac{r}{f}\rho\partial_\theta\sigma\Theta(r - r_p(t)) \quad \text{(A5)}$$

where,

$$\rho(t) = -\sqrt{\frac{4\pi}{3}}\frac{1}{8\pi M}f_0(t) \quad \text{and} \quad \sigma(\theta) = \sqrt{\frac{4\pi}{3}}Y^{10}(\theta) \quad \text{(A6)}$$

This brings the perturbation to,

$$\delta g_{tt} = 4\mu\frac{r^2}{r_p(t)^3}\frac{(r_p(t) - 2M)^2}{r - 2M}\delta(r - r_p(t))\sigma \quad \text{(A7)}$$

$$f^2\delta g_{rr} = -\frac{\mu}{Mr}(r - 2M)(r_p(t) - 2M)\delta(r - r_p(t))\sigma \quad \text{(A8)}$$

$$f\delta g_{tr} = \frac{r\mu}{M}\sqrt{\frac{2M}{r_p(t)}}\left(1 - \frac{2M}{r_p(t)}\right)\left(1 + \frac{r_p(t) - 2M}{r - 2M}\right)\delta(r - r_p(t))\sigma \quad \text{(A9)}$$

We see from (17) and (18) that these are the relevant components in the deformation of the event horizon; $\delta g_{VV} = \frac{1}{4\kappa^2}\frac{1}{V^2}(\delta g_{tt} + 2f\delta g_{rt} + f^2\delta g_{rr})$ and $\delta\hat{\Gamma}^\theta_{VV} = -\frac{1}{2r^2}\partial_\theta\delta g_{VV}$. Since we evaluate at the location of the event horizon, $r = 2M$, we see that these terms vanish when the particle reaches the event horizon. Further, we compute the apparent horizon before the particle touches the horizon and thus the apparent horizon is not affected.

[1] B. P. Abbott *et al.*, "Observation of Gravitational Waves from a Binary Black Hole Merger," *Phys. Rev. Lett.*, vol. 116, no. 6, p. 061102, 2016.

[2] F. J. Zerilli, "Gravitational field of a particle falling in a schwarzschild geometry analyzed in tensor harmonics," *Phys. Rev.*, vol. D2, pp. 2141–2160, 1970.

[3] K. Martel and E. Poisson, "A One parameter family of time symmetric initial data for the radial infall of a particle into a Schwarzschild black hole," *Phys. Rev.*, vol. D66, p. 084001, 2002.

[4] A. Spallicci, "Free fall and self-force: An Historical perspective," *Fundam. Theor. Phys.*, vol. 162, pp. 561–603, 2011. [,561(2010)].

[5] C. O. Lousto and R. H. Price, "Understanding initial data for black hole collisions," *Phys. Rev.*, vol. D56, pp. 6439–6457, 1997.

[6] R. Emparan and M. Martinez, "Exact Event Horizon of a Black Hole Merger," *Class. Quant. Grav.*, vol. 33, no. 15, p. 155003, 2016.

[7] R. Hamerly and Y. Chen, "Event Horizon Deformations in Extreme Mass-Ratio Black Hole Mergers," *Phys. Rev.*, vol. D84, p. 124015, 2011.

[8] P. Mösta, L. Andersson, J. Metzger, B. Szilágyi, and J. Winicour, "The merger of small and large black holes," *Classical and Quantum Gravity*, vol. 32, no. 23, p. 235003, 2015.

[9] V. Moncrief, "Gravitational perturbations of spherically symmetric systems. I. The exterior problem.," *Annals Phys.*, vol. 88, pp. 323–342, 1974.

[10] D. R. Brill and R. W. Lindquist, "Interaction energy in geometrostatics," *Phys. Rev.*, vol. 131, pp. 471–476, 1963.

[11] C. O. Lousto and R. H. Price, "Headon collisions of black holes: The Particle limit," *Phys. Rev.*, vol. D55, pp. 2124–2138, 1997.

[12] P. Anninos, D. Bernstein, S. Brandt, J. Libson, J. Masso, E. Seidel, L. Smarr, W.-M. Suen, and P. Walker, "Dynamics of apparent and event horizons," *Phys. Rev. Lett.*, vol. 74, pp. 630–633, 1995.

[13] S. Detweiler and E. Poisson, "Low multipole contributions to the gravitational self-force," *Physical Review D*, vol. 69, no. 8, p. 084019, 2004.

[14] K. A. Dennison, T. W. Baumgarte, and H. P. Pfeiffer, "Approximate initial data for binary black holes," *Phys. Rev.*, vol. D74, p. 064016, 2006.

[15] T. Baumgarte and S. Shapiro, *Numerical Relativity: Solving Einstein's Equations on the Computer*. Cambridge University Press, 2010.

[16] S. Hayward, "General laws of black hole dynamics," *Phys.Rev.*, vol. D49, pp. 6467–6474, 1994.

[17] A. Ashtekar and B. Krishnan, "Isolated and dynamical horizons and their applications," *Living Rev.Rel.*, vol. 7, p. 10, 2004.

[18] L. Andersson, M. Mars, and W. Simon, "Local existence of dynamical and trapping horizons," *Phys.Rev.Lett.*, vol. 95, p. 111102, 2005.

[19] R. Bousso and N. Engelhardt, "Proof of a New Area Law in General Relativity," *Phys. Rev.*, vol. D92, no. 4, p. 044031, 2015.

[20] A. Bohn, L. E. Kidder, and S. A. Teukolsky, "Toroidal Horizons in Binary Black Hole Mergers," *Phys. Rev.*, vol. D94, no. 6, p. 064009, 2016.

[21] R. A. Matzner, H. E. Seidel, S. L. Shapiro, L. Smarr, W.-M. Suen, S. A. Teukolsky, and J. Winicour, "Geometry of a black hole collision," *Science*, vol. 270, no. 5238, pp. 941–947, 1995.

[22] N. T. Bishop, "The closed trapped region and the apparent horizon of two schwarzschild black holes," *General Relativity and Gravitation*, vol. 14, no. 9, pp. 717–723, 1982.

[23] A. Čadež, "Apparent horizons in the two-black-hole problem," *Annals of Physics*, vol. 83, no. 2, pp. 449 – 457, 1974.

[24] P. Anninos, D. Bernstein, S. Brandt, J. Libson, J. Masso, E. Seidel, L. Smarr, W.-M. Suen, and P. Walker, "Dynamics of apparent and event horizons," *Phys. Rev. Lett.*, vol. 74, pp. 630–633, 1995.

[25] G. B. Cook and A. M. Abrahams, "Horizon structure of initial data sets for axisymmetric two black hole collisions," *Phys. Rev.*, vol. D46, pp. 702–713, 1992.

Chapter 6

Soliton Mechanics

Soliton mechanics

Sharmila Gunasekaran,* Uzair Hussain,† and Hari K. Kunduri‡

Department of Mathematics and Statistics,

Memorial University of Newfoundland St John's NL A1C 4P5, Canada

(Dated: September 21, 2017)

Abstract

The domain of outer communication of five-dimensional asymptotically flat stationary spacetimes may possess non-trivial 2-cycles (bubbles). Spacetimes containing such 2-cycles can have non-zero energy, angular momenta, and charge even in the absence of horizons. A mass variation formula has been established for spacetimes containing bubbles and possibly a black hole horizon. This 'first law of black hole and soliton mechanics' contains new intensive and extensive quantities associated to each 2-cycle. We consider examples of such spacetimes for which we explicitly calculate these quantities and show how regularity is essential for the formulae relating them to hold. We also derive new explicit expressions for the angular momenta and charge for spacetimes containing solitons purely in terms of fluxes supporting the bubbles.

* sdgg82@mun.ca

† uh1681@mun.ca

‡ hkkunduri@mun.ca

I. INTRODUCTION

A striking feature of Einstein-Maxwell theory in four dimensions is the absence of globally stationary, asymptotically flat solutions with non-zero energy - that is, there are 'no solitons without horizons' [1]. This property is closely linked to uniqueness theorems for black holes, and indeed it fails to hold in Einstein-Yang Mills theory for which 'hairy' black holes exist (see, e.g. [2]). In five and higher dimensions, however, non-trivial topology in the spacetime can support the existence of such horizonless solitons even in Einstein-Maxwell supergravity theories. For an asymptotically flat solution, the topological censorship theorem [3] asserts that the domain of outer communication of a spacetime must be simply connected. In four dimensions, that is sufficient to ensure the absence of any cycles in the exterior. In five dimensions, simple connectedness is a weaker constraint, and in particular does not exclude the possibility of 2-cycles ('bubbles'). Physically, these cycles are supported by magnetic flux supplied by Maxwell fields and contribute to both the energy and angular momenta of the spacetime.

In this note we will focus on five-dimensional asymptotically flat stationary spacetimes with two commuting rotational Killing fields, possibly containing a single black hole. In this case it has been shown that the topology of the domain of outer communication is $\mathbb{R} \times \Sigma$, where[1]

$$\Sigma \cong \left(\mathbb{R}^4 \# n(S^2 \times S^2) \# n'(\pm \mathbb{CP}^2)\right) \backslash B, \tag{1}$$

for some $n, n' \in \mathbb{N}_0$ and B is the black hole region, where the horizon $H = \partial B$ must topologically be one of $S^3, S^1 \times S^2$ or $L(p,q)$ [5–8]. The integers n, n' determine the 2-cycle structure of Σ.

[1] In fact, the statement regarding Σ is still true if only one rotational Killing field is assumed, although then there are more possibilities for the horizon topology [7].

In the absence of black holes, soliton spacetimes with 2-cycles supported by flux are known to exist, with a large number of supersymmetric (see the review [9]) and non-supersymmetric examples [10–12]. The largest known family of solutions to our knowledge of these two types appeared in [13] and [14] respectively. These spacetimes carry positive energy. The relationship between the mass of these spacetimes and their fluxes is expressed in a Smarr-type formula, as observed for BPS solitons in supergravity theories by Gibbons and Warner [15]. Subsequently, it was shown that under stationary, $U(1)^2$-invariant variations satisfying the linearized field equations, variations of the mass and magnetic fluxes for general soliton spacetimes are governed by a 'first law' formula [16] (see (11) below).

Furthermore, one can derive a generalised mass and mass variation formula for $\mathbb{R}\times U(1)^2$-invariant spacetimes containing a black hole with an arbitrary number of 2-cycles in the exterior region. Similar to the soliton case it was found that on top of the familiar terms for a black hole, extra terms due to the bubbles are present. However, unlike the pure soliton case, these additional terms are most naturally expressed in terms of variations of an intensive quantity (a potential), as opposed to an extensive quantity (a flux). For Einstein-Maxwell theory, possibly with a Chern-Simons term, the mass formula is [16],

$$M = \frac{3\kappa A_H}{16\pi} + \frac{3}{2}\Omega_i J_i + \Phi_H Q + \frac{1}{2}\sum_{[C]} \mathcal{Q}[C]\Phi[C] + \frac{1}{2}\sum_{[D]} \mathcal{Q}[D]\Phi[D] \tag{2}$$

and the first law of black hole mechanics is,

$$\delta M = \frac{\kappa \delta A_H}{8\pi} + \Omega_i \delta J_i + \Phi_H \delta Q + \sum_{[C]} \mathcal{Q}[C]\delta\Phi[C] + \sum_{[D]} \mathcal{Q}[D]\delta\Phi[D]\ . \tag{3}$$

In the above $[C]$ is a basis for the second homology of Σ, $[D]$ are certain disc topology surfaces which extend from the horizon, Φ are magnetic potentials and $\mathcal{Q}$ are certain 'electric' fluxes defined on these surfaces which we will define precisely below.

This shows that non-trivial spacetime topology plays an important role in black hole thermodynamics, thus providing further motivation to study such objects beyond the obvious implications for black hole non-uniqueness [17].

It should be noted that most explicitly known examples of soliton spacetimes are supersymmetric, in which case the mass variation formula simply follows from the BPS relation. The same is true for the supersymmetric solution describing a rotating black hole with a soliton in the exterior region [17]. Indeed quite generally for BPS black hole solutions one can show that the additional terms arising in (2) and (3) vanish identically. This is analogous to the fact that for BPS black holes in these theories, the surface gravity and angular velocities also vanish identically. For non-supersymmetric solutions describing black holes with exterior bubbles, however, these terms would generically contribute. Examples of such solutions are not explicitly known, although there seems to be no obstruction to their existence, even in the vacuum.

The purpose of this paper is to apply the formalism developed in [16] to explicitly compute the various potentials and fluxes appearing above for some known spacetimes with non-trivial Σ. In so doing we will verify the first variation formula above. We will also derive some new relations that show how the angular momenta and total electric charge of a spacetime may arise solely from the presence of flux through the 2-cycles. Finally, we will reexamine the singly-rotating dipole black ring [18]. The solution is characterized by a local dipole 'charge' resulting from magnetic flux through the S^2 of the ring horizon. The first law for black rings derived in [19] contains additional terms due to the dipole charge and we show how this is recovered using the general formalism of [16]. This will use in a crucial way the disc topology region that lies in the domain of outer communication of the black ring.

II. FIRST LAW FOR BLACK HOLES AND SOLITONS IN SUPERGRAVITY

The mass and mass variation formulae for asymptotically flat, stationary spacetimes invariant under two commuting rotational symmetries has been established for a general five-dimensional theory of gravity coupled to an arbitrary set of Maxwell fields and uncharged scalars. We will be concerned with specific soliton and black hole solutions to five-dimensional minimal supergravity, whose bosonic action is (setting Newton's constant $G_5 = 1$)

$$S = \frac{1}{16\pi}\int_{\mathcal{M}}\left(\star R - 2F\wedge\star F - \frac{8}{3\sqrt{3}}F\wedge F\wedge A\right) \tag{4}$$

Here $F = \mathrm{d}A$ and A is a locally defined gauge potential. The existence of a non-trivial second homology H_2 implies that F is closed but not exact. The theory can be recovered from the general theory considered in [16] upon setting $I = 1$, $g_{IJ} = 2$ and $C_{IJK} = 16/\sqrt{3}$. We will follow this convention throughout when appealing to the construction of potentials and fluxes used in [16]. The equations of motion are

$$R_{ab} = \frac{4}{3}F_{ac}F_b{}^c + \frac{1}{3}G_{acd}G_b{}^{cd}\,, \qquad \mathrm{d}\star F + \frac{2}{\sqrt{3}}F\wedge F = 0 \tag{5}$$

where $G = \star F$. The central observation of [15] was that the non-triviality of the second homology H_2 makes it more natural to work with G rather than the gauge potential A which cannot be globally defined.

Let ξ be the stationary Killing field normalized so that $|\xi|^2 \to -1$ at spatial infinity (in the case of a spacetime containing a black hole, ξ is instead identified with the Killing field which is the null generator of the event horizon). Using the fact that F is closed and invariant under this action, we have a globally defined potential Φ_ξ defined by

$$\mathrm{d}\Phi_\xi \equiv i_\xi F \tag{6}$$

and the requirement $\Phi_\xi \to 0$ at spatial infinity. Note that, even though F is not exact, $i_\xi F$ is. Using Cartan's formula one can show that $i_\xi F$ is in fact closed, and since we assume that the space is simply connected, all closed one-forms are exact. From the Maxwell equation one may define a closed two-form

$$\Theta = 2i_\xi G - \frac{8}{\sqrt{3}} F\Phi_\xi \tag{7}$$

If, in addition to being stationary, the spacetime is invariant under a $U(1)^2$ isometry generated by the Killing fields $m_i = (m_1, m_2)$ (normalized to have 2π-periodic orbits), we also have globally defined magnetic potentials

$$\mathrm{d}\Phi_i = i_{m_i} F \tag{8}$$

and we also fix the freedom by requiring these vanish at an asymptotically flat end. Together (ξ, m_i) generate an $\mathbb{R}\times U(1)^2$ action acting as isometries on $(\mathcal{M}, g, F)$. Using these potentials one can finally deduce the existence of globally defined potentials U_i

$$\mathrm{d}U_i = i_{m_i}\Theta + \frac{8}{\sqrt{3}}\mathrm{d}\Phi_i\Phi_\xi^H \tag{9}$$

which are again fixed by requiring they vanish at the asymptotically flat end. Here Φ_ξ^H is the pullback of Φ_ξ to the horizon if a black hole is present in the spacetime; for a pure soliton spacetime this term is ignored. The potentials and fluxes defined above can be thought of as functions on a 2d orbit space $\mathcal{B} \cong \Sigma/U(1)^2$ [5]. The rank of the matrix $\lambda_{ij} = m_i \cdot m_j$ divides the space into two dimensional interior points, one dimensional boundary segments ($\partial\mathcal{B}$) called rods and zero dimensional points that lie on 'corners' where the segments intersect. A black hole is represented by a compact rod $I_H \cong H/U(1)^2$ where the timelike Killing field goes null. There are two non-compact semi-infinite rods corresponding to the two asymptotic axes of rotation extending out to spatial infinity. The rest of $\partial\mathcal{B}$ contains finite rods I_i where an

integer linear combination $v^i m_i, v^i \in \mathbb{Z}$ of the rotational Killing fields vanishes. This orbit space data thus encodes the action of the isometry group and determines the full spacetime topology up to diffeomorphism [5]. In particular finite rods represent two-dimensional submanifolds which may have the topology of either S^2, or a closed disc D if the corresponding rod is adjacent to I_H. We will discuss specific examples of spacetimes containing such 2-cycles and discs below.

For purely soliton spacetimes (i.e. without black holes), the Smarr formula and mass variation reduce to [16]

$$M = \frac{1}{2}\sum_{[C]} \Psi[C] q[C] \tag{10}$$

$$\delta M = \sum_{[C]} \Psi[C] \delta q[C]. \tag{11}$$

where

$$q[C] = \frac{1}{4\pi}\int_C F \quad \text{and} \quad \Psi[C] = \pi v^i U_i \tag{12}$$

represent the magnetic flux and magnetic potential associated to each element of $[C]$. Note that in (11) the extensive variable $q[C]$ appears naturally in the first law in contrast to (3).

Before discussing specific examples, we would like to present new Smarr-type formulae for the angular momenta and electric charge for purely soliton spacetimes as a sum over fluxes through the 2-cycles. These are useful as they demonstrate how a spacetime can possess such conserved charges in the absence of horizons.

Firstly, consider the angular momenta J_i associated to the rotational Killing field m_i defined by the Komar integrals

$$J[m_i] = \frac{1}{16\pi}\int_{S^3_\infty} \star \mathrm{d}m_i \ . \tag{13}$$

The Maxwell equation and Killing property of the m_i imply the existence of two closed

(though not necessarily exact) two-forms Υ_i defined by

$$\Upsilon_i \equiv 2i_{m_i}G - \frac{8}{\sqrt{3}}F\Phi_i \ . \tag{14}$$

Cartan's formula immediately implies the existence of global potential functions χ_{ij} satisfying $\mathrm{d}\chi_{ij} = i_{m_i}\Upsilon_j$. Note that we can always choose the integration constant so that $\chi_{ij} = 0$ on an interval on which m_i vanishes for fixed j. Now using Stokes' theorem

$$J[m_i] = \frac{1}{8\pi}\int_\Sigma \star\mathrm{Ric}(m_i) = \frac{1}{8\pi}\int_\Sigma \left(-\frac{1}{3}\right)\Upsilon_i \wedge F + \frac{4}{3}\mathrm{d}\star(F\Phi_i) \tag{15}$$

The final term above may be shown to vanish by converting it to an integral over S^3_∞ where Φ_i vanishes. We can evaluate this integral over the orbit space $\mathcal{B}$, giving

$$J[m_i] = \frac{\pi}{6}\int_{\mathcal{B}} \eta^{jk}\mathrm{d}\chi_{ji}\wedge\mathrm{d}\Phi_k = \frac{\pi}{6}\int_{\mathcal{B}}\mathrm{d}[\eta^{jk}\chi_{ji}\wedge\mathrm{d}\Phi_k] \tag{16}$$

where η^{ij} is the antisymmetric symbol with $\eta^{12} = 1$. The final term can be converted to a boundary term on $\partial\mathcal{B}$, and using the fact that the potentials vanish on the semi-infinite rods $I_\pm$, we are left with

$$J[m_i] = \frac{\pi}{6}\sum_i \int_{I_i}\eta^{jk}\chi_{ji}\mathrm{d}\Phi_k \tag{17}$$

This can be further simplified by using the fact that each rod is specified by a pair of integers v^i, so that $v^i m_i$ vanishes By definition $v^i\mathrm{d}\Phi_i = 0$ on the rod, so that $\Phi[C] \equiv v^i\Phi_i$ is constant. By an $SL(2,\mathbb{Z})$ change of basis let us define a new basis $(\hat{m}_1, \hat{m}_2)$ for the $U(1)^2$ generators such that $\hat{m}_1 = v^i m_i$. The other Killing field $\hat{m}_2$ is non-vanishing on the rod except at the endpoints (these correspond to topologically S^2 submanifolds in the spacetime). Note that in the obvious notation, $\hat{\chi}_{1i}, \hat{\Phi}_1$ are constants on the rod. Using $SL(2,\mathbb{Z})$-invariance, $\eta^{jk}\chi_{ji}\mathrm{d}\Phi_k = \eta^{jk}\hat{\chi}_{ji}\mathrm{d}\hat{\Phi}_k$. Putting the above facts together we arrive at

$$J[m_i] = \frac{1}{3}\sum_{[C]}\chi_i[C]q[C] \tag{18}$$

where $q[C]$ are the magnetic fluxes associated to a given cycle C and $\chi_i[C] \equiv -\pi\hat{\chi}_{1i} = -\pi v^j \chi_{ji}$ is a constant associated to each cycle. It is natural to interpret the $\chi_i[C]$ as *magnetic angular momenta potentials* as they encode how the magnetic flux $q[C]$ contribute to the total angular momenta of the spacetime.

Now let us turn to an expression for the total electric charge Q, defined by

$$Q \equiv \frac{1}{4\pi}\int_{S^3_\infty} \star F = -\frac{1}{2\sqrt{3}\pi}\int_\Sigma F \wedge F \tag{19}$$

It may appear counterintuitive that magnetic fluxes contribute to the electric charge, but it should be noted that the Maxwell equation in supergravity is self-sourced. We now proceed to evaluate this over the boundary of the orbit space. Using the definition of the magnetic potentials, we have

$$Q = \frac{\pi}{\sqrt{3}}\int_{\mathcal{B}} \eta^{ij} \mathrm{d}\Phi_i \wedge \mathrm{d}\Phi_j = \frac{\pi}{\sqrt{3}}\int_{\partial\mathcal{B}} \eta^{ij}\Phi_i \mathrm{d}\Phi_j \ . \tag{20}$$

We can now express this as a sum over the 2-cycles using the argument used above for the angular momenta. The result is

$$Q = -\frac{4\pi}{\sqrt{3}}\sum_{[C]} \Phi[C] q[C] \tag{21}$$

where $\Phi[C] = v^i\Phi_i$ are constant magnetic potentials associated to each 2-cycle with corresponding rod vector v^i.

III. EXAMPLES

A. Single soliton spacetime

Our first example is a charged, non-supersymmetric gravitational soliton with spatial slices $\Sigma \cong \mathbb{R}^4 \# \mathbb{CP}^2$ which was concisely analyzed in [15] (see also [11] for a discussion of a generalization which is asymptotically AdS_5). In the following we will

use a different parametrization which is convenient for our purposes. The equations of motion (5) admit the following local solution, invariant under an $\mathbb{R}\times SU(2)\times U(1)$ isometry:

$$\mathrm{d}s^2 = -\frac{r^2 W(r)}{4b(r)^2}\mathrm{d}t^2 + \frac{\mathrm{d}r^2}{W(r)} + \frac{r^2}{4}(\sigma_1^2+\sigma_2^2) + b(r)^2(\sigma_3 + f(r)\mathrm{d}t)^2 \tag{22}$$

$$F = \frac{\sqrt{3q}}{2}\mathrm{d}\left[\left(\frac{1}{r^2}\right)\left(\frac{j}{2}\sigma_3 - \mathrm{d}t\right)\right] \tag{23}$$

where σ_i are left-invariant one-forms on $SU(2)$:

$$\sigma_1 = -\sin\psi\mathrm{d}\theta + \cos\psi\sin\theta\mathrm{d}\phi\,, \quad \sigma_2 = \cos\psi\mathrm{d}\theta + \sin\psi\sin\theta\mathrm{d}\phi\,, \quad \sigma_3 = \mathrm{d}\psi + \cos\theta\mathrm{d}\phi \tag{24}$$

which satisfy $\mathrm{d}\sigma_i = \frac{1}{2}\epsilon_{ijk}\sigma_j\wedge\sigma_k$ and $\psi\sim\psi+4\pi$, $\phi\sim\phi+2\pi$, $\theta\in[0,\pi]$ is required for asymptotic flatness. The functions appearing in the metric are given by

$$W(r) = 1 - \frac{2}{r^2}(p-q) + \frac{q^2+2pj^2}{r^4} \qquad f(r) = -\frac{j}{2b(r)^2}\left(\frac{2p-q}{r^2} - \frac{q^2}{r^4}\right) \tag{25}$$

$$b(r)^2 = \frac{r^2}{4}\left(1 - \frac{j^2q^2}{r^6} + \frac{2j^2p}{r^4}\right) \tag{26}$$

where $p,q,j\in\mathbb{R}$. We will take $m_i = (\partial_{\hat{\psi}},\partial_\phi)$, $\hat{\psi} = \psi/2$, to be our basis for the generators of the $U(1)^2$ action with 2π-periodic orbits.

The parameters (p,q,j) in the above local metric can be chosen to describe a asymptotically flat, charged rotating black holes. However we may obtain a regular soliton spacetime by requiring that the S^1 parameterized by the coordinate ψ degenerates smoothly at some $r=r_0$ in the spacetime, leaving an S^2 bolt, or bubble. We therefore require $g_{\psi\psi} = b(r)^2$ vanishes at r_0. Regularity of the spacetime metric imposes that $W(r_0)=0$. The existence of a simultaneous root fixes

$$p = \frac{r_0^4(r_0^2-j^2)}{2j^4} \qquad q = -\frac{r_0^4}{j^2} \tag{27}$$

In order for $\partial_{\hat{\psi}}$ to degenerate smoothly and avoid a conical singularity at $r=r_0$ requires $W'(r_0)(b^2(r_0))' = 1$, or equivalently

$$(1-x)(2+x)^2 = 1 \tag{28}$$

for $x = x_* = r_0^2/j^2$. This cubic has a unique positive solution at $x \approx 0.870385$, and in particular $r_0^2 < j^2$.

With this inequality it is easy to check that $W(r), b(r)^2 > 0$ for $r > r_0$ and the spacetime metric is globally regular. Further

$$g^{tt} = -\frac{4b(r)^2}{r^2 W(r)} < 0 \tag{29}$$

so the spacetime is stably causal, and in particular the t =constant hpersurfaces are Cauchy surfaces. It can be verified that $g_{tt} < 0$ everywhere, so $\partial/\partial t$ is globally timelike and in particular there are no ergoregions. However, if one uplifts the soliton to six dimensions, we expect it will suffer from the instability discussed in [20].

We thus obtain a 1-parameter family of $\mathbb{R} \times SU(2) \times U(1)$-invariant soliton spacetime.

The S^2 at $r = r_0$ has a round metric

$$\mathrm{d}s_2^2 = \frac{r_0^2}{4}(\mathrm{d}\theta^2 + \sin^2\theta \mathrm{d}\phi^2) \tag{30}$$

and carries a magnetic flux

$$q[C] = \frac{1}{4\pi}\int_{S^2} F = \frac{\sqrt{3}r_0^2}{4j} \tag{31}$$

It is straightforward to read off

$$\Phi_\xi = \frac{\sqrt{3}q}{2r^2}\ , \qquad \Phi_{\hat{\psi}} = -\frac{\sqrt{3}qj}{2r^2}\ , \qquad \Phi_\phi = -\frac{\sqrt{3}qj\cos\theta}{4r^2}\ . \tag{32}$$

A long but straightforward calculation yields, using (7) and (9):

$$\mathrm{d}U_{\hat{\psi}} = \left[\frac{2\sqrt{3}jq}{r^3} - \frac{4\sqrt{3}jq^2}{r^5}\right]\mathrm{d}r \tag{33}$$

$$\mathrm{d}U_\phi = \left[-\frac{2\sqrt{3}jq^2\cos\theta}{r^5} + \frac{\sqrt{3}jq\cos\theta}{r^3}\right]\mathrm{d}r + \left[-\frac{\sqrt{3}jq^2\sin\theta}{2r^4} + \frac{\sqrt{3}jq\sin\theta}{2r^2}\right]\mathrm{d}\theta \tag{34}$$

which leads to

$$U_{\hat{\psi}} = \frac{\sqrt{3}jq}{r^2}\left(\frac{q}{r^2}-1\right)\ , \qquad U_{\phi} = \frac{\sqrt{3}jq\cos\theta}{2r^2}\left(\frac{q}{r^2}-1\right) \tag{35}$$

where the integration constants have been fixed so that the potentials vanish as $r \to \infty$.

On the S^2 'bolt' at $r = r_0$, the Killing field $\partial_{\hat{\psi}} = 2\partial_{\psi}$ degenerates smoothly. The interval structure of the orbit space is given below in the basis of rotational Killing fields orthogonal at infinity $(\partial_{\phi_1}, \partial_{\phi_2})$ where $\partial_{\phi_1} = \partial_{\psi} - \partial_{\phi}$ and $\partial_{\phi_2} = \partial_{\phi} + \partial_{\psi}$. In this basis the two semi-infinite rods can be manifestly seen as axes of rotation with vanishing ∂_{ϕ_1} or ∂_{ϕ_2}.

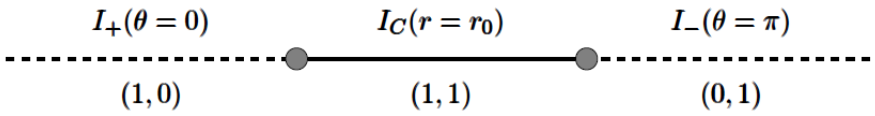

FIG. 1: Rod structure for single soliton spacetime in (ϕ_1, ϕ_2) basis.

We now turn to the computation of the potentials associated to the soliton. Firstly,

$$\Psi[C] = \pi U_{\hat{\psi}}(r_0) = \frac{\sqrt{3}\pi r_0^2(j^2 + r_0^2)}{j^3} \tag{36}$$

We then find

$$\frac{\Psi[C]q[C]}{2} = \frac{3\pi}{8}\left(\frac{r_0}{j}\right)^4 (j^2 + r_0^2) \tag{37}$$

which is indeed the ADM mass of the spacetime, which can easily be read off from the expansion

$$g_{tt} = -1 + \frac{8M}{3\pi r^2} + O(r^{-4}) \tag{38}$$

Finally the first law of soliton mechanics asserts that

$$\mathrm{d}M = \Psi[C]\mathrm{d}q[C] \tag{39}$$

In our explicit example,

$$\mathrm{d}M - \Psi[C]\mathrm{d}q[C] = \frac{3\pi r_0^5}{4j^5}(j\mathrm{d}r_0 - r_0\mathrm{d}j) \tag{40}$$

and the right hand side vanishes as a consequence of the regularity condition $r_0^2/j^2 = x_*$. We emphasize that the Smarr-type relation for the mass does not require regularity of the spacetime to hold, whereas the first law is in fact a finer probe of regularity. Finally one can explicitly check that the electric charge is indeed given by

$$Q = -\frac{4\pi}{\sqrt{3}}\Phi[C]q[C] = -\frac{\sqrt{3}\pi r_0^4}{2j^2}\ . \tag{41}$$

To compute the magnetic angular momentum potentials χ_{ij}, it is convenient to work in the $U(1)^2$ basis $(\partial_\psi, \partial_\phi)$ and then convert to the basis $(\partial_{\phi_1}, \partial_{\phi_2})$ which is orthogonal at the asymptotically flat end, in order to fix integration constants. A long but straightforward calculation yields

$$\begin{aligned} \chi_{\psi\psi} &= -\frac{\sqrt{3}q^2j^2}{4r^4} + \frac{\sqrt{3}q}{4}\ , \qquad \chi_{\phi\psi} = \frac{\sqrt{3}q\cos\theta}{4}\left(1 - \frac{qj^2}{r^4}\right) \\ \chi_{\phi\phi} &= -\frac{\sqrt{3}q^2j^2\cos^2\theta}{4r^4} - \frac{\sqrt{3}q}{4}\ , \qquad \chi_{\psi\phi} = -\frac{\sqrt{3}q\cos\theta}{4}\left(1 + \frac{qj^2}{r^4}\right) \end{aligned} \tag{42}$$

Since the 2-cycle is specified by the vanishing of $\partial_{\hat{\psi}}$, using the formula (18) we find

$$J_\psi = \frac{\pi r_0^6}{4j^3}\ , \qquad J_\phi = 0 \tag{43}$$

where in the second equality we observe that $\chi_{\psi\phi} = 0$ on C using (27) . It is easy to check that these expressions agree with the standard ADM angular momenta computed from the asymptotic fall-off of the metric. As expected, the $SU(2) \times U(1)$-invariant solution has equal angular momenta in orthogonal 2-planes, $J_1 = J_2 = J_\psi$. Note that $J_\psi \neq 0$ for the soliton; indeed, we have the constraint

$$J_\psi = -\frac{2Qq[C]}{3} = \frac{16\pi q[C]^3}{3\sqrt{3}}\ . \tag{44}$$

B. Double soliton spacetime

Our second example is a supersymmetric, asymptotically flat spacetime containing two non-homologous two-cycles. The spatial slices $\Sigma \cong \mathbb{R}^4 \# (S^2 \times S^2)$ where the connected sum with $\mathbb{R}^4$ corresponds to removing a point. The solution is originally given in the more general $U(1)^3$ five-dimensional supergravity [21]. We will quickly review this double soliton solution to the minimal supergravity theory (4) as this particular case does not seem to be reproduced explicitly in the literature. Note that it belongs to the general family of solutions with Gibbons-Hawking base space first analyzed in detail in [22].

The spacetime metric takes the canonical form of a timelike fibration over a hyperKähler 'base space'

$$\mathrm{d}s^2 = -f^2(\mathrm{d}t + \omega)^2 + f^{-1}\mathrm{d}s_B^2 \,, \tag{45}$$

where $V = \partial/\partial t$ is the supersymmetric, timelike Killing vector field and $\mathrm{d}s_M^2$ is a hyperKähler base [22]. The solution has a Gibbons-Hawking hyperKähler base

$$\mathrm{d}s_M^2 = H^{-1}(\mathrm{d}\psi + \chi)^2 + H(\mathrm{d}r^2 + r^2(\mathrm{d}\theta^2 + \sin^2\theta \mathrm{d}\phi^2)) \,, \tag{46}$$

where (r, θ, ϕ) are spherical coordinates on $\mathbb{R}^3$, the function H is harmonic on $\mathbb{R}^3$ and χ is a 1-form on $\mathbb{R}^3$ satisfying $\star_3 \mathrm{d}\chi = \mathrm{d}H$.

The analysis of [22] shows a general technique for constructing solutions of the above form. Defining the following harmonic functions on $\mathbb{R}^3$ [21]

$$H = \frac{1}{r} - \frac{1}{r_1} + \frac{1}{r_2}, \qquad K = \frac{k_0}{r} + \frac{k_1}{r_1} + \frac{k_2}{r_2}, \tag{47}$$

$$L = 1 + \frac{\ell_0}{r} + \frac{\ell_1}{r_1} + \frac{\ell_2}{r_2}, \qquad M = m + \frac{m_1}{r_1} + \frac{m_2}{r_2}, \tag{48}$$

with

$$r_1 = \sqrt{r^2 + a_1^2 - 2ra_1\cos\theta}, \qquad r_2 = \sqrt{r^2 + a_2^2 - 2ra_2\cos\theta} \tag{49}$$

where we assume $0 < a_1 < a_2$, we arrive at a solution provided

$$f^{-1} = H^{-1}K^2 + L \ , \qquad \omega = \omega_\psi(\mathrm{d}\psi + \chi) + \hat{\omega} \ , \tag{50}$$

where

$$\omega_\psi = H^{-2}K^3 + \frac{3}{2}H^{-1}KL + M \ , \tag{51}$$

$$\star_3 \mathrm{d}\hat{\omega} = H\mathrm{d}M - M\mathrm{d}H + \frac{3}{2}(K\mathrm{d}L - L\mathrm{d}K) \ . \tag{52}$$

The Maxwell field is then

$$F = \frac{\sqrt{3}}{2}\mathrm{d}\left[f(\mathrm{d}t + \omega) - KH^{-1}(\mathrm{d}\psi + \chi_i \mathrm{d}x^i) - \xi_i \mathrm{d}x^i\right] \ , \tag{53}$$

where the 1-form ξ satisfies $\star_3 \mathrm{d}\xi = -\mathrm{d}K$. For the above choice of harmonic functions one finds

$$\chi = \left[\cos\theta - \frac{r\cos\theta - a_1}{r_1} + \frac{r\cos\theta - a_2}{r_2}\right]\mathrm{d}\phi \ , \tag{54}$$

and

$$\xi = -\left[k_0\cos\theta + \frac{k_1(r\cos\theta - a_1)}{r_1} + \frac{k_2(r\cos\theta - a_2)}{r_2}\right]\mathrm{d}\phi \ , \tag{55}$$

where we have absorbed the integration constant in χ by suitably shifting ψ. One may also integrate explicitly for $\hat{\omega} = \hat{\omega}_\phi \mathrm{d}\phi$.

For a suitable choice of constants this solution is asymptotically flat provided $\Delta\psi = 4\pi$, $\Delta\phi = 2\pi$ and $0 \leq \theta \leq \pi$. In particular setting $r = \rho^2/4$ and sending $\rho \to \infty$ one finds

$$\mathrm{d}s_M^2 \sim \mathrm{d}\rho^2 + \frac{\rho^2}{4}\left[(\mathrm{d}\psi + \cos\theta \mathrm{d}\phi)^2)^2 \mathrm{d}\theta^2 + \sin^2\theta \mathrm{d}\phi^2\right] \tag{56}$$

with $O(\rho^{-2})$ corrections in the associated Cartesian chart. Finally, choosing

$$m = -\frac{3}{2}(k_0 + k_1 + k_2) \tag{57}$$

and suitably fixing the integration constant in $\hat{\omega}_\phi$, we find $f = 1 + \mathcal{O}(\rho^{-2})$, $\omega_\psi = \mathcal{O}(\rho^{-2})$ and $\hat{\omega}_\phi = \mathcal{O}(\rho^{-2})$. Thus the spacetime is asymptotically Minkowski $\mathbb{R}^{1,4}$.

The free parameters characterizing these local 'three-centre' solutions may be chosen so that globally, the spacetime describes a two-soliton spacetime (see, e.g. [15]). It is clear that the spacetime metric is regular apart from possible singularities at the 'centres' which lie at the points $\mathbf{x_0} = (0, 0, 0)$, $\mathbf{x_1} = (0, 0, a_1)$, and $\mathbf{x_2} = (0, 0, a_2)$ in the usual Cartesian coordinates on the ambient $\mathbb{R}^3$ on the base space. To ensure that the spacetime metric degenerates smoothly at these points, it is sufficient to first require that the base space be smooth. It can be shown that this is in fact the case without any further restriction of parameters (the base space metric approaches, up to a overall sign, the Euclidean metric near the origin of $\mathbb{R}^4$). Note that on the base space, ∂_ψ degenerates smoothly at the centres.

Next to ensure that the spacetime metric is well behaved and has the correct signature, we must have $f \neq 0$ ($f = 0$ would correspond to an event horizon). Equivalently we must ensure f^{-1} does not diverge, which fixes

$$\ell_2 = -k_2^2\,, \quad \ell_1 = k_1^2\,, \quad \ell_0 = -k_0^2\,. \tag{58}$$

Further, since ∂_ψ degenerates on the base, near the centres we have

$$|\partial_\psi|^2 = -f^2\omega_\psi^2 \leq 0 \tag{59}$$

which immediately implies that ω_ψ must *vanish* at these points. It turns out generically ω_ψ actually has simple poles at these points. Removing these requires

$$m_1 = \frac{k_1^3}{2}\,, \quad m_2 = \frac{k_2^3}{2}\,, \quad k_0 = 0\,. \tag{60}$$

Actually imposing that $\omega_\psi = 0$ leads to the so called 'bubble equations'

$$a_2k_1^3 + a_1k_2^3 - 3a_1a_2(k_1 + k_2) = 0 \tag{61}$$

$$a_1(k_1 + k_2)^3 + (a_2 - a_1)(k_1^3 - 3a_1(2k_1 + k_2)) = 0 \tag{62}$$

$$a_2(k_1 + k_2)^3 - (a_2 - a_1)(k_2^3 + 3a_2k_1) = 0 \tag{63}$$

which correspond to the enforcing regularity at $r = 0, r = a_1$, and $r = a_2$ respectively. This leaves a one-parameter family of 2-soliton spacetimes parameterized by (a_1, a_2, k_1, k_2) subject to the three regularity constraints. An analysis of the geometry shows that the spacetime is stably causal ($g^{tt} \leq 0$) [15].

Let us now consider the boundary structure of the orbit space $\mathcal{B} = \Sigma/U(1)^2$, which determines the topology of the spacetime. There is a semi-infinite rod I_+ corresponding to one of axes of symmetry in the asymptotically flat region. The appropriately normalized Killing field which vanishes on this rod is $v_+ = \partial_\psi - \partial_\phi$. In terms of the spherical coordinates on the ambient $\mathbb{R}^3$ associated to the Gibbons-Hawking space, $I_+ = \{r > a_2, \theta = 0\}$. Next, there is a finite rod $I_{C_2} = \{a_1 < r < a_2, \theta = 0\}$ with associated vanishing Killing field $v_2 = -(\partial_\phi + \partial_\psi)$. Note that the Killing field ∂_ψ is non vanishing on C_2 and degenerates smoothly at the endpoints $r = a_1, a_2$ implying that C_2 is a topologically S^2-submanifold in the spacetime. The second 'bubble' corresponds to the interval $I_{C_1} = \{0 < r < a_1, \theta = 0\}$ with associated Killing field $v_1 = -\partial_\phi + \partial_\psi$. The Killing field ∂_ψ is again non-vanishing on this interval and degenerates smoothly at the endpoints $r = 0, r = a_1$. Finally, there is a second semi-infinite rod $I_- = \{r > 0, \theta = \pi\}$ with associated Killing field $v_- = \partial_\phi + \partial_\psi$.

The rod structure is most naturally expressed in terms of the basis of Killing fields $m_1 = v_+, m_2 = v_-$ which have 2π periodic orbits:

$$v_+ = (1, 0)\,, \quad v_2 = (0, -1)\,, \quad v_1 = (1, 0)\,, \quad v_- = (0, 1) \tag{64}$$

from which it is easy to check that the compatibility condition $|\det(v_i^T v_{i+1}^T)| = 1$ is satisfied for adjacent rods.

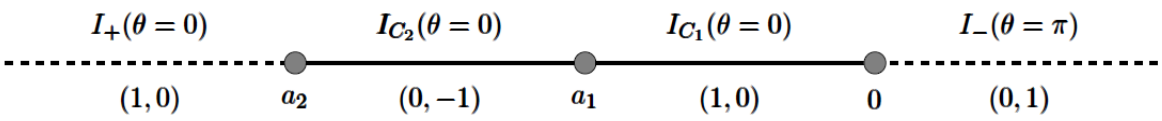

FIG. 2: Rod structure for double soliton spacetime in (ϕ_1, ϕ_2) basis. Here, $\partial_{\phi_1} = \partial_\psi - \partial_\phi$ and $\partial_{\phi_2} = \partial_\phi + \partial_\psi$.

We now turn to a computation of the various intensive and extensive quantities appearing in the first law. The magnetic fluxes through the bubbles C_1, C_2 are found to be

$$q[C_2] = \frac{1}{4\pi}\int_{S^2_2} F = -\frac{\sqrt{3}}{2}(k_1+k_2)\,, \qquad q[C_1] = \frac{1}{4\pi}\int_{S^2_1} F = \frac{\sqrt{3}}{2}k_1 \tag{65}$$

The computation of the 'electric' potentials U_i requires some more work. For a general supersymmetric solution in the timelike class, one can derive the relation

$$i_\xi \star F = \frac{\sqrt{3}}{2} f^2 \star_4 \mathrm{d}\omega - \frac{fG^+}{\sqrt{3}} \tag{66}$$

where $\star_4$ is the Hodge dual taken with respect to the base space and $G^+ = \frac{f}{2}(\mathrm{d}\omega + \star_4 \mathrm{d}\omega)$ is a self-dual 2 form. Using this, and the general form of the Maxwell field leads to the simple expression

$$\Theta = \sqrt{3}\mathrm{d}(f^2(\mathrm{d}t+\omega)) - 4F \tag{67}$$

from which it is manifest that Θ is closed, though not exact, as expected. We then have

$$U_\psi = -\sqrt{3}f^2\omega_\psi + 4A_\psi + 2\sqrt{3}(k_1+k_2) \tag{68}$$

$$U_\phi = -\sqrt{3}f^2\omega_\phi + 4A_\phi \tag{69}$$

where A_ψ, A_ϕ are the components of the gauge field and integration constants have been chosen so that U_i vanish at spatial infinity. As discussed above, $v^i_{C_2}U_i$ and $v^i_{C_1}U_i$

must be constant on the two-cycles C_2 and C_1 respectively. In order to demonstrate this, one must make use of the regularity constraints (61). We find

$$\Psi[C_2] = \pi U_{C_2} \equiv -\pi(U_\psi + U_\phi)|_{I_{C_2}} = -4\sqrt{3}k_1 \tag{70}$$

$$\Psi[C_1] = \pi U_{C_1} \equiv \pi(U_\psi - U_\phi)|_{I_{C_1}} = 4\pi\sqrt{3}(k_1 + k_2) \tag{71}$$

Using this we can indeed verify that

$$\frac{1}{2}\sum_C \Psi[C]q[C] = 6\pi k_1(k_1 + k_2) = M \tag{72}$$

The first law

$$\delta M = \Psi[C_1]\delta q[C_1] + \Psi[C_2]\delta q[C_2] \tag{73}$$

can then be verified explicitly (we emphasize this is independent from (72)). Note that it is straightforward to check that the magnetic potentials are

$$\Phi[C_1] = -\sqrt{3}(k_1 + k_2) = -\frac{1}{4\pi}\Psi[C_1]\ , \qquad \Phi[C_2] = \sqrt{3}k_1 = -\frac{1}{4\pi}\Psi[C_2] \tag{74}$$

and inserting these into (41) for the total electric charge expressed as sum over the basis of 2-cycles, one recovers the usual BPS relation $M = \sqrt{3}Q/2$. The variational formula (73) is surprising as it represents a genuine 'first law' for BPS geometries, whereas for BPS black holes, the first law trivially follows from the BPS condition (i.e. $\delta M = \sqrt{3}\delta Q/2$).

The calculation of angular momenta from the general formula (18) is less straightforward. The difficulty arises from the complexity of the solution, and although it is possible to show that $\mathrm{d}\chi_{ij} = 0$, obtaining the integrated potentials in closed form has proved difficult. However, it should be noted that the asymptotic conditions $v_+^i\chi_{ij} = 0$ on I_+ and $v_-^i\chi_{ij}$ on I_-, as well as the evaluation of $\chi_i[C]$ on each cycle, only require knowledge of χ_{ij} on the 'axes' $\theta = 0, \pi$. Hence we need only integrate for $\chi_{ij}(r, 0)$ and $\chi_{ij}(r, \pi)$ on each segment on the axis (i.e. $I_\pm, I_{C_i}$). Since the χ_{ij} must be continuous

functions of r along the axes across the rod points at $r = a_2, r = a_1$, and $r = 0$, the integration constants arising from integrating separately over each segment are determined completely by the asymptotic conditions. Carrying this out carefully one finds

$$\chi_\phi[C_2] = 2\sqrt{3}k_1(k_1 + 2k_2) \ , \qquad \chi_\phi[C_1] = -2\sqrt{3}(k_2^2 - k_1^2) \tag{75}$$

and

$$\chi_\psi[C_2] = -2\sqrt{3}k_1(3k_1 + 2k_2) \ , \qquad \chi_\psi[C_1] = 2\sqrt{3}(3k_1^2 + 4k_1k_2 + k_2^2) \tag{76}$$

where we have used the regularity constraints (61) to significantly simplify these expressions. Using the expressions for the fluxes (65) we obtain the angular momenta

$$J_\psi = 3\pi k_1(k_1 + k_2)(2k_1 + k_2) \ , \qquad J_\phi = -3\pi k_1k_2(k_1 + k_2) \ , \tag{77}$$

which do in fact agree with the standard ADM angular momenta provided that (61) is used to simplify the latter.

Using the above expressions for the charges (J_ψ, J_ϕ, Q) and fluxes $q[C_i]$, we can derive

$$J_\psi = = \frac{Q}{2}(q[C_1] - q[C_2]) = \frac{8\pi}{\sqrt{3}}q[C_1]q[C_2]\,(q[C_2] - q[C_1]) \ , \tag{78}$$

$$J_\phi = \frac{Q}{2}(q[C_2] + q[C_1]) = -\frac{8\pi}{\sqrt{3}}q[C_1]q[C_2]\,(q[C_2] + q[C_1]) \ . \tag{79}$$

The angular momenta about the $\psi-$ and $\phi-$ directions thus is a measure of the difference and sum of the magnetic fluxes out of the two bubbles.

C. Dipole black ring

As a last example, we consider asymptotically flat dipole black rings[18] where the horizon topology is $S^1 \times S^2$ and $\Sigma \cong \mathbb{R}^4 \# (S^2 \times D^2)$ [23, 24] .The rings are a solution to five dimensional Einstein-Maxwell theory (and also the minimal supergravity theory

because the Chern-Simons term is of no consequence to the solutions). For convenience to match with the conventions used in [18], in this section we take $g_{IJ} = 1/2$ in the general formalism of [16]. The metric is given by

$$ds^2 = -\frac{F(y)}{F(x)}\left(\frac{H(x)}{H(y)}\right)\left(\mathrm{d}t + C(\nu,\lambda)\,R\,\frac{1+y}{F(y)}\,\mathrm{d}\psi\right)^2 \tag{80}$$
$$+\frac{R^2}{(x-y)^2}\,F(x)\left(H(x)H(y)^2\right)\left[-\frac{G(y)}{F(y)H(y)^3}\mathrm{d}\psi^2 - \frac{\mathrm{d}y^2}{G(y)} + \frac{\mathrm{d}x^2}{G(x)} + \frac{G(x)}{F(x)H(x)^3}\mathrm{d}\varphi^2\right]$$

with the gauge potential,

$$A_\varphi = \sqrt{3}C(\nu,-\mu)R\frac{1+x}{H(x)} \tag{81}$$

The functions in the metric are defined as follows,

$$F(\xi) = 1+\lambda\xi, \quad G(\xi) = (1-\xi^2)(1+\nu\xi), \quad H(\xi) = 1-\mu\xi \tag{82}$$
$$\text{with } 0 < \nu \le \lambda < 1\,, 0 \le \mu < 1 \text{ and } C(\alpha,\beta) = \sqrt{\beta(\beta-\alpha)\frac{1+\beta}{1-\beta}},$$

where α and β are any two of the parameters μ, ν and λ.

The following relations remove conical singularities at $y = -1$, $x = -1$ and $x = +1$.

$$\Delta\psi = \Delta\varphi = 2\pi\frac{(1+\mu)^{3/2}\sqrt{1-\lambda}}{1-\nu}\,, \quad \frac{1-\lambda}{1+\lambda}\left(\frac{1+\mu}{1-\mu}\right)^3 = \left(\frac{1-\nu}{1+\nu}\right)^2 \tag{83}$$

Thermodynamic quantities for (80) were calculated in [18]. Here, we specifically focus on rederiving the the extra terms that contribute to the mass using the results in [16]. These extra terms arise from disc topology surfaces denoted by D that meet the horizon. The fluxes and potentials evaluated on these surfaces can be done so on any other surface that is homologous to D with the same boundary as D. Studying the rod structure of the solution reveals a disc topology surface at $x = 1$.

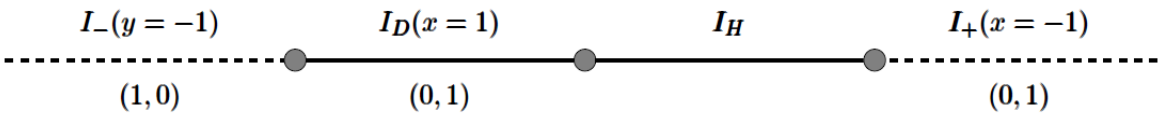

FIG. 3: Rod structure for dipole ring

The disc D is parametrized by (y,ψ) at constant t, ϕ and $x=1$. The flux $\mathcal{Q}[D]$ is given by

$$\mathcal{Q}[D]=\int_{[D]}\Theta=-\frac{\sqrt{3}\pi(\mu+1)R\sqrt{\mu(1-\lambda)(1-\mu)}}{4\sqrt{(\mu+\nu)}} \tag{84}$$

(For usual Einstein-Maxwell theory $g_{IJ}=\frac{1}{2}$ and $C_{IJK}=0$). ∂_φ vanishes at $x=1$. $(v^1,v^2)=(0,1)$ in the $(\hat{\partial}_\psi,\hat{\partial}_\varphi)$ basis, where the Killing fields are normalized to have 2π periodic orbits.

$$\Phi[D]=v^i\Phi_i=-\frac{2\sqrt{3}(1+\mu)R\sqrt{\mu(1-\lambda)(\mu+\nu)}}{\sqrt{(1-\mu)}(1-\nu)} \tag{85}$$

It is easily checked that the potential $\Phi[D]=-2\mathcal{D}$ and flux $\mathcal{Q}[D]=-\frac{1}{2}\hat{\Phi}$ where $\mathcal{D}$ is the local dipole charge and $\hat{\Phi}$ is the magnetic potential introduced[2] in [18]. Therefore, we see that the Smarr relation and first law given in [18]

$$M=\frac{3}{16\pi}\kappa A_H+\frac{3}{2}\Omega_H J+\frac{1}{2}\mathcal{D}\hat{\Phi}\ ,\qquad \delta M=\frac{\kappa\delta A_H}{8\pi}+\Omega_H\delta J+\hat{\Phi}\delta\mathcal{D} \tag{86}$$

match precisely with the derived expressions in (2) and (3). An important point to emphasize is that, although the local dipole charge $\mathcal{D}$ arises as a *flux* integral of F over the S^2 of the black ring [18], in our formalism it arises as the constant value of Φ evaluated on the equipotential disc surface D which ends on the horizon. Hence, although it seems counterintuitive that variations of an 'intensive' variable such as $\Phi[D]$ appear in the general first law, we see that at least in the present case, it is more

[2] The quantities $\mathcal{D}$ and $\hat{\Phi}$ are referred to as $\mathcal{Q}$ and Φ respectively in the notation of [18]. We are using different symbols to avoid confusion with the notation of [16].

naturally interpreted as an extensive variable (the dipole charge). Indeed if one looks at the fall-off of the gauge field A at the asymptotically flat region [26], this quantity can be interpreted as producing a dipole contribution. The fact that $\Phi[D]$ captures, in an invariant way, the dipole charge has also been observed in the context of black lenses [27–29]. In the case of black lenses, there is in fact no natural 2-cycle in the spacetime on which to define a dipole charge as there is for a ring [28].

IV. DISCUSSION

We have explicitly computed the additional terms in the Smarr relation and first law arising from non-trivial spacetime topology in three different geometries, two describing solitons and another describing a black ring. For purely soliton spacetimes, we have complemented the results in [16] with a Smarr type formula for J and Q. These expressions also demonstrate the presence of conserved charges in the absence of a horizon. We have seen that spacetime regularity is crucial for the first law to be satisfied for all examples.

A conjectured relation [30] between dynamical and thermodynamic instability has been established by Hollands and Wald [31]. They have shown that the black p-brane spacetime $M \times \mathbb{T}^p$ associated to a thermodynamically unstable black hole M is itself dynamically unstable. This result of course applies to spacetimes with horizons only, and do not pertain to the soliton spacetimes considered here. Very recently, the linear stability of supersymmetric soliton geometries has been investigated [32] (see also [33] for a rigorous analysis of the scalar wave equation). In particular the authors of [32] have produced evidence that these solutions suffer from a non-linear instability associated with the slow decay of linear waves. It would be interesting if a connection could be found between these studies of dynamical instability and an analogue of

thermodynamic instability using the laws of soliton mechanics discussed in this work.

Acknowledgements

HKK is supported by an NSERC Discovery Grant. This research was supported in part by Perimeter Institute for Theoretical Physics. Research at Perimeter Institute is supported by the Government of Canada and by the Province of Ontario. We thank James Lucietti for a number of useful suggestions and for comments on the draft.

---

[1] G. W. Gibbons, "Supergravity vacua and solitons," in *Duality and supersymmetric theories. Proceedings, Easter School, Newton Institute, Euroconference, Cambridge, UK, April 7-18, 1997*, pp. 267–296. 2011. arXiv:1110.0918 [hep-th]. https://inspirehep.net/record/458559/files/arXiv:1110.0918.pdf.

[2] A. Ashtekar, A. Corichi, and D. Sudarsky, "Hairy black holes, horizon mass and solitons," *Class. Quant. Grav.* **18** (2001) 919–940, arXiv:gr-qc/0011081 [gr-qc].

[3] J. L. Friedman, K. Schleich, and D. M. Witt, "Topological censorship," *Phys. Rev. Lett.* **71** (1993) 1486–1489, arXiv:gr-qc/9305017 [gr-qc]. [Erratum: Phys. Rev. Lett.75,1872(1995)].

[4] In fact, the statement regarding Σ is still true if only one rotational Killing field is assumed, although then there are more possibilities for the horizon topology [7].

[5] S. Hollands and S. Yazadjiev, "Uniqueness theorem for 5-dimensional black holes with two axial Killing fields," *Commun. Math. Phys.* **283** (2008) 749–768, arXiv:0707.2775 [gr-qc].

[6] S. Hollands and S. Yazadjiev, "A Uniqueness theorem for stationary Kaluza-Klein

black holes," *Commun. Math. Phys.* **302** (2011) 631–674, arXiv:0812.3036 [gr-qc].

[7] S. Hollands, J. Holland, and A. Ishibashi, "Further restrictions on the topology of stationary black holes in five dimensions," *Annales Henri Poincare* **12** (2011) 279–301, arXiv:1002.0490 [gr-qc].

[8] S. Hollands and A. Ishibashi, "Black hole uniqueness theorems in higher dimensional spacetimes," *Class. Quant. Grav.* **29** (2012) 163001, arXiv:1206.1164 [gr-qc].

[9] I. Bena and N. P. Warner, "Black holes, black rings and their microstates," *Lect. Notes Phys.* **755** (2008) 1–92, arXiv:hep-th/0701216 [hep-th].

[10] I. Bena, S. Giusto, C. Ruef, and N. P. Warner, "A (Running) Bolt for New Reasons," *JHEP* **11** (2009) 089, arXiv:0909.2559 [hep-th].

[11] G. Compere, K. Copsey, S. de Buyl, and R. B. Mann, "Solitons in Five Dimensional Minimal Supergravity: Local Charge, Exotic Ergoregions, and Violations of the BPS Bound," *JHEP* **12** (2009) 047, arXiv:0909.3289 [hep-th].

[12] N. Bobev and C. Ruef, "The Nuts and Bolts of Einstein-Maxwell Solutions," *JHEP* **01** (2010) 124, arXiv:0912.0010 [hep-th].

[13] I. Bena, S. Giusto, E. J. Martinec, R. Russo, M. Shigemori, D. Turton, and N. P. Warner, "Smooth horizonless geometries deep inside the black-hole regime," *Phys. Rev. Lett.* **117** no. 20, (2016) 201601, arXiv:1607.03908 [hep-th].

[14] I. Bena, G. Bossard, S. Katmadas, and D. Turton, "Non-BPS multi-bubble microstate geometries," *JHEP* **02** (2016) 073, arXiv:1511.03669 [hep-th].

[15] G. W. Gibbons and N. P. Warner, "Global structure of five-dimensional fuzzballs," *Class. Quant. Grav.* **31** (2014) 025016, arXiv:1305.0957 [hep-th].

[16] H. K. Kunduri and J. Lucietti, "The first law of soliton and black hole mechanics in five dimensions," *Class. Quant. Grav.* **31** no. 3, (2014) 032001, arXiv:1310.4810 [hep-th].

[17] H. K. Kunduri and J. Lucietti, "Black hole non-uniqueness via spacetime topology in five dimensions," *JHEP* **10** (2014) 082, arXiv:1407.8002 [hep-th].

[18] R. Emparan, "Rotating circular strings, and infinite nonuniqueness of black rings," *JHEP* **03** (2004) 064, arXiv:hep-th/0402149 [hep-th].

[19] K. Copsey and G. T. Horowitz, "The Role of dipole charges in black hole thermodynamics," *Phys. Rev.* **D73** (2006) 024015, arXiv:hep-th/0505278 [hep-th].

[20] V. Cardoso, O. J. C. Dias, J. L. Hovdebo, and R. C. Myers, "Instability of non-supersymmetric smooth geometries," *Phys. Rev.* **D73** (2006) 064031, arXiv:hep-th/0512277 [hep-th].

[21] I. Bena and N. P. Warner, "Bubbling supertubes and foaming black holes," *Phys. Rev.* **D74** (2006) 066001, arXiv:hep-th/0505166 [hep-th].

[22] J. P. Gauntlett, J. B. Gutowski, C. M. Hull, S. Pakis, and H. S. Reall, "All supersymmetric solutions of minimal supergravity in five- dimensions," *Class. Quant. Grav.* **20** (2003) 4587–4634, arXiv:hep-th/0209114 [hep-th].

[23] A. Alaee, H. K. Kunduri, and E. Martinez Pedroza, "Notes on maximal slices of five-dimensional black holes," *Class. Quant. Grav.* **31** (2014) 055004, arXiv:1309.2613 [gr-qc].

[24] L. Andersson, M. Dahl, G. J. Galloway, and D. Pollack, "On the geometry and topology of initial data sets with horizons," arXiv:1508.01896 [gr-qc].

[25] The quantities $\mathcal{D}$ and $\hat{\Phi}$ are referred to as $\mathcal{Q}$ and Φ respectively in the notation of [18]. We are using different symbols to avoid confusion with the notation of [16].

[26] R. Emparan and H. S. Reall, "Black Rings," *Class. Quant. Grav.* **23** (2006) R169, arXiv:hep-th/0608012 [hep-th].

[27] H. K. Kunduri and J. Lucietti, "Supersymmetric Black Holes with Lens-Space

Topology," *Phys. Rev. Lett.* **113** no. 21, (2014) 211101, arXiv:1408.6083 [hep-th].

[28] H. K. Kunduri and J. Lucietti, "Black lenses in string theory," *Phys. Rev.* **D94** no. 6, (2016) 064007, arXiv:1605.01545 [hep-th].

[29] S. Tomizawa and M. Nozawa, "Supersymmetric black lenses in five dimensions," arXiv:1606.06643 [hep-th].

[30] S. S. Gubser and I. Mitra, "The Evolution of unstable black holes in anti-de Sitter space," *JHEP* **08** (2001) 018, arXiv:hep-th/0011127 [hep-th].

[31] S. Hollands and R. M. Wald, "Stability of Black Holes and Black Branes," *Commun. Math. Phys.* **321** (2013) 629–680, arXiv:1201.0463 [gr-qc].

[32] F. C. Eperon, H. S. Reall, and J. E. Santos, "Instability of supersymmetric microstate geometries," arXiv:1607.06828 [hep-th].

[33] J. Keir, "Wave propagation on microstate geometries," arXiv:1609.01733 [gr-qc].

Chapter 7

Conclusion

In this thesis we have investigated the effect of small disturbances in spacetime to explore various interesting avenues of black hole physics. We explored applications of black hole perturbation theory to the exciting astrophysical problem of black hole mergers, specifically, extreme mass ratio mergers. In the setting of asymptotically AdS black holes and the fluid/gravity duality, we made precise the connection between standard black hole perturbation theory, pioneered by Regge,Wheeler & Zerilli, and the conservation equations of near equilibrium dissipative fluids. We were able to take this connection further to explore the possible extension of the fluid/gravity duality to include non-Newtonian fluids. Finally, we investigated the first law of soliton mechanics on five-dimensional spacetimes that contain solitons or "bubbles of nothing", here we are looking at linearized variations about the solutions too. In this final chapter we will provide a summary of each of the research papers and consider possible future directions.

In Section 1.1.8, we discussed the fluid/gravity duality and saw how the metric for a three dimensional brane can be written in a boosted form which makes the

velocity of the boundary fluid manifest. Then the EFEs are solved in an order-by-order expansion in terms of the gradients of the fluid velocity and it is shown that the constraint equations of the EFEs are the same as the conservation equations of the fluid on the boundary. In Chapter 3 our main goal was to understand precisely how, in the context of the fluid/gravity duality, standard perturbation theory of spherically symmetric black holes is connected with the near-equilibrium fluid dynamics found on a constant-r surface. We reviewed how perturbation theory of spherically symmetric black holes exploits symmetry and makes extensive use of spherical harmonics by expanding the metric perturbation in scalar, vector and tensor harmonics. This bears fruit in the form of a very simple and attractive wave equation, called the master equation with the scalar satisfying this equation called the master function. We accomplished the following: 1) it was shown that the master equation for both the even and odd perturbations was equivalent to conservation equations of the fluid on all constant-r surfaces, 2) we provided expressions for fluid parameters such as energy, velocity, viscosity, etc. in terms of the master function, this allows one to compute these quantities for the fluid on any constant-r surface in the time domain, 3) all expressions concerning the fluid were provided with general boundary conditions. This paper set the stage for more general computations in the fluid/gravity duality specifically in time domain, such as a direct numerical evolution of the master function.

A direct application of the work described in the preceding paragraph was seen in Chapter 4. The master function for the odd perturbations was numerically computed, by using a discretization of the domain which allowed us to time evolve a Gaussian pulse as initial data. Then we extracted the data at a large constant-r Dirichlet surface and computed the viscosity and the shear. It was shown that the viscosity changed with shear, approaching a constant at late times. It was argued that this behaviour is analogous to real world non-Newtonian fluids which have shear dependent

viscosity. This suggests a slight generalization of the fluid/gravity duality to include non-Newtonian fluids. This is still a work in progress but future directions are clear: to compute the even perturbations also and verify that similar non-Newtonian behaviour is found. Another future research endeavour would be to consider non- Newtonian fluid behaviour in spacetimes where the bulk is a brane rather than a black hole, this would be an interesting extension of the formalism of [6].

In Chapter 5 we used perturbation theory to tackle a problem relating to extreme mass ratio black hole mergers. Black hole mergers are currently a very active area of research, both theoretically and observationally. This area of research is primarily fuelled by the recent discovery of gravitational waves [1]. The scenario we considered was of a head-on collision of two black holes where the mass, μ of one the black hole is much smaller than the mass, M, of the other larger black hole, i.e, $\mu/M \to 0$. Given this extreme mass ratio we were able to model the whole problem using perturbation theory. We assumed that the small black hole was a point particle and this led to the master equation having an extra source term that depended on the particle stress tensor. We then integrated this master equation numerically. Specifically, the problem that we were interested in was how the event and apparent horizon of the large black hole deforms. To quantify the deformation of the event horizon we calculated how the null generators of the large black hole's event horizon were perturbed by the gravitational field of the particle. It was found that a prominent role is played by caustics which form at the point of the merger, as a result of nearby null geodesics crossing each other and joining the event horizon surface. For the apparent horizon we found an interesting and surprising result; we found that in the early stages of the merger when the particle is far from the large black hole the apparent horizon and event horizon coincide. As the particle gets closer the event horizon moves outward and grows, but the apparent horizon moves in the opposite direction.

This behaviour is simply explained by the attraction caused by the gravitational field of the particle on outward directed null geodesics that initially coincided with the even horizon. This attraction makes their expansion positive. Similarly the geodesics that were in the interior with slightly negative expansion now have zero expansion due to the gravitational field of the particle, hence the zero expansion surface, which is the apparent horizon, move inwards. A weakness of our approach is that any features related to the deformation of the small black hole are not present since it is assumed to be a particle. A natural future direction of research is to match the two complementary regimes of analysis, i.e, ours and that of [17]. This can be done by using techniques of matched asymptotic expansion.

Finally in Chapter 6 we applied the first law of soliton mechanics, that was derived in [38], to three five dimensional asymptotically flat solutions. The first law of soliton mechanics is a generalization of the first law of black hole mechanics to include spacetimes in higher dimensions with a non trivial topology in the domain of outer communication. Specifically, we considered spacetimes that have non-trivial two-cycles known as solitons or "bubbles of nothing". The main aim of our work was to explicitly verify the law for these examples and to see what role regularity plays. These bubbles are usually believed to be held up by charge to prevent them from collapsing, a research direction is to better understand the nature of the potentials that arise in the first law. Another direction is to extend the law to asymptotically AdS spacetimes, since these are five dimensional spacetimes their duals, via the AdS/CFT duality, are four dimensional conformal field theories, which are relevant in the real world. This would require a way to deduct divergent volume terms that appear in the Smarr relation and first law.

Bibliography

[1] B. P. Abbott et al. Observation of Gravitational Waves from a Binary Black Hole Merger. *Phys. Rev. Lett.*, 116(6):061102, 2016.

[2] N. Ambrosetti, J. Charbonneau, and S. Weinfurtner. The Fluid/gravity correspondence: Lectures notes from the 2008 Summer School on Particles, Fields, and Strings. 2008.

[3] R. L. Arnowitt, S. Deser, and C. W. Misner. Dynamical Structure and Definition of Energy in General Relativity. *Phys. Rev.*, 116:1322–1330, 1959.

[4] I. Bakas. Energy-momentum/Cotton tensor duality for AdS(4) black holes. *JHEP*, 01:003, 2009.

[5] V. Balasubramanian and P. Kraus. A Stress tensor for Anti-de Sitter gravity. *Commun. Math. Phys.*, 208:413–428, 1999.

[6] S. Bhattacharyya, V. E. Hubeny, S. Minwalla, and M. Rangamani. Nonlinear Fluid Dynamics from Gravity. *JHEP*, 02:045, 2008.

[7] I. Booth. Black hole boundaries. *Can. J. Phys.*, 83:1073–1099, 2005.

[8] J. D. Brown and J. W. York, Jr. Quasilocal energy and conserved charges derived from the gravitational action. *Phys. Rev.*, D47:1407–1419, 1993.

[9] V. Cardoso and O. J. C. Dias. Rayleigh-Plateau and Gregory-Laflamme instabilities of black strings. *Phys. Rev. Lett.*, 96:181601, 2006.

[10] G. Chalmers and K. Schalm. Holographic normal ordering and multiparticle states in the AdS / CFT correspondence. *Phys. Rev.*, D61:046001, 2000.

[11] Z. W. Chong, M. Cvetic, H. Lu, and C. N. Pope. General non-extremal rotating black holes in minimal five-dimensional gauged supergravity. *Phys. Rev. Lett.*, 95:161301, 2005.

[12] G. Compere, K. Copsey, S. de Buyl, and R. B. Mann. Solitons in Five Dimensional Minimal Supergravity: Local Charge, Exotic Ergoregions, and Violations of the BPS Bound. *JHEP*, 12:047, 2009.

[13] J. Daintith. *Biographical Encyclopedia of Scientists, Third Edition*.

[14] T. Damour. Black-hole eddy currents. *Phys. Rev. D*, 18:3598–3604, Nov 1978.

[15] A. Einstein. Näherungsweise Integration der Feldgleichungen der Gravitation. *Sitzungsberichte der Königlich Preußischen Akademie der Wissenschaften (Berlin), Seite 688-696.*, 1916.

[16] R. Emparan. Rotating circular strings, and infinite nonuniqueness of black rings. *JHEP*, 03:064, 2004.

[17] R. Emparan and M. Martinez. Exact Event Horizon of a Black Hole Merger. *Class. Quant. Grav.*, 33(15):155003, 2016.

[18] R. Emparan and H. S. Reall. A rotating black ring solution in five dimensions. *Phys. Rev. Lett.*, 88:101101, Feb 2002.

[19] R. Emparan and H. S. Reall. Black Holes in Higher Dimensions. *Living Rev. Rel.*, 11:6, 2008.

[20] A. Fetter and J. Walecka. *Theoretical Mechanics of Particles and Continua*. Dover Books on Physics. Dover Publications, 2012.

[21] J. L. Friedman, K. Schleich, and D. M. Witt. Topological censorship. *Phys. Rev. Lett.*, 71:1486–1489, Sep 1993.

[22] J. P. Gauntlett, J. B. Gutowski, C. M. Hull, S. Pakis, and H. S. Reall. All supersymmetric solutions of minimal supergravity in five- dimensions. *Class. Quant. Grav.*, 20:4587–4634, 2003.

[23] G. W. Gibbons. Supergravity vacua and solitons. In *Duality and supersymmetric theories. Proceedings, Easter School, Newton Institute, Euroconference, Cambridge, UK, April 7-18, 1997*, pages 267–296, 2011.

[24] S. Gillessen, F. Eisenhauer, S. Trippe, T. Alexander, R. Genzel, F. Martins, and T. Ott. Monitoring stellar orbits around the Massive Black Hole in the Galactic Center. *Astrophys. J.*, 692:1075–1109, 2009.

[25] R. Gregory and R. Laflamme. Black strings and p-branes are unstable. *Phys. Rev. Lett.*, 70:2837–2840, 1993.

[26] J. Griffiths and J. Podolskỳ. *Exact Space-Times in Einstein's General Relativity*. Cambridge Monographs on Mathematical Physics. Cambridge University Press, 2009.

[27] S. Gunasekaran, U. Hussain, and H. K. Kunduri. Soliton mechanics. *Phys. Rev.*, D94(12):124029, 2016.

[28] T. Harmark. Stationary and axisymmetric solutions of higher-dimensional general relativity. *Phys. Rev.*, D70:124002, 2004.

[29] S. W. Hawking. Black hole explosions? *Nature*, 248:30–31, Mar. 1974.

[30] S. W. Hawking and G. F. R. Ellis. *The large scale structure of space-time*, volume 1. Cambridge university press, 1973.

[31] O. Heaviside. *Electromagnetic Theory*. Number v. 1 in Electrician series. "The Electrician" printing and publishing Company, limited, 1893.

[32] M. Henningson and K. Skenderis. The Holographic Weyl anomaly. *JHEP*, 07:023, 1998.

[33] S. Hollands, A. Ishibashi, and R. M. Wald. A Higher dimensional stationary rotating black hole must be axisymmetric. *Commun. Math. Phys.*, 271:699–722, 2007.

[34] S. Hyun, W. T. Kim, and J. Lee. Statistical entropy and AdS / CFT correspondence in BTZ black holes. *Phys. Rev.*, D59:084020, 1999.

[35] P. Kanti. Black Holes at the LHC. *Lect. Notes Phys.*, 769:387–423, 2009.

[36] A. Komar. Positive-definite energy density and global consequences for general relativity. *Phys. Rev.*, 129:1873–1876, Feb 1963.

[37] H. K. Kunduri. Spacetime topology and the laws of black hole-soliton mechanics. *Entropy*, 19(1), 2017.

[38] H. K. Kunduri and J. Lucietti. The first law of soliton and black hole mechanics in five dimensions. *Classical and Quantum Gravity*, 31(3):032001, 2014.

[39] R. Loganayagam. Entropy Current in Conformal Hydrodynamics. *JHEP*, 0805:087, 2008.

[40] C. O. Lousto and R. H. Price. Understanding initial data for black hole collisions. *Phys. Rev.*, D56:6439–6457, 1997.

[41] J. M. Maldacena. The Large N limit of superconformal field theories and supergravity. *Int. J. Theor. Phys.*, 38:1113–1133, 1999. [Adv. Theor. Math. Phys.2,231(1998)].

[42] K. Martel and E. Poisson. A One parameter family of time symmetric initial data for the radial infall of a particle into a Schwarzschild black hole. *Phys. Rev.*, D66:084001, 2002.

[43] K. Martel and E. Poisson. Gravitational perturbations of the Schwarzschild spacetime: A Practical covariant and gauge-invariant formalism. *Phys. Rev.*, D71:104003, 2005.

[44] J. McClintock and R. Remillard. Black hole binaries. 2003.

[45] G. Michalogiorgakis and S. S. Pufu. Low-lying gravitational modes in the scalar sector of the global AdS(4) black hole. *JHEP*, 02:023, 2007.

[46] C. Misner, K. Thorne, and J. Wheeler. *Gravitation*. 1971.

[47] J. A. Muñoz, E. Mediavilla, C. S. Kochanek, E. E. Falco, and A. M. Mosquera. A Study of Gravitational Lens Chromaticity with the Hubble Space Telescope. *Astrophysical Journal*, 742:67, Dec. 2011.

[48] R. Myers and M. Perry. Black holes in higher dimensional space-times. *Annals of Physics*, 172(2):304 – 347, 1986.

[49] NASA. Nasa's nustar sees rare blurring of black hole light, 2014.

[50] M. Natsuume. AdS/CFT Duality User Guide. *Lect. Notes Phys.*, 903:pp.1–294, 2015.

[51] R. Penrose. Gravitational collapse and space-time singularities. *Phys. Rev. Lett.*, 14:57–59, 1965.

[52] H. Poincare. Sur la dynamique de l' electron. *Note de H. Poincare*, 1905.

[53] E. Poisson. *A relativist's toolkit : the mathematics of black-hole mechanics*. Cambridge, UK: Cambridge University Press, 2004.

[54] T. Regge and J. A. Wheeler. Stability of a Schwarzschild singularity. *Phys. Rev.*, 108:1063–1069, 1957.

[55] K. Schwarzschild. On the gravitational field of a mass point according to Einstein's theory. *Sitzungsber. Preuss. Akad. Wiss. Berlin (Math. Phys.)*, 1916:189–196, 1916.

[56] N. Scientist. Explore 100 years of general relativity, 2015.

[57] A. Strominger and C. Vafa. Microscopic origin of the Bekenstein-Hawking entropy. *Phys. Lett.*, B379:99–104, 1996.

[58] L. B. Szabados. Quasi-local energy-momentum and angular momentum in general relativity. *Living Reviews in Relativity*, 12(1):4, 2009.

[59] E. H. Telescope. Event horizon telescope, 2017.

[60] K. Thorne, R. Price, and D. MacDonald. *Black Holes: The Membrane Paradigm*. Silliman Memorial Lectures. Yale University Press, 1986.

[61] W. G. Unruh. Experimental black-hole evaporation? *Phys. Rev. Lett.*, 46:1351–1353, May 1981.

[62] P. C. Vaidya. Newtonian Time in General Relativity. *Nature*, 171:260–261, 1953.

[63] M. Van Raamsdonk. Black Hole Dynamics From Atmospheric Science. *JHEP*, 05:106, 2008.

[64] R. M. Wald. *General relativity*. Chicago Univ. Press, Chicago, IL, 1984.

[65] E. Witten. Anti-de Sitter space and holography. *Adv. Theor. Math. Phys.*, 2:253–291, 1998.

[66] F. J. Zerilli. Gravitational field of a particle falling in a schwarzschild geometry analyzed in tensor harmonics. *Phys. Rev. D*, 2:2141–2160, Nov 1970.